Dynamic Scheduling and Control of MEA Absorption Processes for CO_2 Capture Using gProms

by

Farhan Ahmad

A thesis

presented to the University of Waterloo

in fulfilment of the

thesis requirement for the degree of

Master of Applied Science

In

Chemical Engineering

Waterloo, Ontario, Canada, 2019

Author's Declaration

I hereby declare that I am the sole author of this thesis. This is a true copy of the thesis, including any required final revisions, as accepted by my examiners.

I understand that my thesis may be made electronically available to the public.

Abstract

There are three general approaches for the mitigation of carbon emissions from fossil fuel fired power plants; pre-combustion, oxyfuel and post-combustion carbon capture. The post-combustion absorption process using MEA (methyl-ethanol-amine) is selected for this work due to its maturity in research and capability of it being retrofitted on existing power plants.

Previous research included work on solvent development selections, model development, steady state simulation, dynamic simulation and control and optimization. A rigorous dynamic model used in this work is based on the model developed by (Nittaya, 2014) and (Harun, 2012) and includes six PI controllers implemented in gProms v5.1. 80% of the energy cost requirements by post combustion carbon capture system (PCCCS) are for the solvent regeneration. Due to the fluctuation in the electricity demand, appropriate scheduling of the PCCCS can reduce operating costs associated with carbon capture as demonstrated by (Alie, 2013).

Controller performance analysis usually involves either disturbance rejection or servo-control tests but not a combination of both scenarios. Since the %CC schedule was developed to compliment a power generation schedule that generates flue-gas accordingly, this work evaluates the controller in the presence of both flue gas disturbances and %CC set-point changes simultaneously.

It was found that the flue gas disturbances worked in favour of achieving the desired set-points and the controller performed better (~53%) than when evaluated without the influence of the disturbance. This work showed that tuning the controller for the intended schedule improved the response of the controller by about ~58% over the IMC tuned controller (that was estimated around similar operating conditions).

It was determined that following the proposed schedule resulted in a decrease of 7% in energy consumption in comparison with capturing at a fixed capture rate. Fluctuations in the day-to-day electricity demand can be modelled using a correlation between the proposed schedule and the power generated. This work proposed a linear correlation between the two that resulted in a similar set-point schedule being generated. In conclusion, a series of PI controllers may be used to control the highly non-linear MEA based post-combustion carbon capture process provided the controllers are tuned in accordance to the set-point schedule.

Acknowledgements

I would like to thank Professor Peter Douglas for providing me with the opportunity to pursue the MASc degree at the University of Waterloo and provide guidance throughout the research.

I would also like to thank my friends Shafe Assaf, Saad Taimoor, Elodie Papp, Victor Guiguer, Majd Tabbara, Tuhin Poddar, Mohammed Al Katheri, and Ian Tivendale, my brother (Faraz Ahmad) and his wife (Umber Deshmukh) for supporting and encouraging me throughout the course of the degree.

Dedicated to my beloved parents

Parvez Ahmad and Zehra Parvez

Table of Contents

List of Figures

List of Tables

List of Nomenclature

English letters

$a_{g/l}$	Specific gas-liquid interfacial area (m^2/m^3)
a_p	Total surface area of packing (m^2/m^3)
a_w	Wetted surface area of packing (m^2/m^3)
A_{tube}	Cross-sectional area of a tube (m^2)
A_T	Cross-sectional area of a tank (m^2)
$\%CC$	Percent carbon capture (%)
$C_{g,i}$	Molar concentration in gas phase (mol/m^3)
C_i^l	Molar concentration at gas-liquid interfacial (mol/m^3)
$C_{l,i}$	Molar concentration in liquid phase of component *I* (mol/m^3)
$C_{p,i}$	Specific heat capacity of component *i* (J/mol/K)
C_v	Valve sizing coefficient (m^2)
d_c	Column diameter (m)
$D_{g,i}$	Diffusivity in the gas phase of component i (m^2/s)
D_{tube}	Diameter of tube (m)
d_p	Nominal diameter of the packing element (m)
E	Enhancement factor for pseudo-first-order reaction (dimensionless)
E_2	Enhancement factor for irreversible second order reaction (dimensionless)
E_{cond}	Energy holdup in the condenser (J)
E_{reb}	Energy holdup in the reboiler (J)
E_{tank}	Energy holdup in the tank (J)
f_{leak}	Leakage fraction of a valve
F	Molar flow rate (mol/s)
F_{in}	Molar flow rate at the inlet (mol/s)
g	Gravitational constant (m/s^2)
h_T	Liquid level in the tank (m)
H	Enthalpy (J/mol)
H_l	Liquid enthalpy at the outlet (J/mol)
H_v	Vapour enthalpy (J/kg)
k_g	Mass transfer coefficient in gas phase ($mol/kPa/m^2/s$), ($mol/Pa/m^2/s$)

k_l	Mass transfer coefficient in liquid phase (m/s)
L	Superficial liquid mass velocity (kg/m^2/s)
L_B	Liquid level of reboiler drum (m)
N_i	Molar flux (mol/m^2/s)
mw_L	Molecular weight of the outlet liquid stream from valve (g/mol)
M	Dimensionless parameter, Hatta number
$M_{i,reb}$	Molar holdup of component *i* in the reboiler (mol)
p_g	Gas partial pressure (kPa)
p_g^l	Gas partial pressure at gas-liquid interfacial (kPa)
q_g	Interfacial heat transfer in gas phase (J/m^3/s)
q_l	Interfacial heat transfer in liquid phase (J/m^3/s)
Q_{cond}	Condenser duty (W)
Q_{reb}	Reboiler duty (W)
Q_{tank}	Make-up tank duty (W)
R_g	Ideal gas constant (8.314x10^{-3} m^3. kPa/mol/K)
t	Time (s)
T	Temperature (K)
T_{cond}	Condenser temperature (K)
T_g	Gas temperature (K)
T_{tube}	Temperature of the tube (heat exchanger, K)
T_{shell}	Temperature of the shell side of the heat exchanger (K)
T_l	Liquid temperature (K)
u	Velocity (m/s)
U	Overall heat transfer coefficient
V_1	Valve 1 stem position (Buffer tank)
V_2	Valve 2 stem position (Absorber sump tank)
V_3	Valve 3 stem position (Reboiler surge tank)
V_{SP}	Valve stem position
V_{SP}^{act}	Actual valve stem position
x_i	Molar fraction of component *i*
y_{CO_2}	Vapor fraction (molar) of CO_2

z	Element of height (m)

Greek Symbols

α	Fractional valve opening
ΔP	Pressure drop
μ_g	Gas viscosity (kg/m/s)
μ_l	Liquid viscosity
ρ_g	Density of gas (kg/m^3)
ρ_l	Density of liquid (kg/m^3)
ρ_m	Molar density (mol/m^3)
τ_v	Valve's time constant (min)
σ_{ct}	Critical surface tension of packing material
σ_l	Surface tension of liquid

Chapter 1: Introduction

With the rise in population, comes a rise in the demand of energy. Due to the recent rise in concern for climate change and global warming, there is a great deal of research in the fields of mitigating greenhouse gas emissions; namely carbon dioxide. The electric power sector is the single largest contributor to world-wide carbon emissions. Most countries are attempting to reduce their carbon emissions with renewable energy sources (e.g. hydro, wind and solar) as well as the use of lower carbon intensive fuels such as natural gas. However, they are not capable of replacing their dependency on coal and all projections indicate the use of coal will continue to increase

A lot of work on Carbon Capture and Storage (CCS) from fossil fuels has been undertaken in the last couple decades. Three major categories of CCS processes include pre-combustion, oxyfuel and post-combustion. Pre-combustion and oxyfuel combustion require implementation during the design phase due to the changes needed to operate the power plant with the CCS. Absorption based post-combustion carbon capture is popular from its existing well demonstrated technology.

In order to better understand the process, standalone steady-state models were developed to study the behaviour of the process at various operating parameters. This along with lab-scale testing, provided insights to the process, the capabilities of the solvent used and the basis to develop dynamic models. A significant amount of research has been conducted on the individual components within the CCS system.

To minimize costs, steady state optimisation studies have been undertaken. More recently, dynamic modelling and control studies have been undertaken, most of which focused on the well-established MEA absorption process. Investigators have implemented and studied various controller designs such as linear controllers and model predictive controllers. Most of the studies focused on the disturbance rejection (flue-gas disturbances) and/or servo control scenarios. However, they have not investigated the combined effect of both disturbances and simultaneous set-point manipulation throughout the day.

The objective of this research is then to continue research on the dynamic operation of the post combustion CCS absorption process using the MEA solvent. In particular we examine the optimal

operation of an absorption process integrated with a power plant within an electrical grid of generating stations in the face of varying electricity demand resulting in flue gas disturbances.

1.1 Outline of the Thesis

Chapter 2 is the literature review where a summary of the previous work relating to the background, modelling, scheduling and control of the carbon capture process is presented.

The process description is elaborated in Chapter 3 that includes a detailed process description including the equipment dimensions and the nominal values used for this work.

Chapter 4 comprises of the results and discussions associated with this work. The chapter discusses the key findings of this work surrounding modelling issues, non-linearity analysis, linearized modelling, the assessment of a series of PI controllers on servo-control, disturbance rejection and a mixture of both scenarios, and the possibility of modelling a schedule based on a measured disturbance.

The final chapter is conclusions and recommendations where a summary of the findings in this work and recommendations for future work are provided.

Chapter 2: Literature Review

2.1 Background

In the 1970's, the average temperature of the earth was decreasing leading to then popular belief of global cooling. As time passed during the post-industrial age, the average temperature began to rise at an alarming rate leading to the modern belief of global warming (Peterson, Connolley, & Fleck, 2008). This temperature anomaly is due to difference in the amount of energy being absorbed by the earth than released by it.

One of the reasons for this rise in the net absorption of energy is due to the increase in greenhouse gas (GHG) emissions; namely carbon dioxide. Amongst the various GHG, carbon dioxide has the least impact (per same amount of mass) in comparison to the other GHG's. However, due to the quantity of carbon dioxide present throughout the atmosphere (EPA, 2016), it has earned the number one spot on global impact due to GHG.

As water temperature rises, the coral reefs undergo a process called bleaching and consistent bleaching could lead to "severe" effects including some acclimation and genetic adaptation (Hoegh-Guldberg, 1998). Another impact of the rising temperatures is the possible melting of the West Antarctic Ice Sheet (WAIS) increasing the sea level by 4 to 6 meters (O'Neill, 2002). The paper suggests a limit of 2 °C above 1990 global average is enough to avoid WAIS.

There are agreements made between countries throughout the world to combat climate change. The goal of the Kyoto agreement was to reduce the GHG emissions by 5% below the levels in 1990 by the end of 2012. (O'Neill, 2002) investigated the impact of the climate change provided we do not achieve the goals set out by the Kyoto protocol. The 2015 Paris agreement re-evaluated the current status of the emissions and created new goals for the countries to achieve. According to the Article 2 of the agreement, aims to reduce the global temperature to 2 °C above pre-industrial levels and try to achieve 1.5 °C by 2025 without threatening food production (Paris Climate Change Conference, 2015).

While reducing carbon emissions from every sector is beneficial, focusing on the largest carbon emitters, the power industry, will have a greater impact; (Scott, Gilfillan, Markusson, Chalmers, & Haszeldine, 2012) discussed the dominance of fossil fuels as a global source of electricity in the

future (2035 based on trends from (IEA, 2011). The paper also mentioned the importance of CCS (Carbon Capture and Storage) to mitigate the emissions from the associated power plants.

2.2 Carbon Capture Systems (CCS)

A typical coal fired plant operation is described in the following Figure (1) where the energy stored in the coal is converted into thermal, mechanical and electrical energy. This is done by burning the coal to heat water and produce generate steam which then spins turbines to generate electricity. NO_x, SO_x and particulates are normally removed from the flue gas before being vented to the atmosphere thereby still releasing significant amounts of carbon in the form of CO_2.

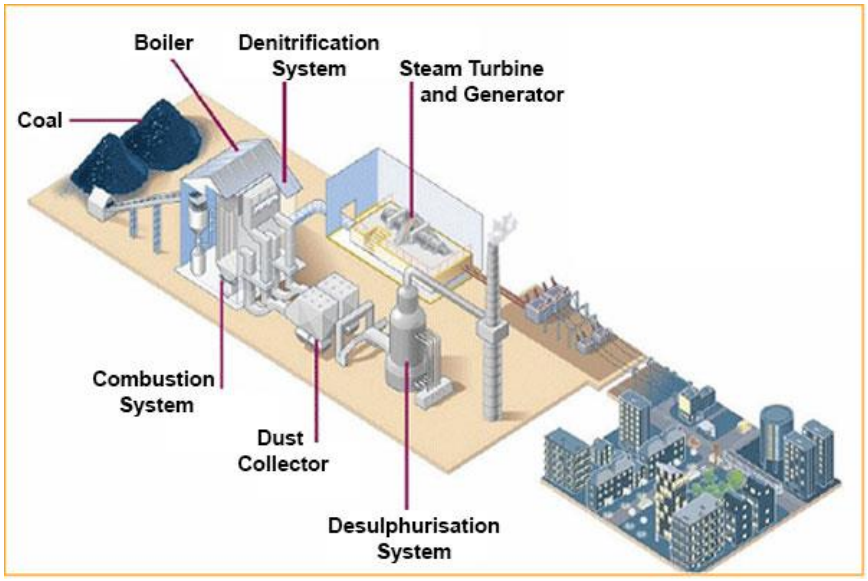

Figure 1 Coal Fired Power Plant (Natural Resources Canada, 2016)

Installing a carbon capture system on existing generating stations as well as upcoming requires proper evaluation of the various carbon capture options. There are several proposed methods for capturing CO2 from power plants, which fall under three main categories presented in Figure 2, (Song, et al., 2018); pre-combustion, oxy-fuel and post combustion Carbon capture system (CCS).

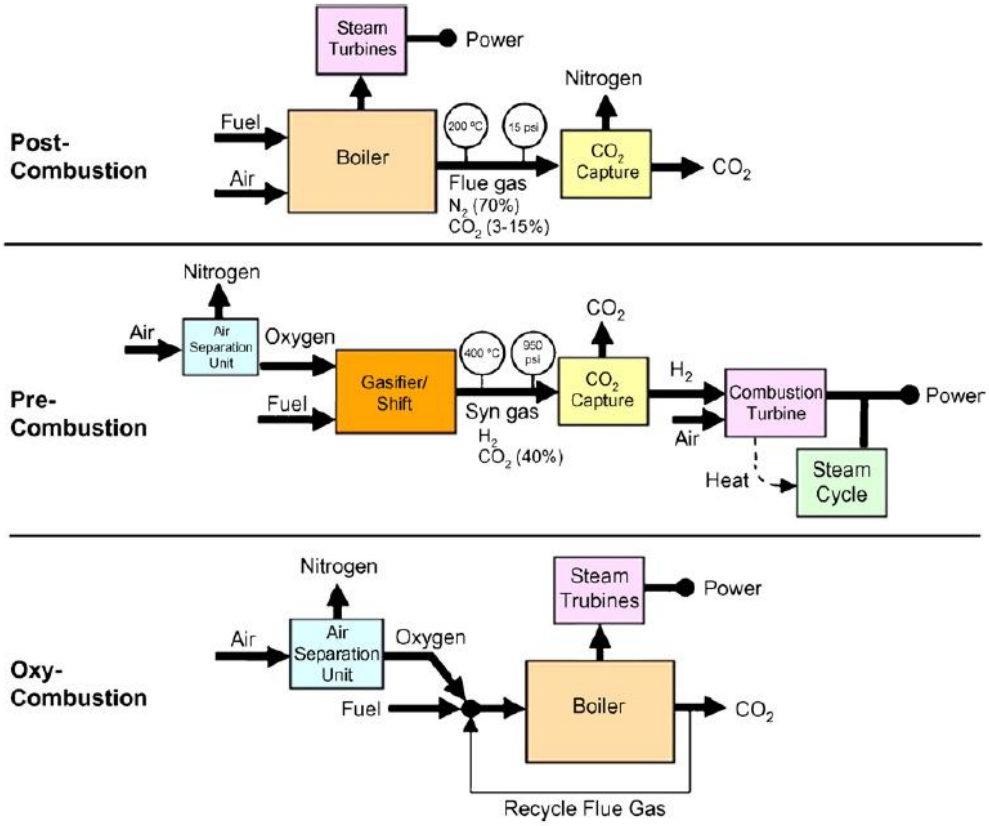

Figure 2 Various CCS Options (Song, et al., 2018)

Post-combustion carbon capture, requires no modifications to the plant itself and in principle, can be installed on an existing PC boiler process. The flue-gas enters the capture unit and using either physical or chemical adsorption/absorption, the CO_2 is extracted from the flue-gas before being treated to recycle the solvent. The captured stream of highly concentrated CO_2 is sent for compression and storage (Figure 2). One major benefit is that existing boilers require little to no modifications. They do have one major drawback as well, the energy requirements for this capture process is very high requiring either additional source of energy or can lower the overall output of the power plant (to the area) by about 30-35% (Oyenekan & Rochelle, 2006).

(Singh, 2003) conducted an economic study between the post-combustion MEA/oxyfuel capture process where it was determined that oxyfuel capture had the potential of achieving lower operating costs than the MEA combustion but requires higher capital costs. There are multiple variations of post-combustion, namely physical adsorption and chemical absorption. MEA is a popular solvent because of its high selectivity in absorbing carbon dioxide from the flue gas at low concentrations and pressures. However, the MEA absorption process has a high energy

requirement for solvent (MEA) recovery accounting up to 80% of the overall CCS energy costs and resulting in a significant de-rating of the power plants.

Pre-combustion CO_2 capture requires modification of the combustion process. The oxygen (or steam/air) and fuel react in the gasifier to produce syngas (CO and H_2) (Figure 2). The CO and steam are reacted in the water-gas shift reactor to produce CO_2 and additional H_2. The H_2 is used to generate electricity and the CO_2 is sent for capture (Jansen, Gazzani, Manzolini, Dijk, & Carbo, 2015). The main benefits of the pre-combustion process include lower energy penalty and lower usage of water. However, the process itself is complex and expensive to construct.

Figure 2 also outlines the oxyfuel CO_2 capture process which requires design modifications to the boiler and cannot be easily retrofitted to an existing PC process. Conventional PC (Pulverized Coal) boilers burn coal in an air (O2 - N2) environment whereas oxy-combustion boilers burn coal in and O2 – CO2 environment. Burning in the presence of O_2 will yield very high flame temperatures that need to be controlled by recycling the flue-gas back into the boiler. Benefits of using an oxyfuel combustion include higher efficiency of the boiler, lower flue gas amounts and high CO2 concentrations within the flue gas resulting in smaller post-combustion treatment facilities. (Lockwood, 2014) provides a comprehensive review of the oxyfuel process and Stanger (Stanger, et al., 2015) highlights the developments made in the last decade in the field of capturing CO_2 using oxyfuel combustion on various types of boilers.

In the late 1970s and early 1980s, there were several CO_2 capture plants that were forced to close down due as the recovered CO_2 was too expensive for the enhanced oil recovery (EOR) operations (Herzog H. , 2010). About 80% of the stored CO_2 is used in EOR (Chapel, Marix, & Ernest, 1999). In 2000, Hezorg (Herzog H. J., 2000) conducted a study in the economics of CO_2 capture in terms of the policies at the time.

According to the (Global CCS Institute, 2018), there are currently 43 large scale CCS facilities of which 18 are operational, 5 under construction and 20 under development. As research develops in terms of usability, efficiency and costs; these procedures become practical enough to be implemented for the benefits they propose (costs now seem reasonable to implement overpaying carbon tax for the companies involved). Recently, hybrid combinations of various technology have begun to be investigated as well (Song, et al., 2018).

For the purposes of this work, the control study is conducted on the most mature chemical absorption-based post-combustion carbon capture process. Figure 3 (Wang, Zhao, Otto, Robinius, & Stolten, 2017) presented in the review paper described a general chemical absorption post-combustion capture process that includes two major components; an absorber and a stripper column. The absorber column is designed for the flue-gas contacts and is absorbed by the solvent. This solvent is then retrieved in the stripper column using heat. The heat exchanger is added to the system to help lower energy costs of the process and the reboiler/condenser are placed to maintain temperatures of the solvent entering the column (condenser) and adjust the temperatures of the mixture in the stripper column (reboiler). Finally, the separated pure stream of CO_2 is sent for compression and storage. A detailed process description specific with equipment dimensions and parameters for his work will be provided in the next chapter.

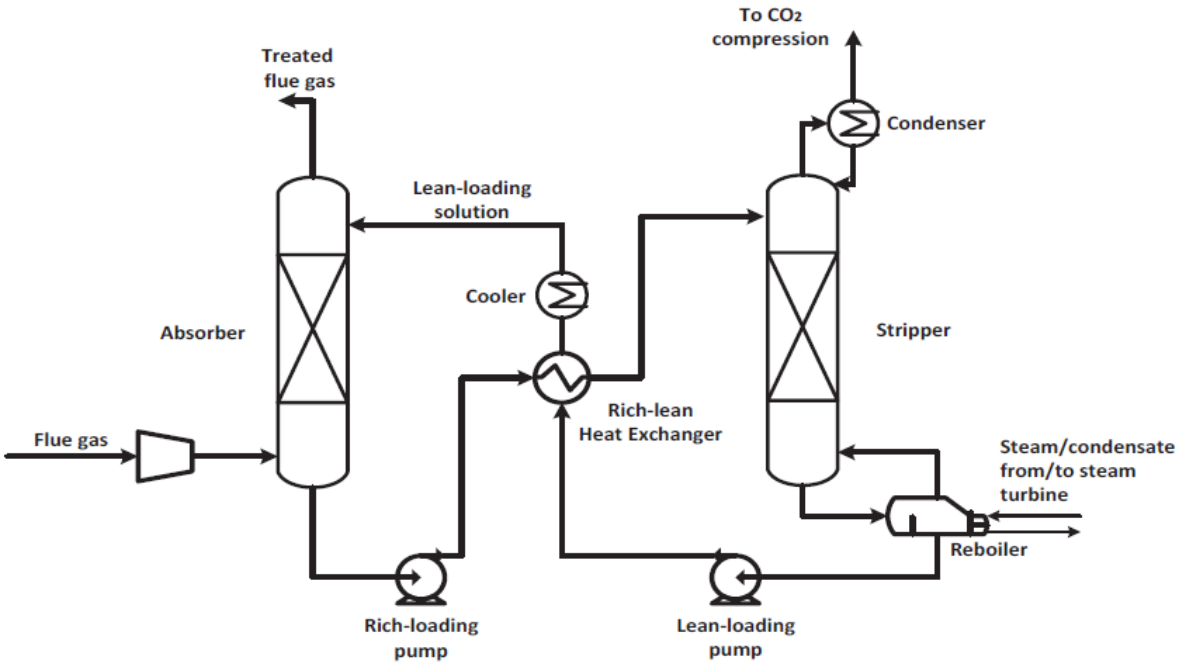

Figure 3 Chemical Absorption based CO2 Capture (Wang, Zhao, Otto, Robinius, & Stolten, 2017)

The solvent must selectively separate the maximum amount of CO2 from the flue-gas stream while allowing the remaining components to pass through. Table 1 (Luis, 2016) below describes various options within a post combustion scenario (physical and chemical).

Overview of CO_2 removal processes in a post-combustion scenario [8].

Process name	Solvent/reagent + additives	CO_2 in treated gas (ppm)
Physical absorption systems		
Purisol (NMP)	N-methyl-2-pyrrolidone	Less than 50
Rectisol	Methanol	Less than 10
Fluorsolv	Propylene carbonate	Function of pressure
Selexol	Polyethylene glycol dimethyl ether	Function of pressure
Processes with chemical reagents		
MEA	Water/monoethanolamine (20%)	Less than 50
Promoted MEA	Water/MEA (25–30%) + amine guard	Less than 50
Benfield	Water/K_2CO_3 (25–30%) + DEA, etc	500–1000
Vetrocoke	Water/K_2CO_3 + As_2O_3 + glycine	500–1000
Catacarb	Water/K_2CO_3 (25–30%) + additives	500–1000
Lurgi	Water/K_2CO_3 (25–30%) + additives	500–1000
Carsol	Water/K_2CO_3 + additives	500–1000
Flexsorb HP	Water/K_2CO_3 amine promoted	500–1000
Alkazid	Water/K_2-methylaminopropionate	To suit
DGA	Water/diglycolamine (60%)	Less than 100
MDEA	Water/methyl diethanolamine (40%) + additives	100–500
Hybrid systems		
Sulfinol	Sulphones/DIPA	Less than 100
TEA–MEA	Triethanolamine/monoethanolamine Water/sulpholane/MDEA	Less than 50

Table 1 Solvent Selection table based on amount of CO_2 present in treated gas (Luis, 2016)

Other works by (Salazar, Diwekar, Joback, Berger, & Bhown, 2013) show various solvents and the pros/cons associated with them using MEA as the basis. For the purposes of this work, the widely researched MEA will be used.

MEA is produced by combining ammonia and ethylene oxide. However, there are associated drawbacks to using MEA in the CCS which include equipment corrosion, toxicity and solvent degradation at high temperatures (which are required for CO2 separation) over time. The largest operating cost component of the chemical absorption process is due to the high energy costs of the solvent recovery (80% of the capture costs).

2.3 Dynamic Modelling and Control

Much work has been conducted on steady state modelling, techno-economic simulations, design and optimisation ((Singh, 2003) (Alie, 2013) (Harun, 2012) (Nittaya, 2014)). However, dynamic modelling and control research are newer.

(Lawal, Want, Stephenson, & Yeung, 2009) developed a dynamic equilibrium and a rate-based model for the absorber in the CO_2 capture that was validated against a pilot plant. The rate-based model provided a better representation of the data than did the equilibrium model. Based on the

model, it was also determined that the absorber can be operated normally under partial load as well.

(Harun, 2012) developed a model for the entire MEA process as well as a simple control structure for it. The absorber and the desorber (stripper) columns were a rate-based dynamic rigorous model. This model is used as the model for this work.

The relative non-linearity between key variables of the process was investigated by (Wu, et al., 2018, b). This paper described the process non-linearity when key variables (capture rate, flue gas flowrate and reboiler temperature) are altered as well as their interactions. It was also noted that operating at capture rates below 90% have a response much closer to linearity than operating at ranges above 90% and the influence of the flue-gas flowrate on the non-linearity of the process is minimal. The reboiler temperature, on the other hand, is highly influential so it was determined to keep it as tightly under control as possible.

The majority of the linear process models operate near a fixed nominal operating point and the non-linear models based on first-principle models is computationally demanding making control design difficult (Liao, et al., 2018). The paper also investigated the development of a simulation model for the PC combustion-based process based on piece-wise linear models (Simulink) and quantified the non-linear characteristics of key variables such as CO_2 capture rate, reboiler temperature, condenser temperature and lean solvent temperature (gProms).

2.4 Scheduling

(Rao & Rubin, 2006) investigated the capital and variable costs for CO_2 capture and discussed the various regions of maintaining the capture rate (fixed capture rate) depending on the constraints such as heat requirements and loss of power generation.

(Chalmers & Gibbins, 2007) suggested to store the rich solvent during peak hours and recover the solvent during off-peak hours. Additional solvent and tanks were required to meet the requirements adding costs for the CCS.

Normally, CO_2 capture is assumed to be constant with the boiler that generates the flue-gas operating at full capacity. (Alie, 2013)'s work investigated benefits of flexible CO_2 capture and scheduling electricity generation for a system of units (generators) based on IEEE RTS '96 (IEEE

Transactions on Power Systems, 1999). The work also involved evaluating the benefits of CO_2 capture based on various prices of CO_2. The system included nuclear, hydro, coal and oil as the sources of energy. Firstly, the cost to performance for each source of energy was evaluated and then re-evaluated with one of the generators operating with PCCCS. However, it is estimated that installing a PCCCS to a nominal 500 MWe unit will have a de-rate of 31% for an average capture rate of 85%. Some of other challenges faced by MEA CCS (Post-Combustion) include loss of sorbent and corrosion of the equipment (Rao A. B., 2002).

Figure 4 and 5 were based on information from (Douglas, 2018) and Alie (2013). Figure 4 represents the schedule for the generating station (based on different capture rates) and the corresponding capacity factor (fraction of power generation utilized for electricity) for the 350 MW coal fired 'Austin Generating Station', one of 24 generating stations in the fleet within the IEEE 96' scenario.

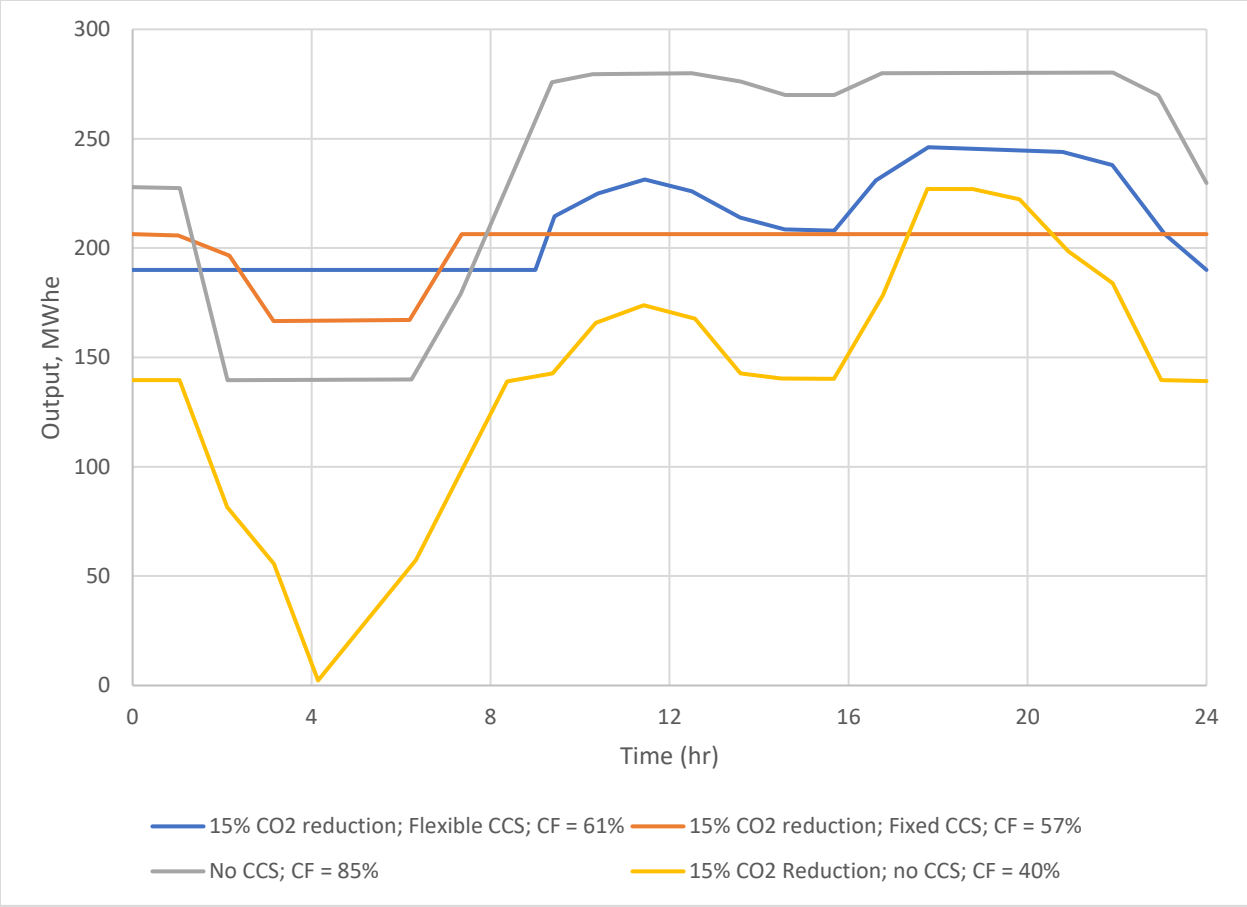

Figure 4 Power Plant Output in Various Scenarios

Not having any constraints allows the generator to operate at a capacity factor of 0.85 for the duration of the day. Now having a constraint of 15% CO_2 reduction without CCS drops the capacity factor down to 0.40. Adding CCS with a fixed capture rate of 85% improves the capacity factor up to 0.57 and using a variable capture rate allows the capacity factor to reach 0.61. This is lower than not having any constraints on the performance of the generator but is significantly better than having to reduce the emissions without CCS. The figure also represents the scheduling of the Austin power generator for the various scenarios. The schedule of power generator operation is used as a basis for the disturbance in this work.

The variable capture rate for the power generation schedule posed in the previous figure is shown in Figure 5.

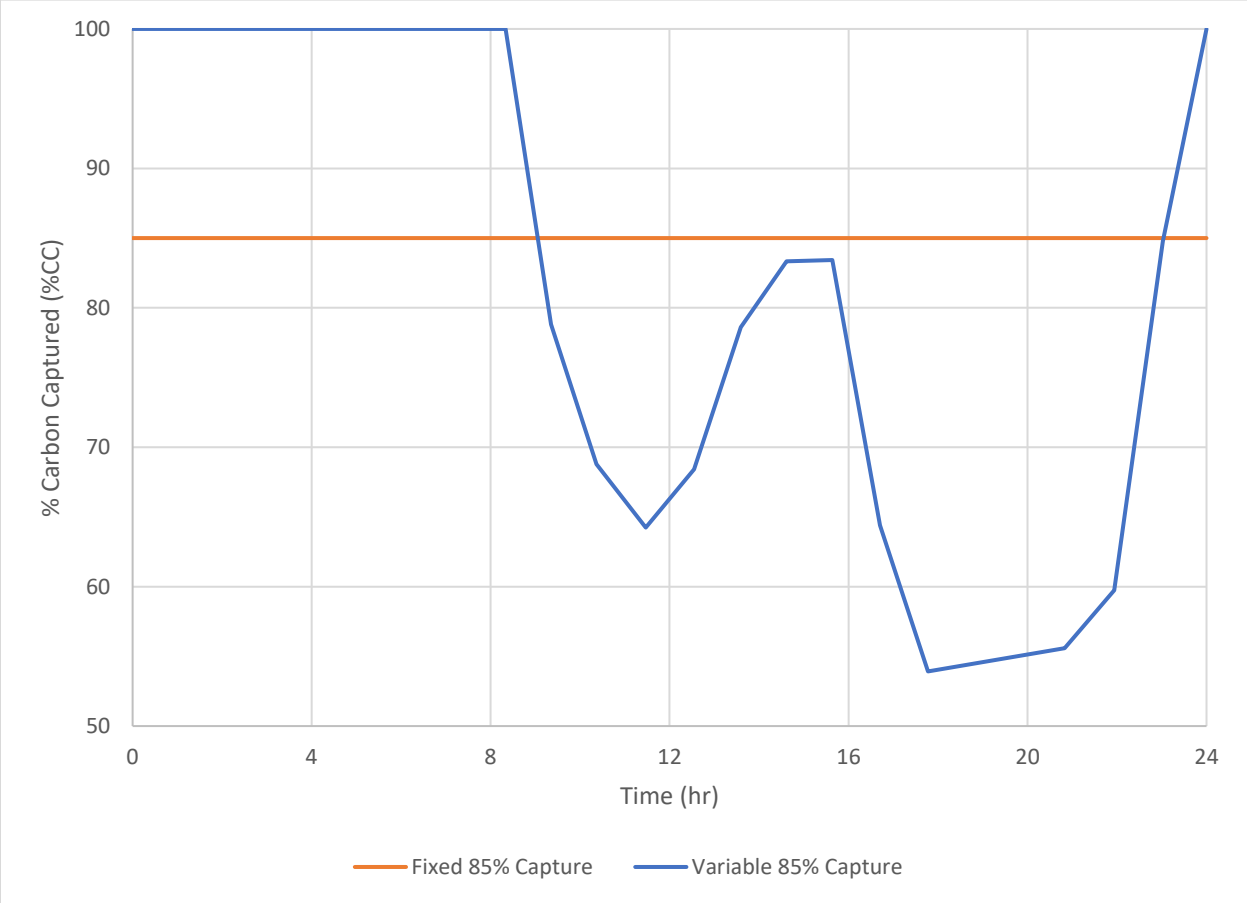

Figure 5 Proposed CCS Schedule

The schedule is designed to capture close to 100% when the demand of energy is low and capture lower amounts as the demand changes throughout the day (working hours). Using the variable capture rate allows for minimizing capture costs while achieving the desired capture goal of 85%. This schedule is used as the basis for the set-point schedule in this work.

(Mechleri, Lawal, Ramos, Davison, & Dowell, 2017) evaluated the fluctuations of the electricity prices throughout the day and identify relevant operating regions for the process. The paper investigated the change in flue-gas based on the demand but decided to hold the capture rate fixed at 90%.

2.5 CCS Control

(Lin, Chang, Wong, Jang, & Ou, 2011) stated the importance of avoiding flooding and poor wetting conditions for the absorber and the stripper column when manipulating suggesting they cannot be shut down or turned on at will. The work consisted of evaluating the variability in the capture rate (varying between 50%, 70%, 90%) based on different manipulated variables and electricity prices.

(Nittaya, 2014) modified the controllers developed by Harun (2012) and found six manipulated variables and six key controlled variables. All six controlled variables were paired with a manipulated variable using linear PI controllers based on RGA analysis and heuristics. The control scheme presented in this work is used as the basis for the control structure in this work (the control scheme will be presented in detail in the next section).

(Zhang, Turton, & Bhattacharyya, 2016) compared the performance of linear PID controllers and LMPC (Linear Model Predictive Control) and showed that there is significant interaction between CO_2 capture rate and the reboiler temperature using Aspen Plus and Aspen Plus Dynamics. The PID controllers were tuned according to various tuning rules (within Aspen) such as IMC, Ziegler-Nichols, Tyreus-Luyben, IAE, ISE, ITAE and Cohen-coon and the controllers were paired based of an RGA (Relative Gain Array) analysis. It was noted that the performance of the LMPC performed significantly better than PID in all aspects and the performance of the PID controller is expected to deteriorate with aggressive disturbances.

(Oh, Binns, Cho, & Kim, 2016) evaluated the energy requirements for MEA-based CO_2 capture process and the optimal conditions at which to operate for a minimized energy requirement. The work proposed tweaks to the MEA-capture process such as flue-gas splitting, multiple-solvent feeding, split-stream/semi-lean and absorber intercooling that have the potential to improve the energy efficiency of the process.

A model-free adaptive control (MFAC) was proposed by (Li, Ding, Wang, & Oko, 2018) using on-line tuning. To assist in computational time of the controller parameters, the model uses neural networks that was validated against the first-principle models. This controller performed better than linear PID's and linear MPC's due to the constantly changing parameters.

(Wu et al, 2018, a) explored the implementation of a Multi-Model Predictive Control (MMPC) by having multiple MPC's based on models of the PCCS at various operating points. This model was capable of operation over a wide range of operating conditions and was able to reject flue-gas variation (using two manipulated and two controlled variables) much better than linear PI's or LMPC's. However, this work does not show the interaction between the disturbance in the flue-gas and the capture rate but rather as two separate studies.

This work is based on the control structure developed by (Nittaya, 2014). One of the objectives of this work is to demonstrate the applicability of several linear PI controllers (6 control pairs) on a highly non-linear application of Carbon Capture using chemical absorption in the presence of disturbance as well as set-point scheduling.

This work focuses on the scheduling and control part of the process. All the mentioned research investigates either disturbance rejection or servo control related issues. This work aims to investigate the combination of both disturbance and servo control related applications (an alternative approach to evaluating control performance).

2.6 Summary of Papers

A summary of all the researched papers are summarized in the table presented in the following page (Table 2).

Article Information			Analysis Type				Controller		Controller Tests		
First Author	**Year**	**CCS Focus**	**Steady-State**	**Dynamic**	**Economics**	**Scheduling**	**PI**	**MPC**	**Disturbance Rejection**	**Servo-Control**	**Combined**
Chapel, D.G.	1999	CCS Development	✓		✓						
Herzog, H.J.	2000	CCS Economics	✓		✓						
Rao, A.B.	2002	Techno-economic assessment	✓		✓						
Oyenekan, B.	2006	Stripper Column PCC Modifications	✓								
Rao, A.B.	2006	Cost-Effective CO2 Control Levels	✓		✓						
Abu-Zahra, M.R.M.	2007	MEA Technical Performance	✓								
Hannah, C.	2007	PCC - Process Modification Suggestions	✓		✓						
Lawal, A	2009	Dynamic CCS Absorber		✓							
Herzog, H.J.	2010	CCS Scaling	✓		✓						
Lin, Y.	2011	Control for CCS Plant Flexible operation		✓			✓			✓	
Harun, N.	2012	CCS Dynamic Model		✓			✓			✓	
Alie, C.	2013	CCS Fleet Scheduling				✓					
Salazar, J.	2013	PCC Solvent Analysis	✓		✓						
Nittaya, T.	2014	PI Controller					✓		✓	✓	
Lockwood, T.	2014	Oxyfuel Review	✓		✓						
Rohan, S.	2015	Oxyfuel Review	✓	✓		✓					
Patricia, L.	2016	MEA Alternatives for CO2 Capture	✓								
Zhang, Q.	2016	Model Development and MPC (PCCS)		✓				✓	✓		
Oh, S.	2016	Energy minimization for MEA CCS	✓		✓						
Yuan, W.	2017	PCCS Review	✓		✓						
Mechleri, E.	2017	PCC Control for flexible operation		✓	✓		✓		✓	✓	
Song, C.	2018	Hybrid (CCS Review)	✓		✓	✓					
Wu, X.	2018	Process non-linearity Analysis		✓			✓			✓	
Peizhi, L.	2018	PCC Model Development	✓	✓							
Ziang, L.	2018	Model-Free adaptive control for MEA		✓			✓	✓		✓	
Wu, X.	2018	MMPC for flexible operation		✓				✓	✓	✓	
Ahmad, F. (This work)	2019	Dynamic scheduling and control	✓	✓		✓	✓		✓	✓	✓

Table 2 Literature Review Summary

Chapter 3: Process Description

The process flowsheet and process variables and parameters are described below. Figure 6 represents the process flowsheet. A101 is the absorber; the flue gas (1) is blown into the bottom of the absorber and comes in contact with the lean MEA solution (2). A102 represents the absorber sump tank where rich MEA solution accumulates before flowing (3) to the desorber (D101) through valve V2. The rich MEA (3 and 5) passes through a heat exchanger (HX) that transfers heat from the lean MEA (9) to the rich MEA (5) in an effort to reduce heating costs in the desorber column (D101). The rich MEA stream (5) enters the desorber (D101) at the top and comes in contact with steam produced by the reboiler (R102) separating the CO_2 from the MEA. Fluctuations in the Q_{reb} are compensated for by adding a surge tank (R101). The separated CO_2 is then cooled using the condenser (C1) before being transported for storage. The lean MEA (9) passes through the heat exchanger (HX) entering the make-up tank (T1) where additional water and MEA are added to system compensating for the losses of MEA through the system. Once the MEA is diluted with the water to make the required composition, valve (V1) controls the flowrate of the lean MEA (2) from the make-up tank (T1) into the absorber (A101) for carbon capture.

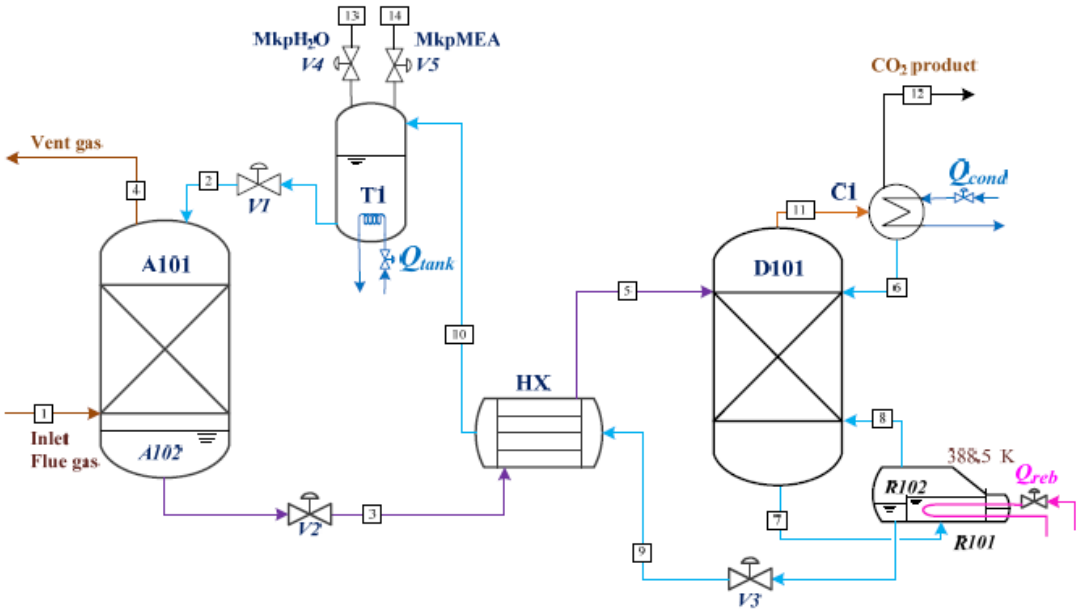

Figure 6 Post Combustion Carbon Capture Model, Nittaya (2014)

The nominal values for the process and control variables are presented in Table 3 below.

Variable		Nominal steady-state value
MV1	Condenser heat duty (Qcond)	8.6 kW
MV2	Buffer tank heat duty (Qtank)	164.3 kW
MV3	Reboiler heat duty (Qreb)	153.6 kW
MV4	Outlet valve position of the buffer tank (V1)	32 % opening
MV5	Outlet valve position of the absorber sump tank (V2)	50% opening
MV6	Outlet valve position of the reboiler surge tank (V3)	50% opening
CV1	Condenser temperature (Tcond)	313.8 K
CV2	Lean amine temperature (Ttank)	312.8 K
CV3	Reboiler temperature (Treb)	388.4 K
CV4	Percentage of CO_2 removal (%CC)	96.30%
CV5	Liquid level in absorber sump tank (L2)	0.3 m
CV6	Liquid level in reboiler surge tank (L3)	0.3 m

Table 3 Nominal steady state values of the process variables (Nittaya, 2014)

Following the starting variables, the parameters for the various equipment in the process is presented below (Table 4) along with their sources. These parameters include the dimensions, operating temperature and pressure and constants for the equipment used within the modelling environment.

Parameter	Value	Remark
Absorber (A101)		
Internal diameter (m)	0.43	(Dugas, 2006)
Height (m)	6.1	(Dugas, 2006)
Packing size (mm)	IMTP#40	(Dugas, 2006)
Nominal size	0.038	(Dugas, 2006)
Specific area (m2/m3)	143.9	(Dugas, 2006)
Operating temperature (K)	314-329	(Dugas, 2006)
Operating pressure (kPa)	101.3 – 103.5	(Dugas, 2006)
Stripper (D101)		
Internal diameter (m)	0.43	(Harun et al., 2012)
Height (m)	601	(Harun et al., 2012)
Packing size (mm)	IMTP#40	(Harun et al., 2012)
Operating temperature (K)	350-380	(Harun et al., 2012)
Operating pressure (kPa)	159.5 – 160	(Harun et al., 2012)
Reboiler (R101)		
Operating temperature (K)	383-393	(Harun et al., 2012)
Operating pressure (kPa)	160	(Harun et al., 2012)
Condenser (C1)		
Operating temperature (K)	312-315	(Nittaya, 2014)
Operating pressure (kPa)	159	(Nittaya, 2014)
Cross heat exchanger (HX)		
Internal diameter of shell (m)	0.305	(Edward, 2008)
Internal diameter of tube (m)	0.148	(Edward,2008)
Outer tube diameter of tube (m)	0.19	(Edward,2008)
Buffer tank (T1)		
Internal diameter (m)	2	(Nittaya, 2014)
Absorber sump tank (A102)		
Internal diameter (m)	0.43	(Nittaya, 2014)
Reboiler surge tank (R102)		
Internal diameter (m)	0.43	(Nittaya, 2014)
Valves		
Flow coefficient of V1 (m2)	1.01 * 10E-3	(Nittaya, 2014)
Flow coefficient of V2 (m2)	0.85 * 10E-3	(Nittaya, 2014)
Flow coefficient of V3 (m2)	0.85 * 10E-3	(Nittaya, 2014)

Table 4 Equipment parameters (Various Sources)

3.1 Modelling Issues:

The gProms equation solvers have significantly changed over the last couple of years. The model developed by Harun and Nittaya was developed using gProms (v3.2), whereas this work was performed using gProms (v5.1).

The default solver for v3.2 was DASOLV and the default solver for v5.1 is DAEBDF. Both solvers use a form of backward differential formulas. However, due to the changes in the convergence formulas and how they interact with the equations, the new default solver, (DAEBDF) was unable to converge the earlier code that was solved with DASOLV, the older solver. Using the default solver did not require any additional input from the user indicating the solver and tolerances. The changes to the solvers configuration resulted in poor initialization and convergence of the model. Manipulating equations to make the model more robust required rewriting several equations to avoid the usage of division. Manipulating certain variable limits heavily affected the ability of the model to converge. Chemical kinetics and mass transfer equations along with the upper and lower limits on the molar concentration were the primary causes of the model failing to converge with the new solver. However, an updated "DASOLV" solver was used to assist in the convergence along with the manipulation of equations

This leads to the issue with debugging model's that are developed on an equation-oriented platform (gProms) in comparison to a sequential modular one such as Aspen Hysys. Within gProms, the solver compiles all the equations and variables and verifies if the system as a whole has one unique solution. All the variables are solved simultaneously leading to a significantly lower simulation time. However, when an error occurs, the equation where the error has taken place is often not the source of the error. In sequential modular systems such as AspenPlus or Hysys solves each block (unit operation) of the process (A101, HX, …) one block at a time using the output of the previous block as the input to the next component until the system produces repeated results indicating convergence. In this simulation environment, when an error occurs, the source of error is often in the block where the error has occurred, making debugging much easier.

These issues led to surprising number of unexpected errors when running the models developed by (Harun, 2012) and (Nittaya, 2014) and resulted in significant editorial changes (e.g.

rewriting/rearranging equations and adjusting limits on the various variables) and debugging efforts.

Chapter 4: Results and Discussion

4.1 Aspen Steady State Analysis

The first part of the results investigates the linearity of the process and conditions that would assist in operating the process in a linear manner. A steady state model was developed in Aspen Hysys using the parameters shown above. Valves and the buffer tank were omitted from the model as they require dynamics to process results and they will be investigated in gProms v5.1.

The impact of manipulating the energy consumed by the reboiler (Figure 7) and the condenser (Figure 8) at various inlet flue-gas flowrates and inlet CO_2 concentrations on the condenser temperature, reboiler temperature and the CO_2 purity from the condenser were investigated. The influence of various inlet flue-gas flowrates and inlet CO_2 concentrations on the overall capture capability is also investigated.

The tests involved manipulating the MV's from 20% below their nominal value to 20% above their nominal values and observing the responses on the controlled variables. Using the steady state values, the gain between each increment was evaluated to see the operating range at which the process behaves linearly. The gains are evaluated as the difference between the two steady state observed values for the controlled variables divided by the difference in the manipulated variables (Watts).

4.1.1 Reboiler Duty

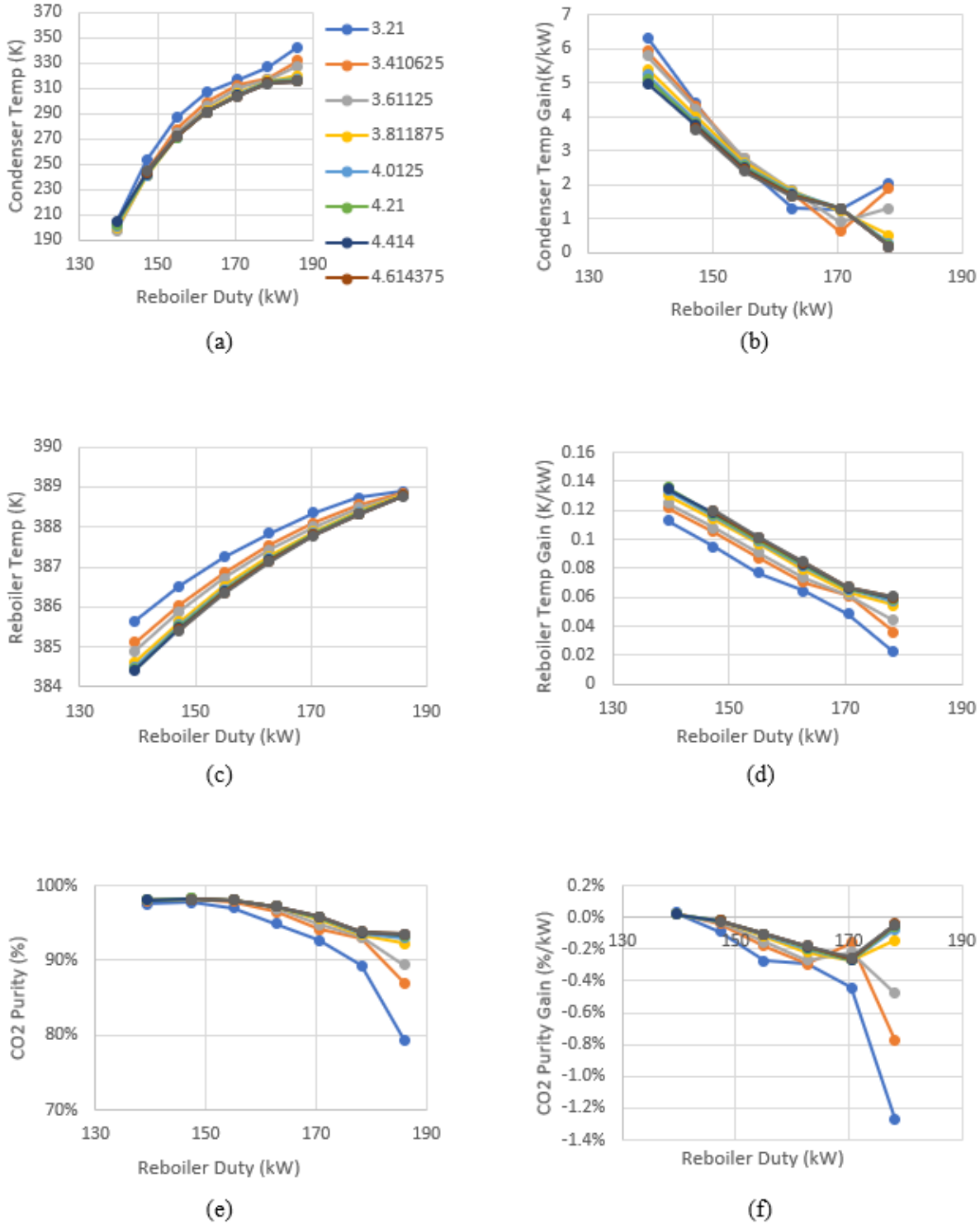

Figure 7 Response and respective gains of condenser temperature, reboiler temperature and CO2 purity as a function of reboiler duty

With respect to the energy of the reboiler, values below -10% of the nominal value failed to converge for all flowrates and concentrations. The nominal value for the reboiler duty was 155,000 Watts, which translates to the manipulating range of the duty from 139,000 Watts to 17,825 Watts at increments of 7,750 W. The legend on Figure 7(a) is the same for all the remaining figures within Figure 7.

As the energy of the reboiler increases, the temperature of the condenser increases significantly from ~204 K to ~320 K (including all flowrates) as the reboiler duty is increased from -10% of the nominal value to +20% of the nominal value Figure 7(a). Figure 7(b) shows the gain of the condenser temperature at each reboiler duty increment. Ideally, for a linear process, a flat horizontal line is to be expected. However, the gain changes with each increasing watt of the reboiler duty. As the duty increases, there is a trend towards linearity suggesting operating at high reboiler duties for a wider linear operating range.

Switching over to the effect of reboiler duty on the reboiler temperature, the temperature varies from ~384 K to 389 K Figure 7 (c, d). The trends are similar to that of the condenser temperature, with a very small increase per watt. Although the range of variation is small, it is essential to maintain the temperature of the reboiler constant around 388/389 K to improve the process in terms of behaving in a linear manner as shown by (Wu, et al., 2018, b). This again suggests that the reboiler duty be kept at the higher end.

However, when it comes to the CO_2 purity from the product stream, increasing the reboiler duty significantly affects it (Figure 7(e, f)). Increasing the reboiler duty increases the overall temperature of the desorber column and while holding the condenser duty constant, additional MEA that was to be recovered in the column now passes through reducing the purity of the product (CO_2) stream as well as reducing the amount of MEA recovered by the column increasing costs to replace it. In regard to the linearity of the process, operating at high reboiler duty leads to a larger change in the gain suggesting that the operation be held at lower reboiler duties to maintain a linear effect CO_2 purity.

The effect of varying the flowrates follow a parallel trend on the controlled variables while manipulating the MV. This suggests that a linear approximation can be used for a wide range of inlet-flowrates.

4.1.2 Condenser Duty

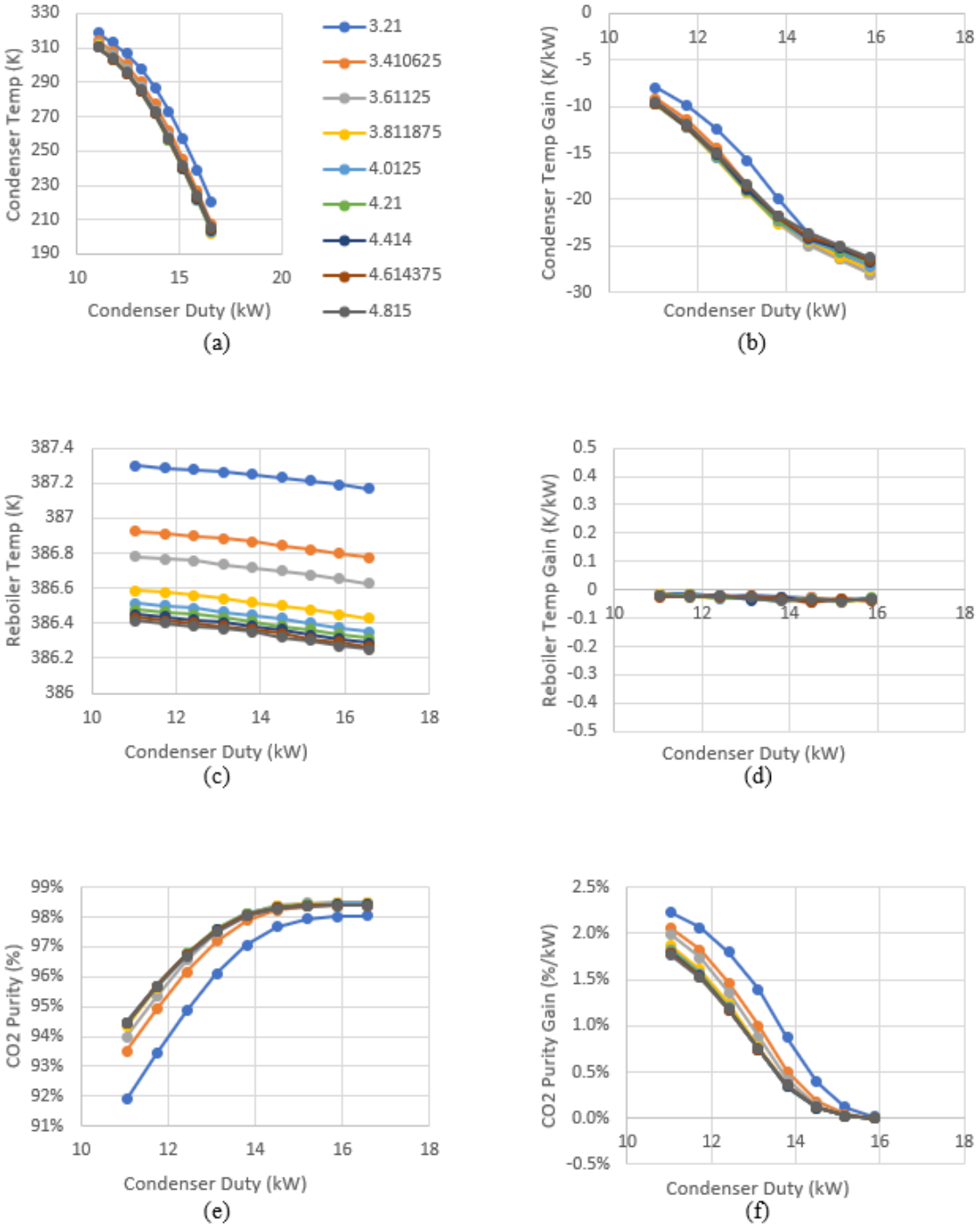

Figure 8 Response and respective gains of condenser temperature, reboiler temperature and CO2 purity as a function of condenser duty

When the condenser duty is increased, this means that additional energy is removed from the stream passing through it (increased -ve duty). Moving over to the effect of the condenser duty on the controlled variables, it has an opposite response to the one from the reboiler duty. All the legends are the same for Figure 8 (a to f). The condenser duty was manipulated from 11040 W to 16560 W with each incremental step being 690 W (5% of the nominal value).

Removing additional energy from the condenser will drop the condenser temperature as indicated by Figure (8, a). The temperature drops from around ~310 K to ~210 K (inclusive of all flowrates). When looking at the gains, the gains change at a higher rate initially and appear to behave linearly at higher condenser duties (Figure 8, b).

When observing the response of the reboiler temperature, the flowrate has a larger impact than the effect of the condenser duty (Figure 8, c and d). Varying the condenser duty changes the temperature by less than ~0.5 K. As the change is significantly small, the gains can be assumed to have linearly throughout the range of the condenser duty. However, the nominal value is to be adjusted based on the flowrate of the inlet flue-gas.

Cooling the fluid passing through the condenser condenses the MEA primarily increasing the purity of the product stream (CO_2 purity) as the condenser duty increases (Figure 8, e). The nominal value is at the inflection point which is a relative optimum as any additional duty added to the condenser to remove heat from the passing stream will yield lower and lower benefits (since the process approaches near 100% purity) as shown by the gains in Figure 8 (f) dropping to near 0 values.

For a more linear response to manipulations in the condenser duty, higher duty values should be chosen. However, operating at high condenser and reboiler duties will result in additional unwanted costs. The effect of the other manipulated variables and controlled variables will be investigated by using the dynamic model developed by (Harun, 2012) and (Nittaya, 2014).

4.1.3 Overall %CC as a function of disturbances

When comparing the influence of the Q_{reb}, Q_{cond}, flue-gas flowrate and flue-gas concentration on the overall capability of the absorber, the absorber is unaffected by the Q_{reb} and Q_{cond} in a steady-state environment because the assumption is that the buffer tank between the heat exchanger and the absorber for the return feed manipulates the concentration and flowrate of the lean MEA into the absorber to a fixed constant.

Therefore, the main influencers to the capture rate from the absorber are the flowrate and concentration of flue-gas entering the absorber from the power plant. Looking at Figure 9, holding the lean MEA concentration and flowrate constant along with a fixed inlet flue-gas flowrate; varying the inlet CO_2 concentration results in a relatively linear performance below 97%.

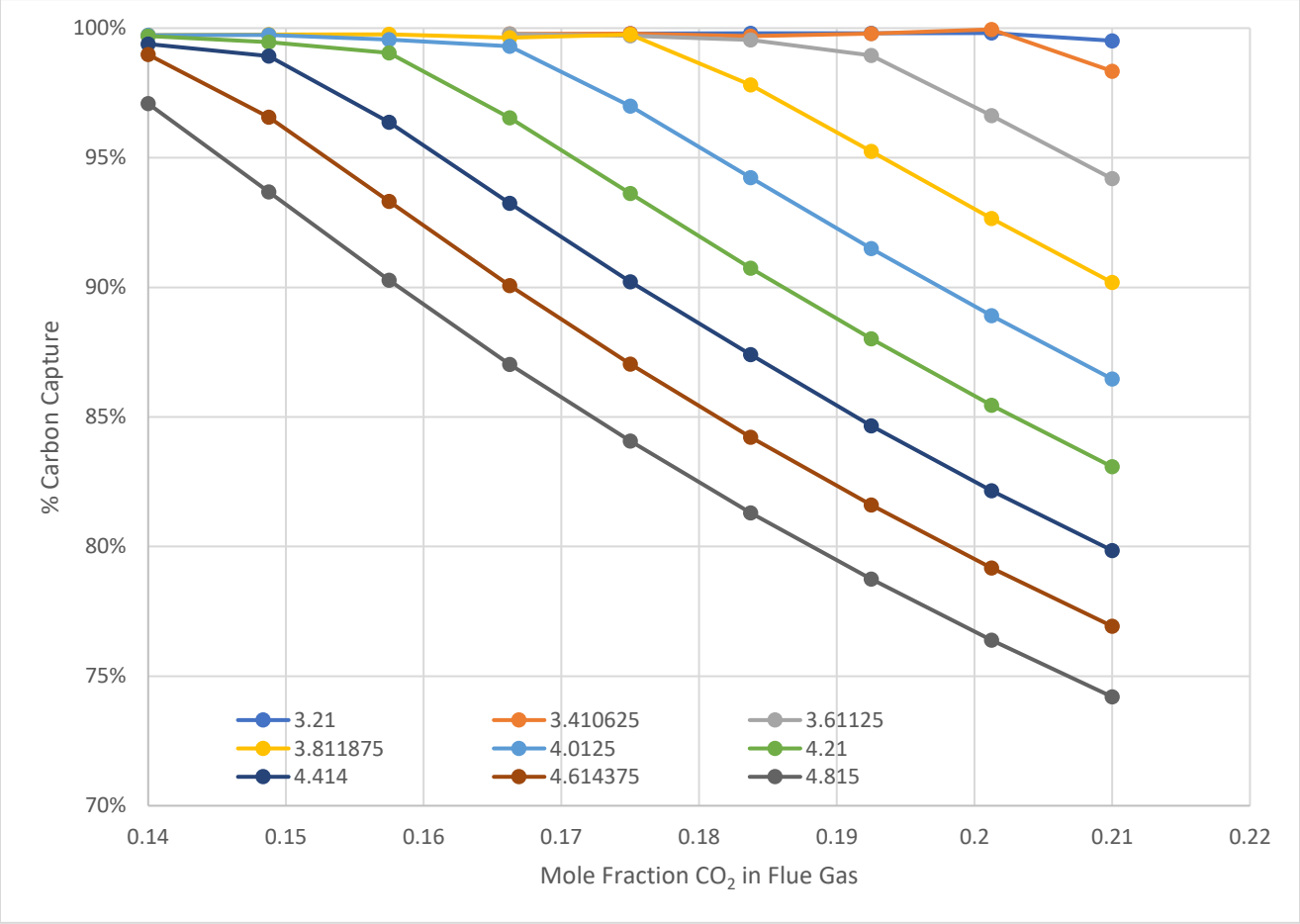

Figure 9 Change in %CC as inlet CO2 mole fraction is increased at various flowrates (mol/s)

The concentration of CO_2 was varied from -20% to +20% of the nominal value (0.175 mole frac CO_2) with each increment being 5% of 0.175.

Looking at Table 5, the difference between each iteration indicates all flowrates follow the same trend when varying the CO_2 concentration.

%CC Difference									
Flowrate/CO_2 Conc	**0.140**	**0.149**	**0.158**	**0.166**	**0.175**	**0.184**	**0.193**	**0.201**	**0.210**
3.210						0.01%	0.01%	0.00%	-0.30%
3.411					0.01%	-0.09%	0.10%	0.16%	-1.61%
3.611					-0.07%	-0.16%	-0.60%	-2.33%	-2.43%
3.812		0.02%	0.01%	-0.13%	0.13%	-1.94%	-2.57%	-2.58%	-2.48%
4.013		0.00%	-0.18%	-0.25%	-2.31%	-2.76%	-2.73%	-2.60%	-2.44%
4.210		-0.23%	-0.42%	-2.50%	-2.92%	-2.88%	-2.73%	-2.57%	-2.37%
4.414		-0.47%	-2.55%	-3.13%	-3.03%	-2.81%	-2.74%	-2.51%	-2.30%
4.614		-2.42%	-3.25%	-3.25%	-3.02%	-2.83%	-2.62%	-2.43%	-2.25%
4.815		-3.41%	-3.40%	-3.24%	-2.96%	-2.78%	-2.55%	-2.36%	-2.18%

Table 5 Change in %CC as inlet CO_2 mole fraction increases at various flowrates

As the concentration of CO_2 in the inlet stream is increased, the change in %CC increases before decreasing for all the flowrates. The change in the rate at which the %CC decreases with the increase in inlet CO_2 concentration decreases (after the initial drop) at a slower rate indicating an approach towards linear response as the concentration increases. This is attributed to the fact that as the amount of CO_2 entering the absorber increases, the MEA is able to capture additional amount of CO_2. Since the amount of MEA entering the absorber is fixed, the MEA will reach a saturation point beyond which any additional CO_2 entering the system will pass through the absorber leaving through the vent as they cannot be absorbed by the MEA. On the other hand, as the system is starved of CO_2 at low inlet CO_2 concentrations (varies at different flue-gas flowrates) with excess MEA flowing through the absorber, almost all the CO_2 is captured, and the change is only witnessed beyond a certain concentration at each inlet flue-gas flowrate.

This work involves manipulating the power generated by the power plant. As the source of power generation is coal, the concentration of the CO_2 generated from coal will remain within a relatively small range. The flowrate of flue-gas generated will depend on the power generated from the power plant. As additional power is generated to supply the demand, additional flue-gas is generated fluctuating the flowrate of flue-gas throughout the day with a much larger range in comparison to the inlet CO_2 concentration. Figure 10 below represents the change in %CC, holding the inlet CO_2 concentrations constant and increasing the inlet flue-gas flowrate from -20% nominal value to 20% nominal value with each increment being 5% each (of the nominal value). The trends are similar to those of holding the inlet flue-gas flowrate fixed and varying the inlet CO_2 concentration. At first, when the flowrate is -20%, there is very little mass of CO_2 entering the carbon capture system (CCS) which leads to almost all the CO_2 being absorbed by the MEA passing the absorber. Then as the flowrate begins to increase, allowing for additional CO_2 to enter the absorber, some of the CO_2 manages to pass through the absorber and leave uncaptured.

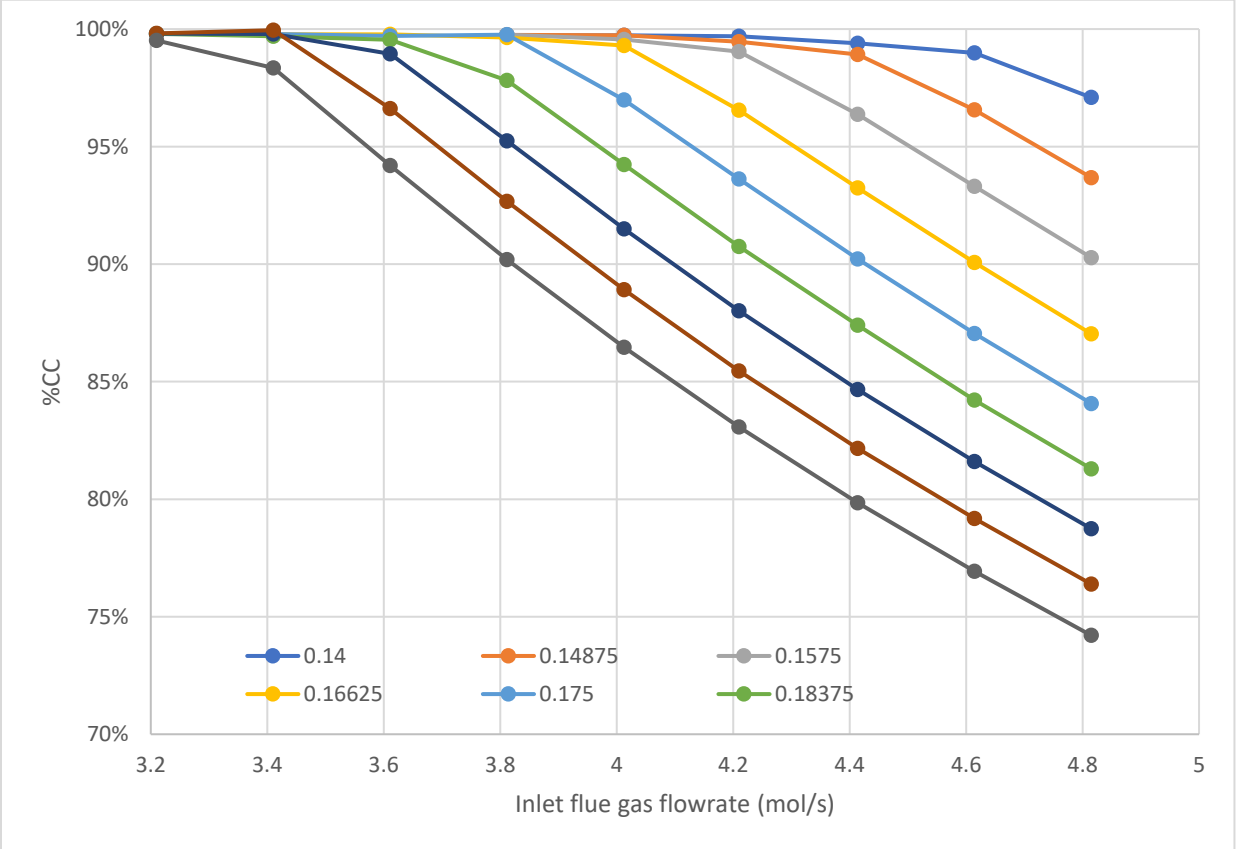

Figure 10 Change in %CC as inlet flue gas flowrate increases at various inlet CO2 concentrations

The gains for the chart above are displayed below in Table 6. The trend follows very closely to that of the previous table. The change in the gains first drop to incorporate the additional CO_2 in the system, once the MEA's capability in absorbing CO_2 approaches a maximum, a smaller and smaller portion of the additional CO_2 is absorbed by the MEA.

%CC Difference									
CO2 Conc/Flowrate	**3.210**	**3.411**	**3.611**	**3.812**	**4.013**	**4.210**	**4.414**	**4.614**	**4.815**
0.140					0.00%	-0.04%	-0.31%	-0.41%	-1.89%
0.149					-0.01%	-0.28%	-0.54%	-2.36%	-2.88%
0.158					-0.21%	-0.51%	-2.67%	-3.06%	-3.04%
0.166			0.00%	-0.14%	-0.33%	-2.76%	-3.30%	-3.18%	-3.03%
0.175		0.00%	-0.08%	0.05%	-2.77%	-3.37%	-3.41%	-3.17%	-2.97%
0.184		-0.10%	-0.15%	-1.73%	-3.59%	-3.49%	-3.34%	-3.18%	-2.93%
0.193		-0.01%	-0.85%	-3.70%	-3.74%	-3.49%	-3.36%	-3.06%	-2.86%
0.201		0.14%	-3.33%	-3.96%	-3.76%	-3.46%	-3.29%	-2.98%	-2.79%
0.210		-1.17%	-4.15%	-4.01%	-3.72%	-3.39%	-3.23%	-2.92%	-2.72%

Table 6 Change in gains as inlet flue gas flowrate increases at various inlet CO_2 concentrations

This indicates that the nominal values for the inlet CO_2 concentration and the inlet flue-gas flowrate operate at the inflection point. Manipulating either of the variables in either direction can be approximated by a unique linear response. This also indicates that there is a good ratio of MEA and the amount of CO_2 entering the absorber.

4.2 Open Loop Testing

Figure 11 and 12 represent the response of the process without controllers when the flowrate of the inlet flue gas is manipulated to -10%, -5%, +5%, and +10% of the nominal flowrate.

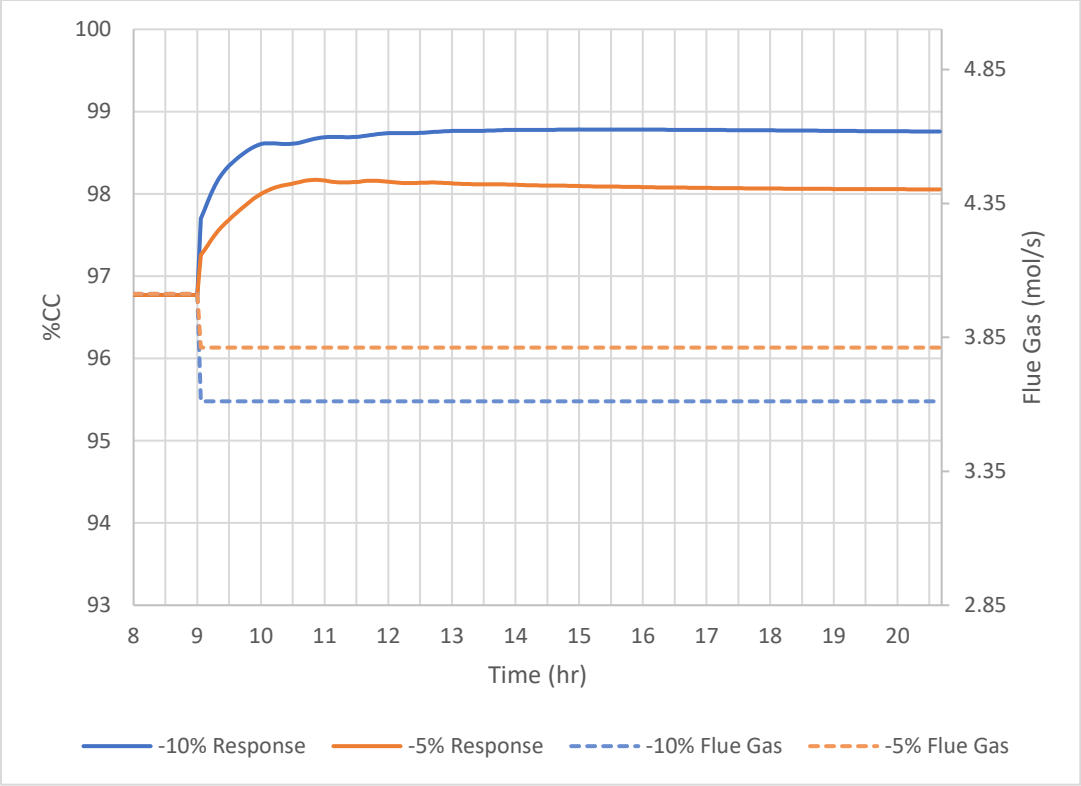

Figure 11 %CC Response to negative change in flue-gas flowrate

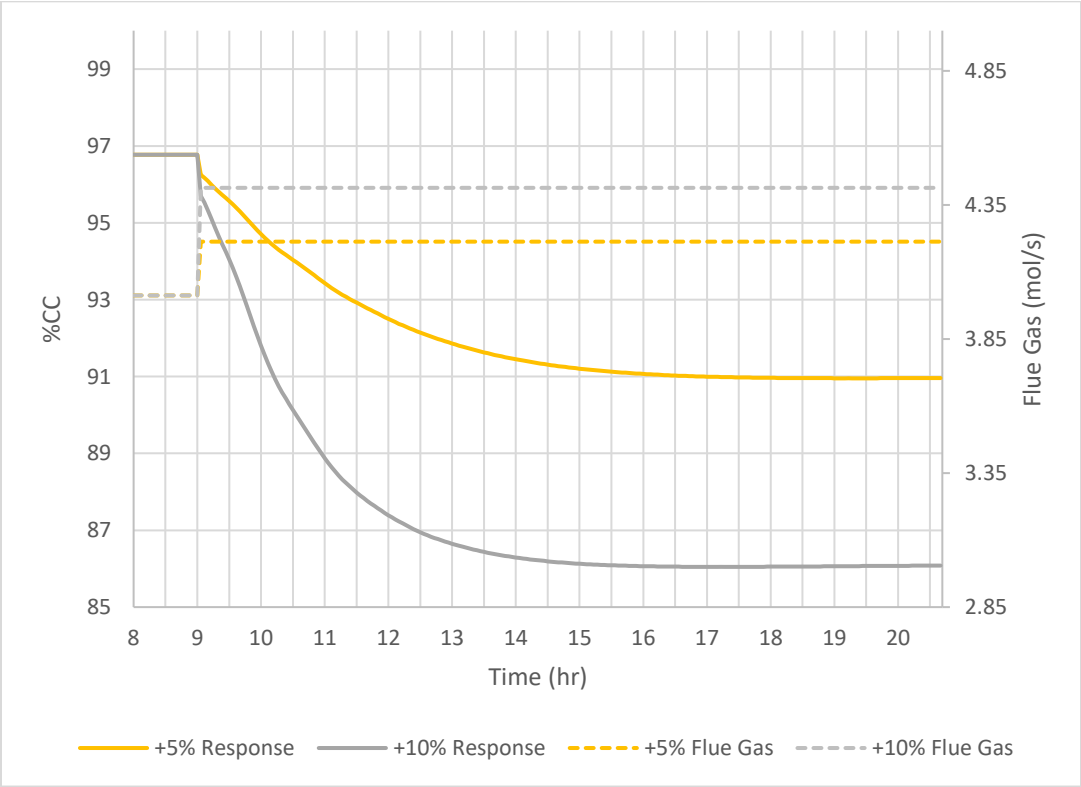

Figure 12 %CC Response to positive change in flue-gas flowrate

Figure 11 shows the response of %CC when the flue gas is reduced by 5% and 10%, respectively. Reducing the flue gas by 5%/10% results in an increase in %CC by 1.3%/2% over a ~14-hour period. As the flue gas entering the absorber is lowered without manipulating the flowrate of MEA, the increased residence time within the absorber allows the present MEA to capture additional CO_2 entering the system.

Increasing the flue-gas flowrate results in a much larger change in %CC (Figure 12). An increase of 5%/10% in the flue-gas flowrate reduced the %CC by 5.8%/10.7% respectively over a ~17-hour period. This is different from the response of %CC when the flue-gas flowrate was reduced highlighting the non-linearity of the process. Appropriate controller and tuning parameters must, therefore, be selected based on the operating region of the carbon capture process.

4.3 RGA Analysis

The process has six manipulated variables and six controlled variables, leading to a total 720 combination of pairings. The Relative Gain Analysis (RGA) (Bristol, 1966) provides insight on the interaction between the manipulated variable and the controlled variable. This analysis is used to find suitable pairings that lead to reduced interactions between the manipulated variable and the controlled variables.

Considering the non-linear nature of the process, the gains of each manipulated variable were calculated cantered around their nominal steady state values (Table 7). Several runs surrounding the nominal steady state value at various degrees of manipulation of the manipulated variables (MV) were averaged from the dynamic model (gProms) for each process gain.

CV/MV	Q_{reb} (W)	Q_{cond} (W)	Q_{tank} (W)	V1	V2	V3
%CC (%)	0.23	-0.21	-0.12	-43.64	-3.27	-3.62
Treb (K)	0.08	-0.02	-0.04	-25.09	-0.27	-1.23
Tcond (K)	2.14	-9.11	-1.40	-322.44	-7.13	-17.31
Ttank (K)	0.14	-0.04	-0.42	203.01	1.86	1.70
L2 (m)	7.11E-04	-2.68E-04	-3.72E-05	1.50	-1.33	0.02
L3 (m)	5.77E-04	8.84E-05	5.81E-05	1.69	0.03	-1.12

Table 7 Process Gains (CV/MV)

The RGA matrix is obtained by the following equation

$$\lambda_{ij} = K_{ij}H_{ij}$$

Where K_{ij} is the i-jth element of the steady state gain matrix K and H_{ij} is the i-jth element of H where $H = (K^{-1})^T$. Special note should be made that the multiplication performed here is element-by-element multiplication rather than matrix multiplication. Once the RGA matrix is obtained, the goal is to select positive values closest to one. The RGA matrix and best pairings are shown in the table below (Table 8).

CV/MV	Qreb	Qcond	Qtank	V1	V2	V3
%CC	11.49	-0.12	-6.30	-3.20	-0.36	-0.51
Treb	-8.29	-0.03	4.73	4.14	0.06	0.38
Tcond	-1.89	1.16	1.27	0.40	0.01	0.04
Ttank	-0.22	0.00	1.29	-0.06	0.00	0.00
L2	-0.07	0.00	0.00	-0.21	1.29	-0.01
L3	-0.03	0.00	0.00	-0.07	0.00	1.10

Table 8 RGA matrix and controller pairings

RGA performs best with a linear system; with highly non-linear systems, the RGA pairings may lead to different results depending on the set of steady state operation conditions surrounding the evaluation. Since the RGA only involves steady-state gains, it does not take dynamics into account.

When dealing with small manipulations around a fixed set-point or rejecting the influence of the disturbance on the process, the control structure proposed by the RGA analysis is a good choice. However, to obtain the capture schedule proposed (Figure 5) using a set of linear PI controllers is a more challenging task as the capture rates range from ~40% to ~99% due to the non-linearity of the process.

According to Wu et al. 2018 (b), being able to tightly control the reboiler temperature will lead a relatively linear interaction between the inlet flue gas flowrate and capture rates. Based on (Nittaya, 2014)'s work, an alternative control scheme was chosen as it was designed to hold the temperature of the reboiler as stable as possible. All the pairings in control are similar to the one determined

by the RGA analysis except the valve controlling the flowrate into the reboiler (V2) is used to control the temperature of the reboiler (T_{reb}) and the valve controlling the flowrate of lean MEA into the absorber column (V1) is now used to control the level in the absorber sump tank (L2). The tuning parameters estimated by (Nittaya, 2014) as well will be used as the base case for operating the controller (Table 9).

4.4 Controller Tuning

CV	MV	K_c	τ_I (sec)	Set point
L2	V1	0.5	240	0.31 m
L3	V3	0.5	60	0.32 m
T_{cond}	Q_{cond}	12	97	315.4 K
T_{tank}	Q_{tank}	40	250	314 K
T_{reb}	V2	0.5	500	388.5 K
%CC	Q_{reb}	80	250	96.30%

Table 9 PI controller gains, time constants and set points

The controlled process would have to maintain a fixed set-point in the presence of a disturbance. Considering the carbon capture process specifically, assuming that the power generated from the power plant fluctuates based on the demand; a typical disturbance is the variability in the flue-gas generated by the power plant that enters the absorber in the CCS plant. In order to see the capability of the controller, a 5% and 10% increase and decrease in the nominal flue-gas flowrates were tested. Figures 13 and 14 show the performance of the controller in maintaining a fixed %CC set-point in the presence of disturbance (-10%, -5%, +5%, and +10% flue-gas flowrates).

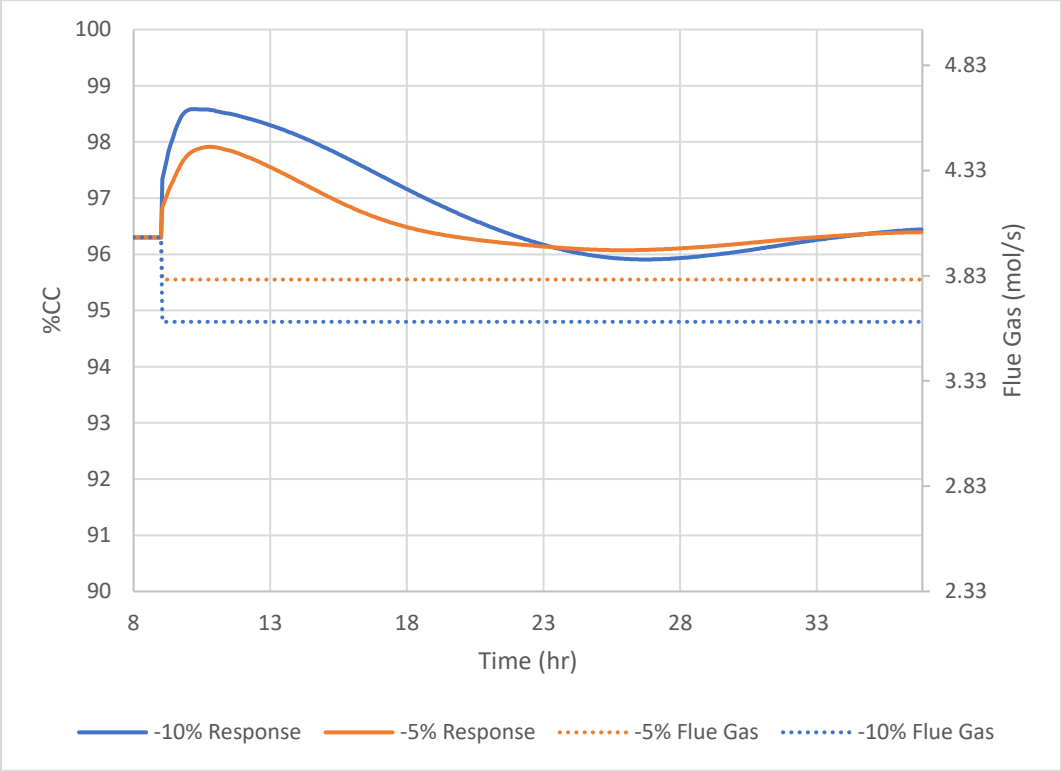

Figure 13 %CC Response to negative change in flue-gas flowrate with controller

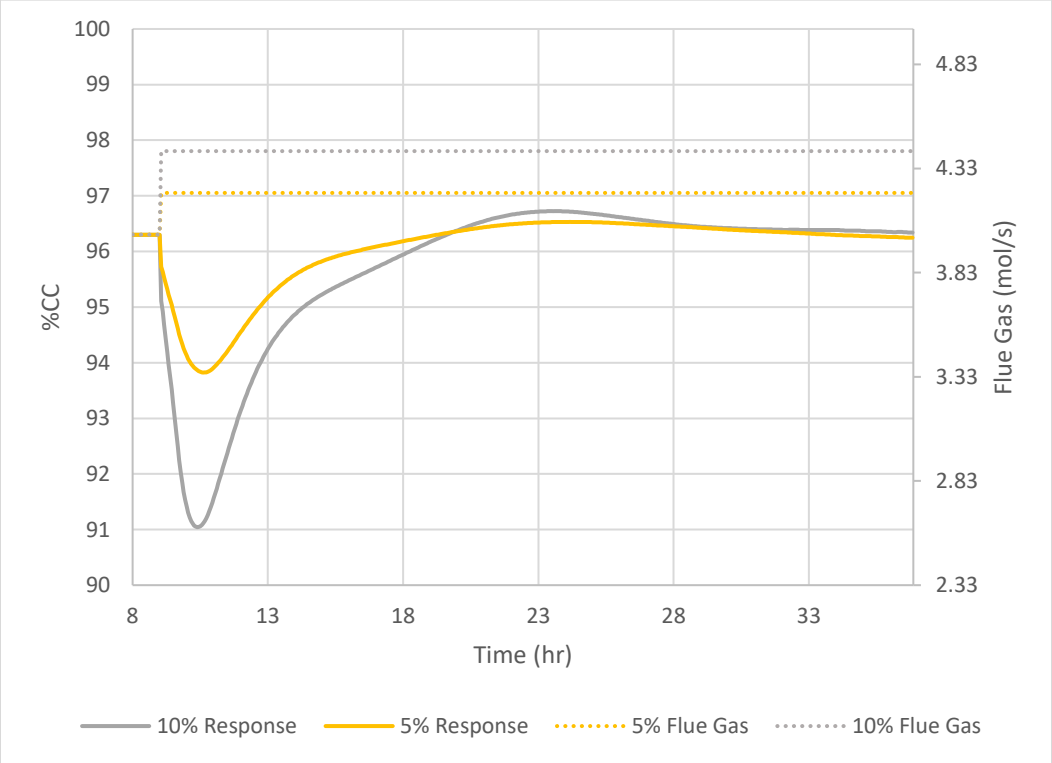

Figure 14 %CC response to positive change in flue-gas flowrate with controller

Figure 14 shows the response of %CC to a negative step decrease in flue-gas flow rate as the controller adjusts the manipulated variables to maintain a fixed capture of 96.3%. A reduction in the flue-gas flowrate allows additional contact time between the CO_2 and the MEA as well as a lower amount of CO_2 overall being present in the absorber resulting in an increase in the %CC at first. The controller adapts and manipulates the associated variables to lower the %CC back to the original set-point. A decrease of 5% in the flue-gas flowrate results in an increase of ~1.5% CC before the process is able to reduce the effect of the decreased flowrate and a 10% decrease leads to an increase of ~2.2% CC from the nominal value before approaching the desired set-point. Both fluctuations resulted in the process approaching initial steady state values after 35+ hours which is longer than the process approaching steady-state without the controller.

It is important to note that an initial decrease in the disturbance (inlet flue-gas flowrate) by 5% resulted in an increase of %CC by 1.5% and an additional decrease of 5% in the disturbance resulted in an additional increase of 0.7%. This is due to multiple factors including the process non-linearity and the maximum capture capability of the process. As the capture rates approach 100%, additional decrease in the amount of CO_2 present will yield lower additional gains on the %CC.

A 5% increase in the flue gas lowered the %CC by ~2.3% and a 10% increase in the flue-gas lowered the %CC by ~5.3% before moving back to the original set-point. The additional 5% increase of the disturbance resulted in a larger drop of %CC (3%). Both runs approached steady state around ~29 hours after the disturbance was introduced which is significantly lower than when the flowrate (flue-gas) was decreased. This is also attributed to the non-linearity in the process. additional influx of CO_2 into the process reduces the %CC as the contact time between the CO_2 and the MEA reduces. As the process is not constrained by the upper limit of capture, the additional increase in the disturbance results in an even greater drop in the %CC.

This is vastly different from comparing the decrease in the flue-gas flowrate. The non-linearity of the process effects the time constants of the variables as well due to the usage of linear PI controllers. In the case of decreasing flue-gas flowrate runs, the increase of %CC was by ~1.5 – 2.2% resulting in the manipulation of the associated manipulated variables according to the gain

resulting in a slower response than anticipated. As the process dynamics change over time (along with the MV changing to lower the %CC), the effect of the MV on the CV changes as well resulting in an overshoot of the target adding to the time required to approach steady state. Whereas analysing the response of increasing flue-gas flowrate on %CC, the %CC is capable of lowering based on the amount of disturbance and is not capped (relatively). The drop in %CC manipulates the MV more "aggressively" to make up the difference between the set-point and the %CC quicker resulting in lowering the time needed to approach steady state.

As the model solver (DASOLV) in gProms v5.1 was different from the version in gProms v3.2, a test was performed to compare the results using the different versions. A servo control test was performed in which the %CC set point was changed from 96.3% to 90%. The results shown below in Figure 15 (left) are similar to that of the original model developed by Harun (2012) and Thanita (2014) (Figure 15, right).

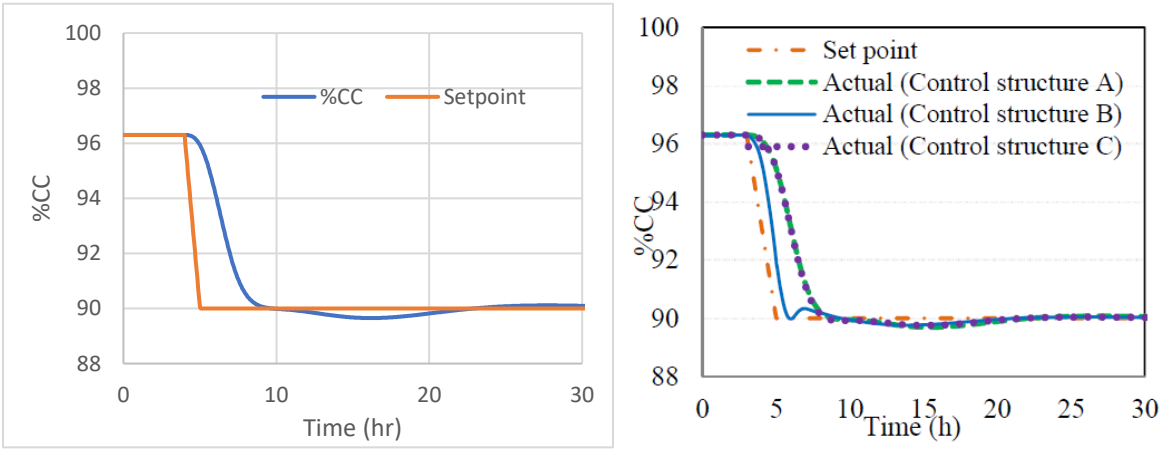

Figure 15 %CC Response to %CC set-point changes

The controller configuration chosen was "Control Structure C" from Thanita (2014) that pairs MV and CV according to Table 9 as the configuration was designed to maintain a stable reboiler temperature which helps a linear PI controller work for a wider range of set-points. The %CC set-point was dropped from 96.3% to 90% in an hour which was the same case in Thanita's run. The response of controller C from the model implemented on gProms v3.2 is the same as the response on gProms v5.1. The process in both cases takes about 25 hours to approach near steady-state at the new set-point. A response lag of ~1 hour is important when trying to follow a constantly

changing set-point. As the set-point constantly changes direction and rate, this does not mean that the process will be following the same schedule with ~1-hour delay. It may not even be able to achieve the desired set-points as the set-points may change direction as seen in the upcoming analysis. Nevertheless, it appears from these servo control tests that this CCS process is flexible, in that it can move smoothly from one steady state to another one.

4.5 Proposed Capture Rate Schedule

The %CC schedule proposed by Alie's work (2013) and Professor Douglas (2018) (Figure 5) was broken into a series of ramps with each ramp being half hour (Figure 16). Start-up and shutdown processes are not considered in this schedule. This is an important assumption as the nominal value of the capture rate is 96.3% which is very high. As the amount of CO_2 captured by the absorber approaches 100%, the harder it becomes for the absorber to absorb additional amounts of CO_2.

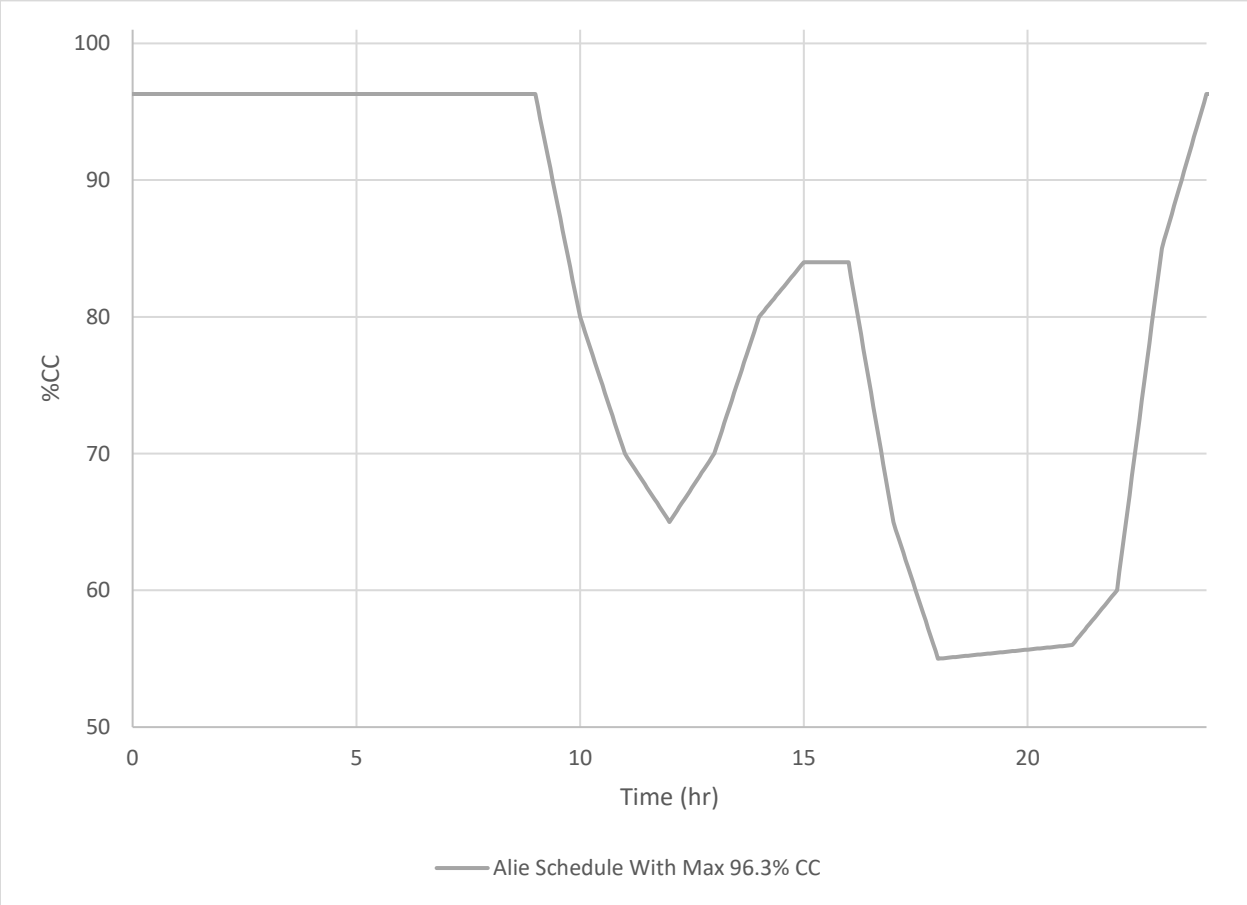

Figure 16 Proposed %CC schedule implementation

The aim of this work is to investigate the dynamic performance of the MEA absorption in the face of various disturbances. The disturbances that impact the process are both external load disturbances in the form of flue gas variations as well as operator-imposed set-point changes. One can imagine that flue gas variations will occur due to dynamic changes in the power plant. Operator imposed set-point changes are envisioned in the case where the utility wishes to change the amount of CO_2 captured during the day. For example, during periods of high electricity demand it may be advantages to reduce the amount of CO_2 that is captured and vice versa.

A decentralized set of linear controllers on a highly non-linear process as the process is deviating away from the nominal values. The schedule ranges from 96.3% to 55% with erratic changes in between resulting in a lack of time for the process to stabilize at those set points. The schedule was extended with a fixed capture rate of 96.3% after the 24-hour mark in all the cases to observe the process approaching and stabilizing at a high capture rate set-point.

4.6 Controller Response to Large Set-point Changes

The first schedule implemented on the process was a series of simple changes in the set-point resembling the proposed schedule in Figure 5. The goal behind this test was to observe the process under a large set-point change without the influence of flue-gas fluctuation. Rather than having random fluctuations of the set-point, every change implemented was derived observing the minimum and maximum of the proposed operating schedule every time the schedule changes direction (from negative slope to positive slope or vice versa).

The process response (Figure 17) can be compared against two series of set-points, one being the set-point implemented on the system and the other being the proposed capture rate (Figure 5).

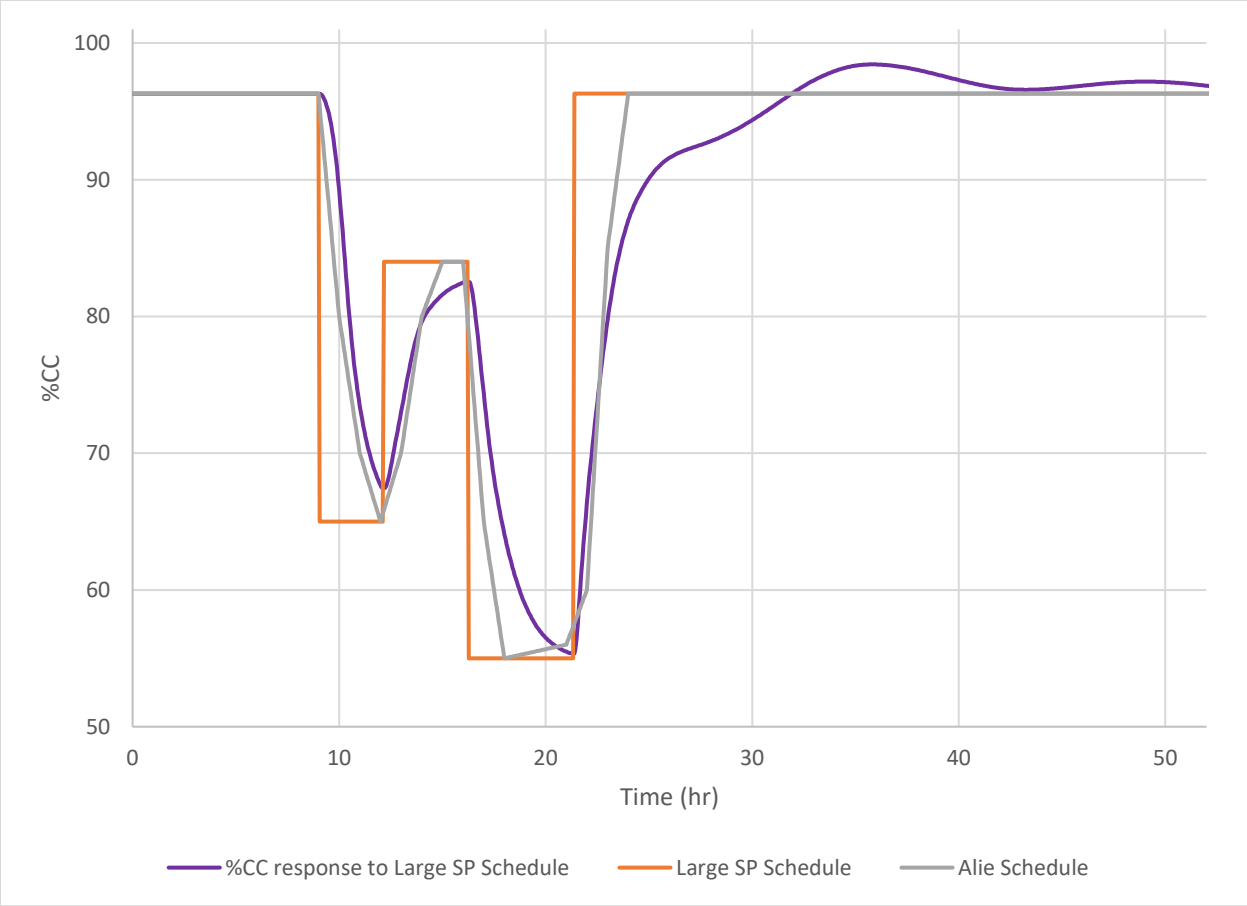

Figure 17 Process response to large set-point changes

When comparing to the instantaneous %CC set point changes, the process performs relatively poorly. This is because the set-point changes are instantaneous, and the process dynamics cannot react to such erratic changes. Although the response cannot react quickly to instantaneous set point changes, able to maintain stability with the large set-point changes, and reach the desired set-point desired had there been enough time for the process to reach a new steady state. Generally, in highly non-linear systems, the gains change with different manipulations of the set-point leading to different gains by the monitored variable (%CC).

On the other hand, when comparing the response to the proposed operating schedule (Figure 5), the response follows a trajectory acceptable to the requirement all the way up to the end. While the response is not ideal, it is intriguing that the process dynamics allow the response to closely imitate the desired schedule. The process performs better when approaching set-points that are

lower than the current (%CC at time t) in comparison to the set-points that are higher. The last and largest step change from 55% to 98.6 shows the process non-linearity as the response follows a similar pattern to the previous step changes at first, followed by a non-linear trajectory when approaching close to the desired set-point. Cycling through this set-point on a regular basis may lead to slight variations in the response as the process takes 20+ hours to stabilize at the nominal steady-state value again (to start the cycle for the following day).

4.7 Controller Response to Proposed Schedule

Once it was determined that the process was able to react to various large set-points changes, albeit, with a relatively large lag, the set-points were converted to a series of ramps to mimic the schedule proposal in Figure 5. On a commercial scale, this is the kind of schedule that would be implemented. This test was conducted to see the performance of the linear PI controller on the scheduled set-point. Figure 18 shows the schedule implemented in gProms which is very similar to the proposed schedule (Figure 5) as well as the associated process response to the set point schedule.

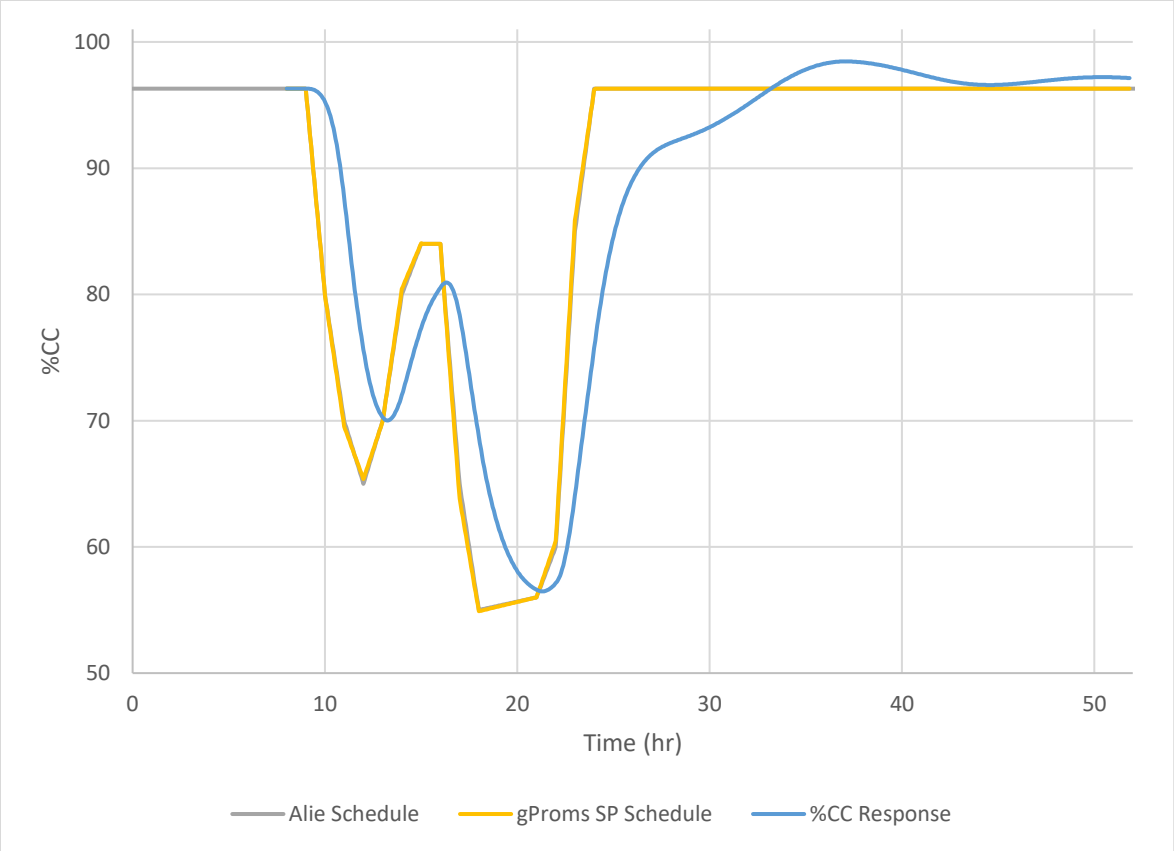

Figure 18 Process response to ramp set point changes

Although, the process response to that schedule is rather underwhelming, it generally is able to track the changes in the set-point. Similarly, to the previous test, the process performs better when obtaining lower capture rates in comparison to capturing higher rates. In real world applications, this trying to achieve the desired capture rates would be tedious if the set-points are adjusted so that the process is able to meet the desired rates. This may work if we assume that the power generation is fixed.

4.8 Controller Response to Shifted Schedule

Assuming that the demand of power from the fleet is expected to follow a similar pattern on average throughout the year and knowing that there is a lag of approximately 0.5 hour on the process response to the schedule, the set-points can be shifted so that the process response follow's the desired schedule as shown in the figure below (Figure 19).

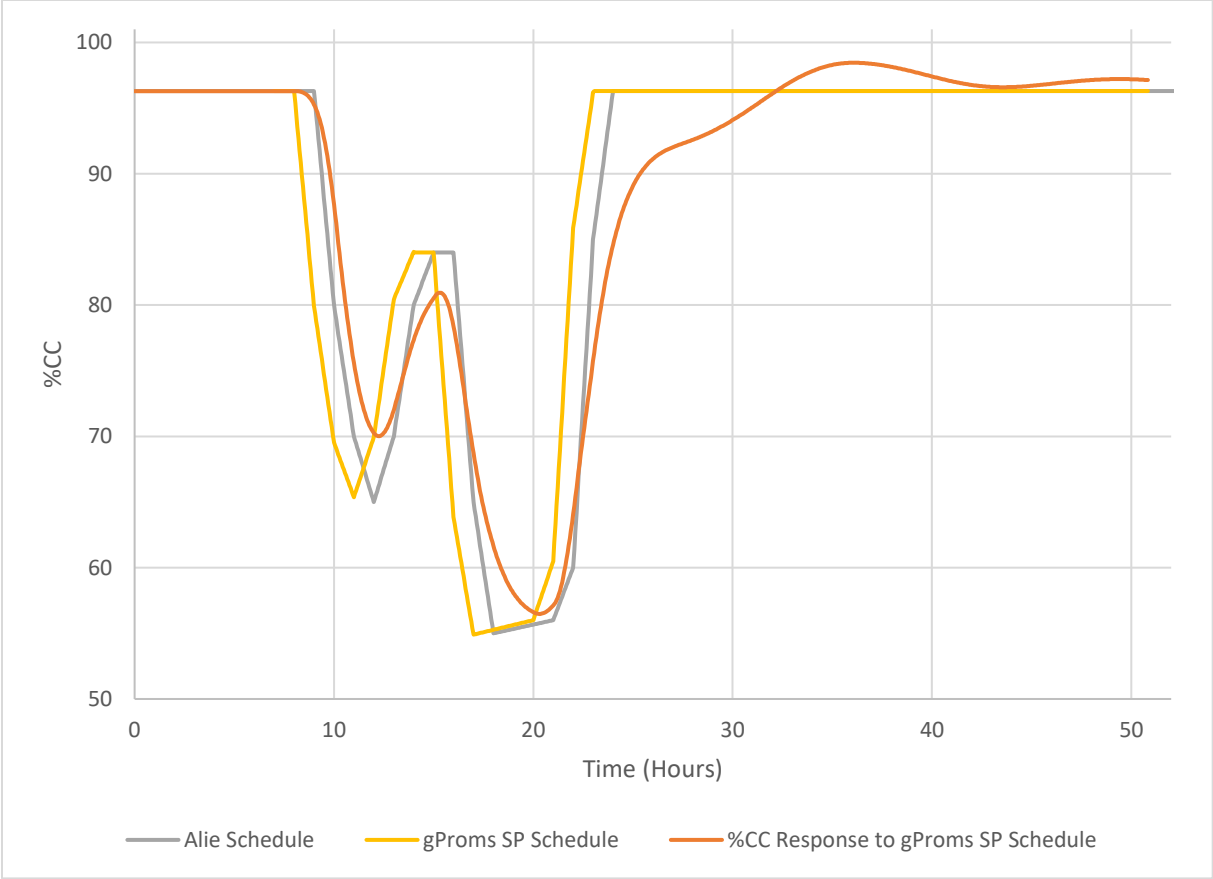

Figure 19 Process response to predicting set-points an hour early

In this scenario, the set-points mimic the schedule but are shifted by 0.5 hours. The process response to the set-points is the same as the response to the previous case. However, this response is a lot more desirable when compared against the proposed operating scheme (Figure 5). The process is still unable to reach the minimum set-points (similar to the previous case) but is following the trajectory with minimal delay.

Typically, to improve the controller performance at this stage is to tune the controller parameters based on tuning guidelines. However, there is one factor that is to be accounted for in the carbon capture rates. This schedule was derived to improve the capacity factor of the Austin power plant (IEEE Transactions on Power Systems, 1999) which means that the power plant can operate at a variable rate throughout the day. This results in varying flue-gas generation based on the amount of power generated (Figure 18).

4.9 Flue-gas flowrate disturbance

The variation in power generation was converted into percent difference every half hour. The same variation was implemented to the flue-gas flowrate resulting in a disturbance to the system (Figure 20). This disturbance occurs along with the set-point changes taking place. Increasing the flue-gas into the absorber will yield a lower capture rate as there is less time for the MEA to come in contact with the passing CO_2. As the power output of the Austin power plant increases when the demand increases, so does the flue gas.

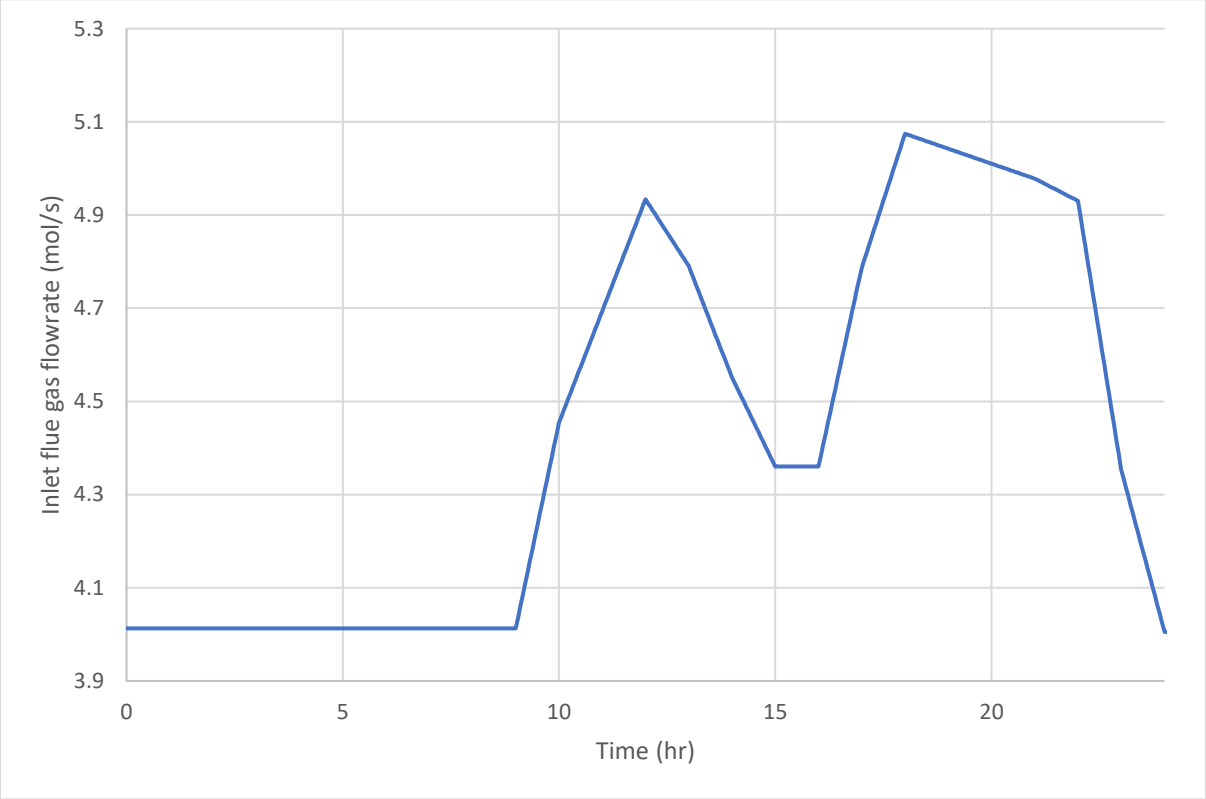

Figure 20 Implementation of flue gas disturbance in gProms

4.9.1 Open loop response to flue gas disturbance

To evaluate the extent of variation in capture rates caused by the disturbance, the flue-gas flowrate fluctuation was implemented in the carbon capture system without the influence of controllers, i.e. a so-called open loop test. The implementation of the disturbance in gProms was similar to that of the proposed schedule as a series of ramps (half hour each). The disturbance ranges from 4.01 mol/sec to 5.07 mol/sec.

As expected, it can be seen in Figure 21 that the disturbance resembles the proposed schedule pattern (Figure 5).

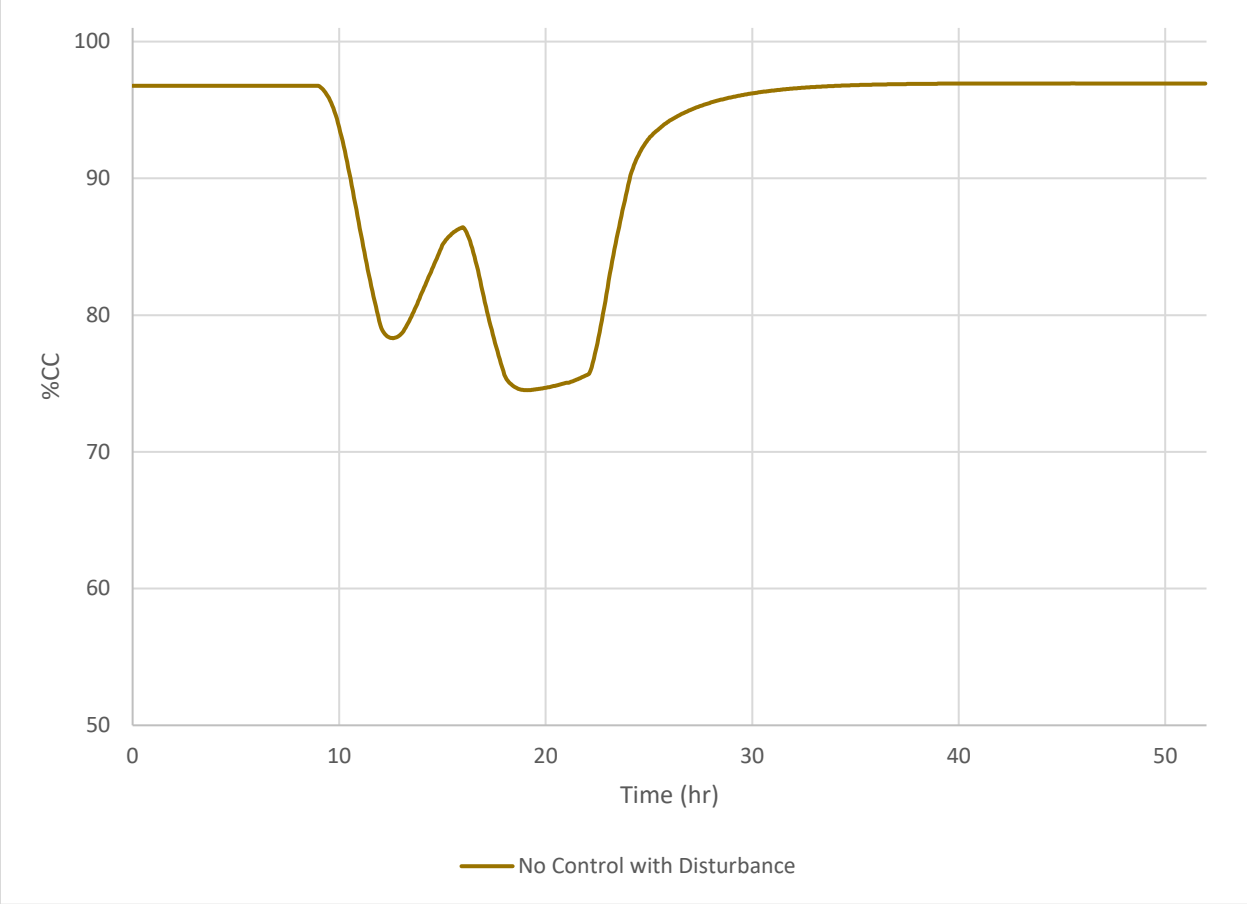

Figure 21 Open loop response to flue gas disturbance

This is beneficial in achieving a better response from the controller, as this disturbance aids the process in achieving the desired set-points. The disturbance results in the system deviating from the nominal value of 96% down to 74%.

4.9.2 Closed loop response to disturbance

The goal of the proposed schedule is to minimize energy costs of the capture system allowing for additional power generation while maintaining capture requirements improving the overall efficiency of the power plant with a carbon capture system. Trying to capture a fixed amount of

CO_2 from the varying power generation schedule will require much higher energy than varying the capture rates along with the disturbance during peak hours (Figure 32)

To capture a fixed capture rate, the Q_{reb} must be increased significantly in order to counter the effect of the increase in flue-gas flow rate. The controller is unable to reject the disturbance and keep a fixed capture rate of 98.5% resulting in poor performance of the controller (Figure 22).

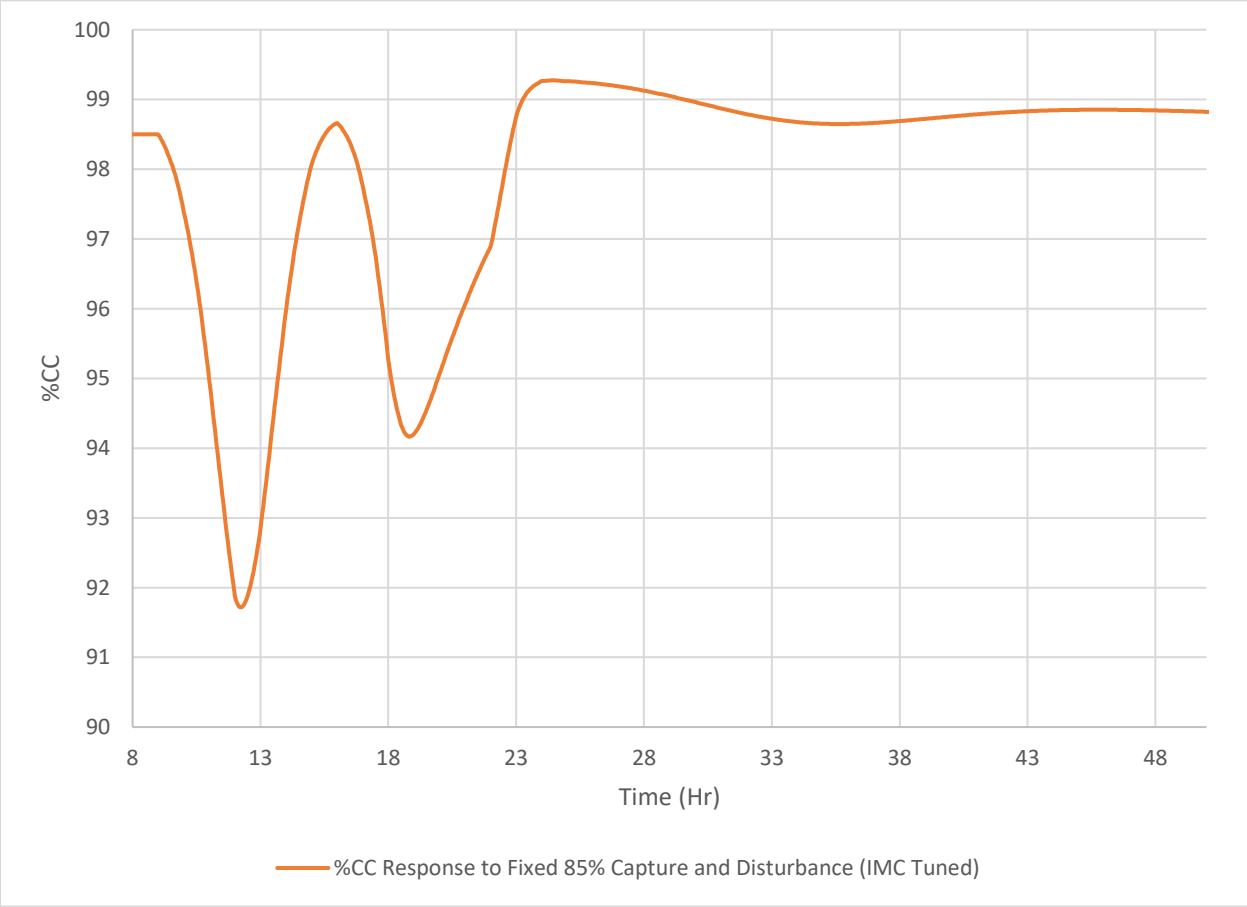

Figure 22 Closed loop response to flue gas disturbance

4.9.3 Closed loop Response to Proposed Schedule with Flue Gas Disturbance

Combining the flue gas disturbance with the set-point changes was performed on gProms by changing the associated parameters simultaneously at each interval. The response of the system in the presence of the disturbance and the schedule is shown in Figure 23 below.

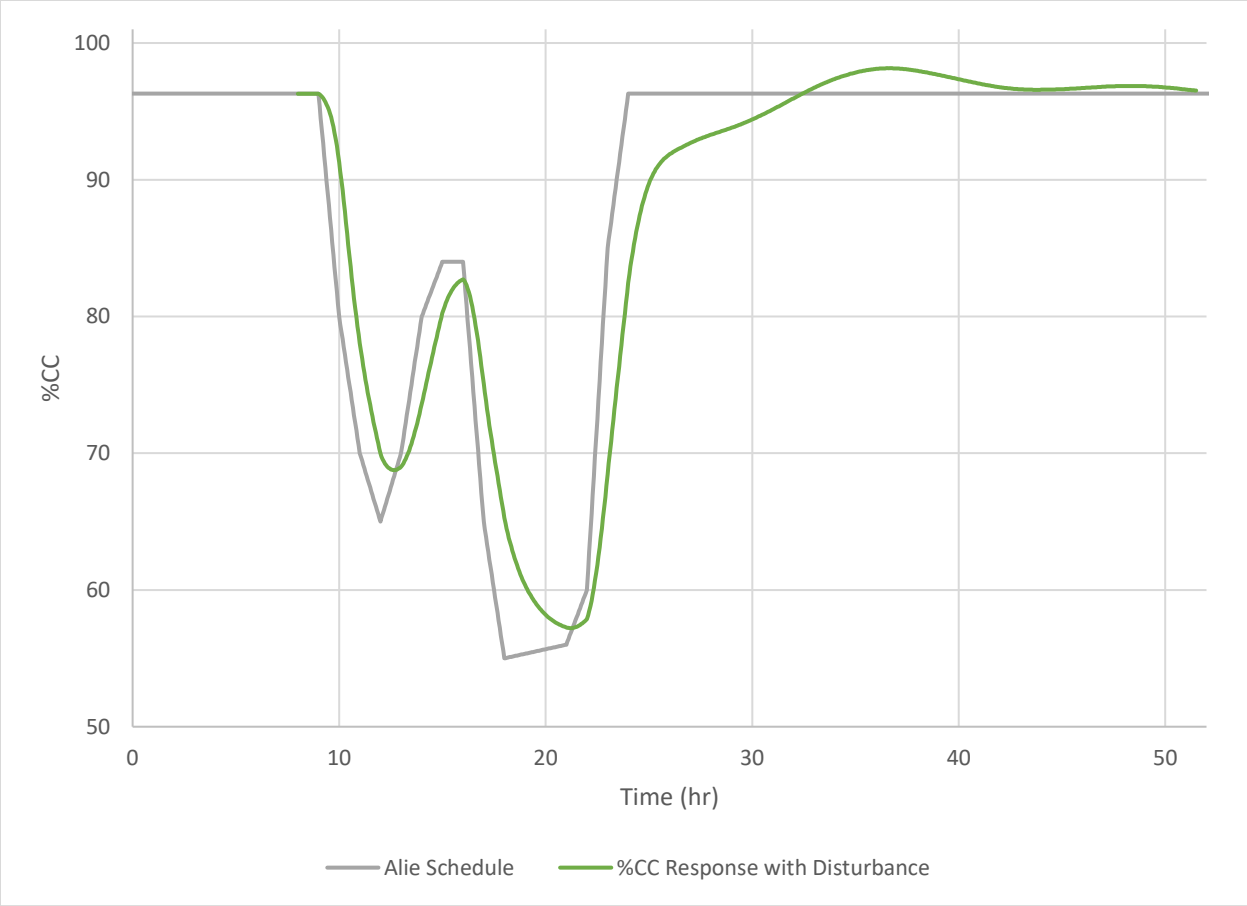

Figure 23 Closed loop response to %CC schedule with flue gas disturbance

In comparison to trying and maintaining a fixed capture rate, the performance of the controller on the set-point schedule is improved significantly, the lag as well as the difference between the minimum of the set-point and the process response minimum is reduced. This reduces the necessity of relying on predicting the disturbance in the flue-gas flowrate. As seen in Figure 23, there is still quite a bit of room for improvement in the performance of the controller throughout the entire time-period.

4.10 Re-tuning Controllers for specific application

In order to improve the performance of the controller, a more aggressive change needs to be made when the manipulated variables are changed (Qreb in this scenario). A rule of thumb tuning map from (Cooper, 2004) is used as a guideline to tune the controller. The time-constant for the Q_{reb}/%CC controller was changed from 250 (seconds) down to 100 (seconds) significantly

increasing the aggressive behaviour of the controller. The figure (Figure 24) below represents a typical approach in tuning the performance of PI controllers (Cooper, 2004).

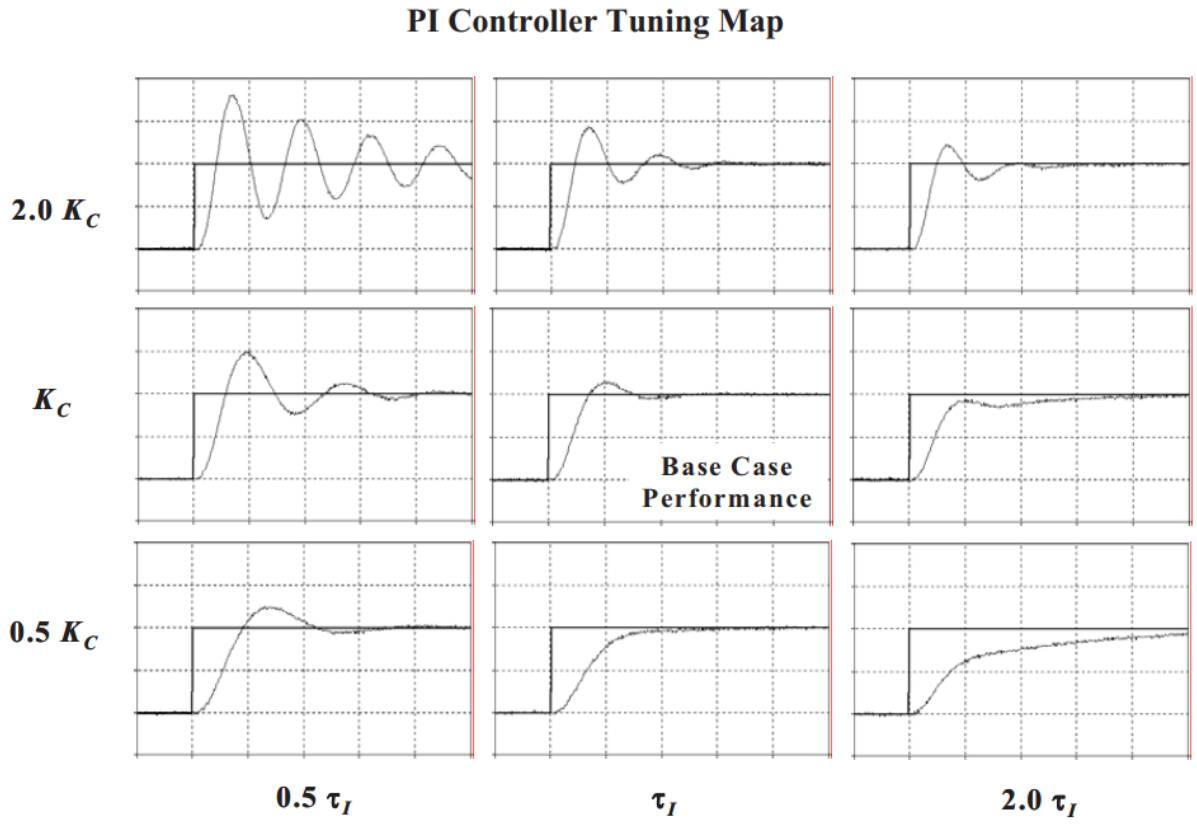

Figure 24 PI Controller Tuning Map ((Cooper, 2004)

4.10.1 Re-tuned Controller Response to Fixed Set-point with Disturbance

Implementing the newly tuned controller on a fixed carbon capture rate, yields in better response to the fluctuation in the flue-gas flowrate as seen in Figure 25. However, the controller's ability to reject disturbance is still poor. There is a lot of room for improvement suggesting alternative controllers be implemented when focusing on disturbance rejection such as model predictive controllers.

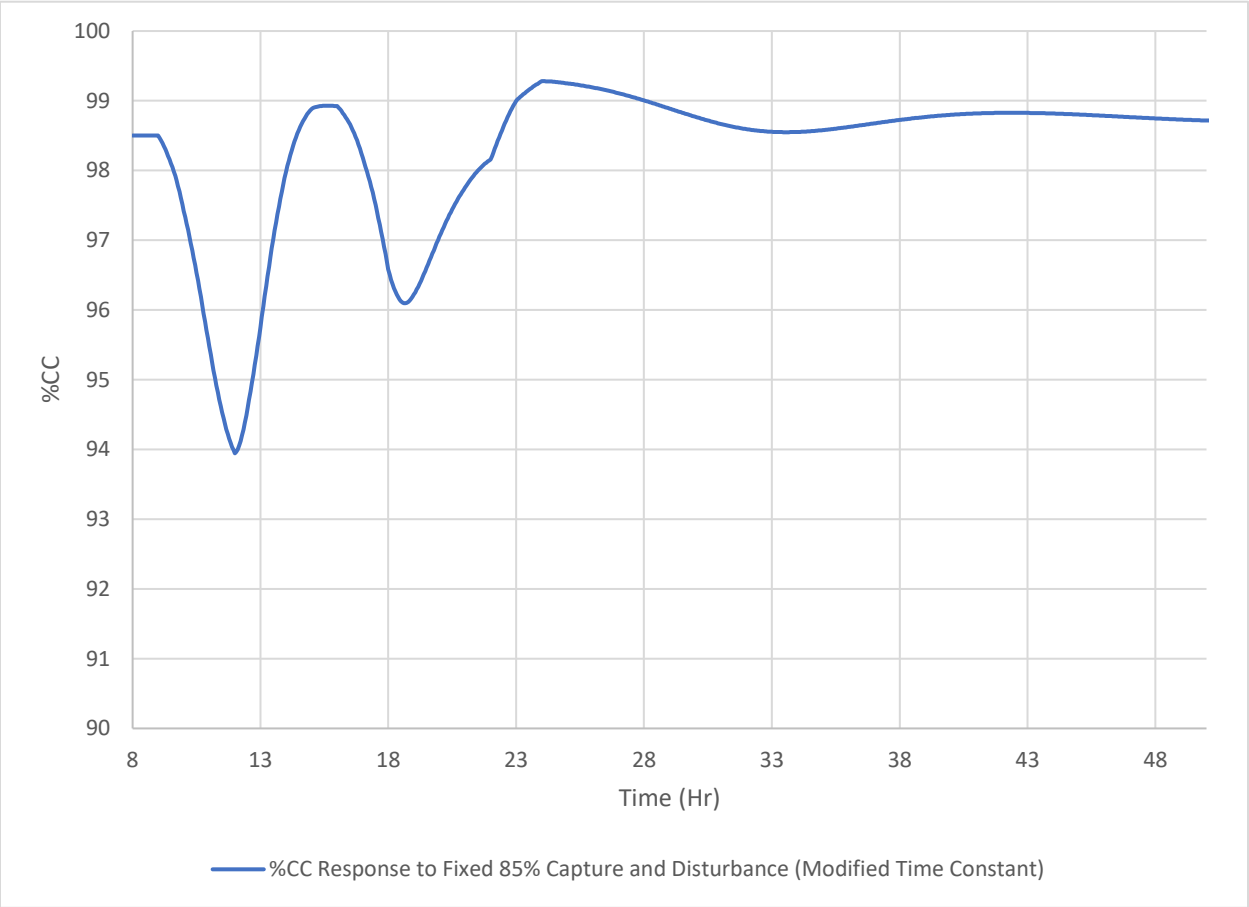

Figure 25 Closed loop response to fixed set-point with flue gas disturbance and re-tuned controller parameters

The next test conducted was to implement the schedule along with the disturbance in flue-gas flowrates with the updated time-constant controller (Figure 26). The lowered time constant on the controller leads to a larger response from the manipulated variable when a disturbance occurs. This helps in reducing the lag followed by the process response. The downside to tuning a controller to be more aggressive is likely overshooting and extended oscillations before the process reaches steady state.

4.11 Re-Tuned Controller Response to Proposed Schedule

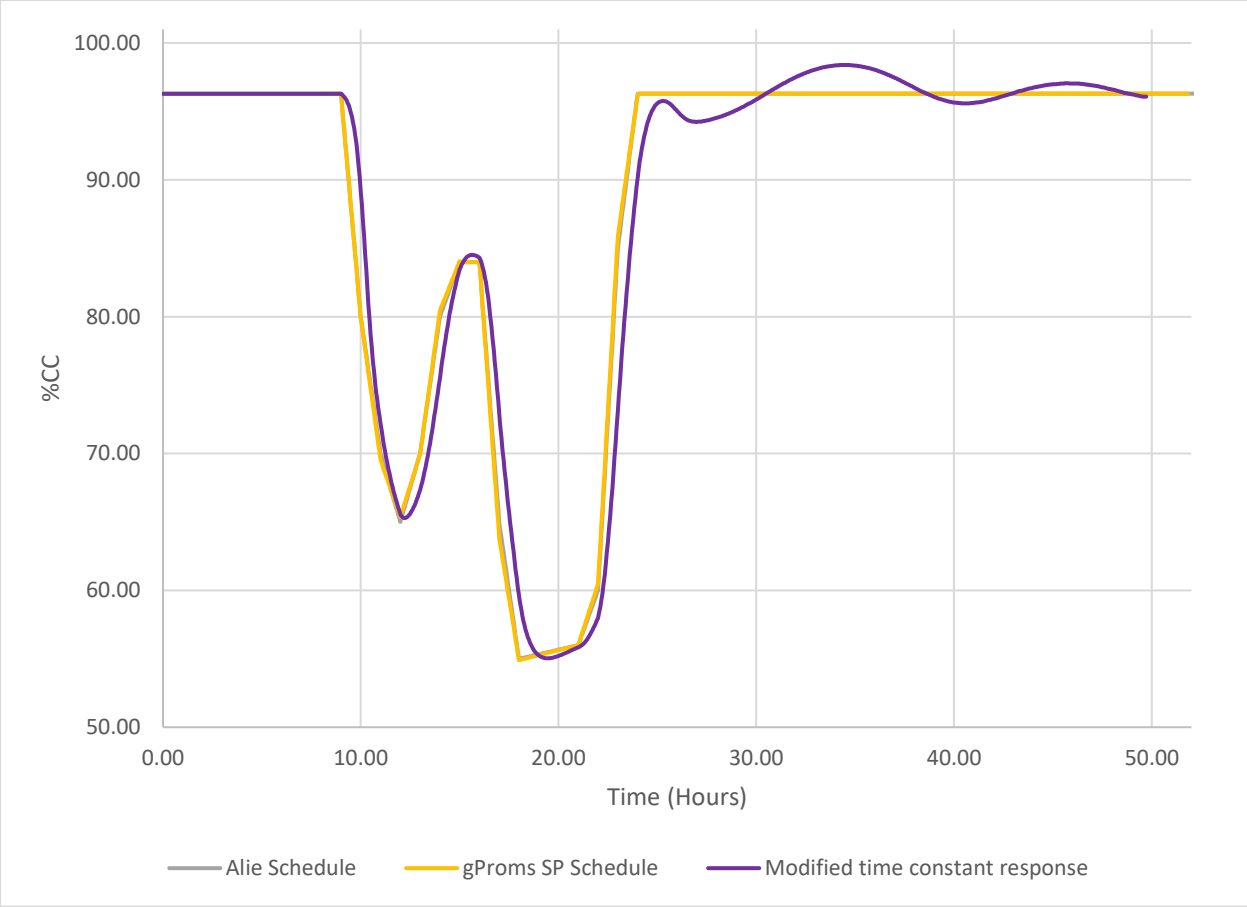

Figure 26 Process response to ramp set-point with updated controller parameter and disturbance

Looking at Figure 26, the re-tuned controller was able to incorporate the disturbances and was able to achieve the desired set-points with acceptable lag. The performance of this controller on the process indicates the feasibility of using PI controllers on this process.

The re-tuned parameters work well with the current schedule, however, an adjustment to the schedule will likely require re-tuning of the controller parameters. For example, changing the nominal steady state value from 96.3% to 98.5% (increasing the rate at which the %CC will have to drop in order to achieve 69.5% by the 11th hour) will yield a different response. This is shown by the comparison of the two cases mentioned above. The set-point is changes as it would in the proposed schedule with one starting from 96.3% and the other 98.5% down to 69.5% at the 11th hour and held constant at 69.5% until the process reaches steady state.

4.12 Effect of Set-point Magnitude on Controller Performance

The Figure (27) below represents the schedule implemented for the other runs. The %CC set-point changes from 96.3% at the 9th hour down to 69.5% at the 11th hour.

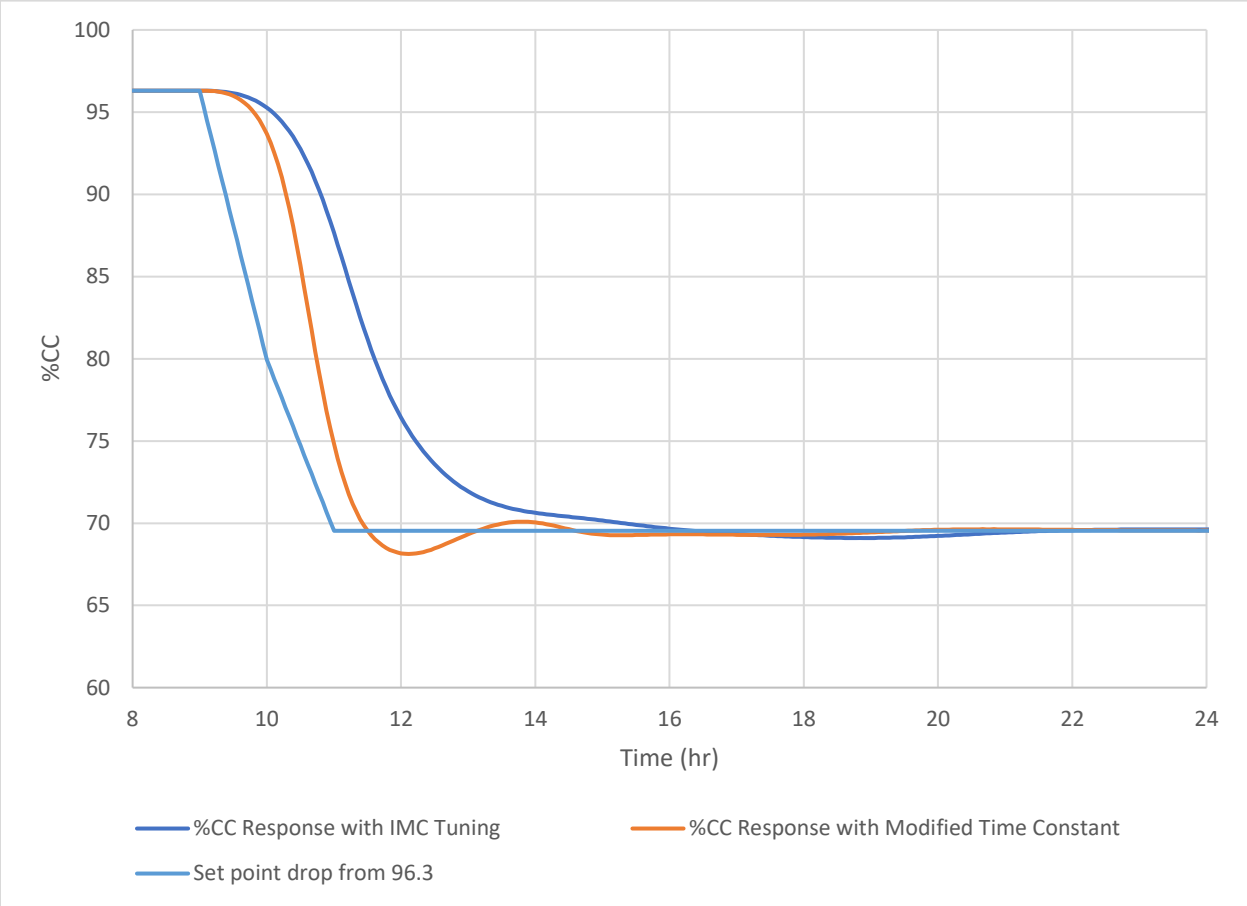

Figure 27 IMC tuned and modified controller response to set point changing from 96.3% to 69.5%

The IMC tuned controller performs smoothly achieving close to steady state around the 21st hour with almost zero overshoot. The modified controller is able to achieve near steady-state response around the 17th hour with some overshoot of about ~1.5% below the desired set-point. This falls in line with the tuning guidelines used to modify the controller response where lowering the time constant results in a much more aggressive response, lowering the lag of the process with the drawback of an increased overshoot and oscillations.

Changing the nominal steady-state value to 98.5 results in a larger drop to achieve the same desired set-point of 69.5% at the 11th hour (Figure 28).

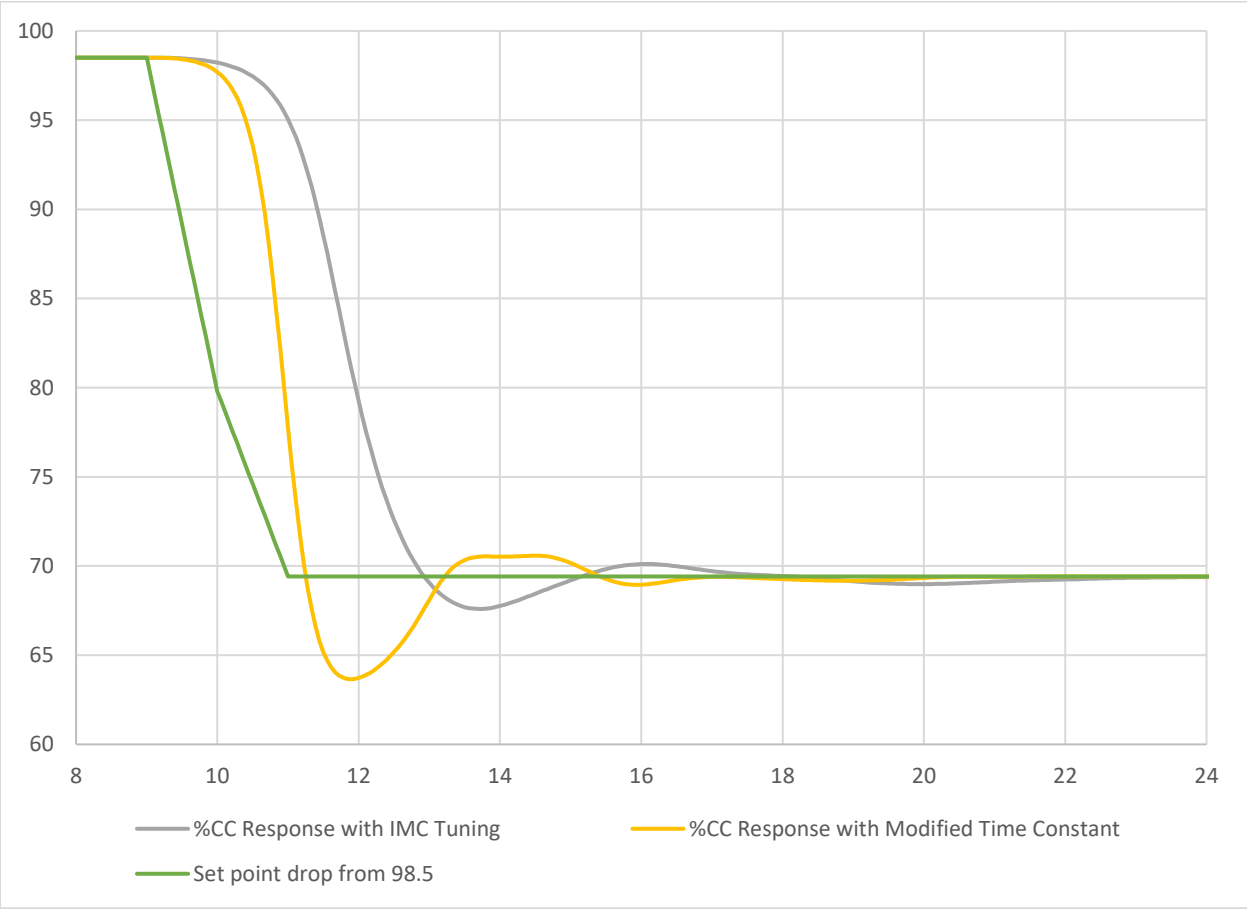

Figure 28 IMC tuned and modified controller response to set point changing from 98.5% to 69.5%

This adds an additional 2.2% drop resulting in significantly different responses from the controllers. The IMC tuned controller still lags about ~2 hours in achieving the various desired set-points, overshoots by ~1.8% CC and stabilizes around the 23rd hour meaning that the process response is sluggish and requires a while in stabilizing. The modified controller has a much lower lag with a much larger overshoot of ~6% CC below the set-point and reaches steady state around the same time as the IMC controller.

Comparing the two responses (previous two figures) show the response of two different tuning parameters on a process with a slight adjustment to the set-points. This highlights the issue with applying linear PI controllers on a highly non-linear process. In the case of post-combustion CCS

process, the linear PI controllers can be tuned according to a set schedule. However, the controllers will require additional tuning based on the changes to schedule on a regular basis. A small change of 2.2% on the schedule resulted in vastly different process response for the two controllers. Depending on the process constraints and the acceptable overshoot throughout the day, different parameters are to be implemented.

4.13 Controller Performance Error Evaluation

In order to evaluate the performance of the controller, the error is to be evaluated. Integrated square error emphasis the error difference between compared variables. For the first set of comparisons, the response of the runs is compared against its respective set-points. Figure 29 compares the different runs without the influence of inlet flue gas flowrate. The large SP changes too drastically resulting in a significantly higher error due to the response delay of the process and the error begins to stabilize around ~3550. Switching over to the ramp set-point schedule results in much lower error as the changes in %CC are changing along with the process response reducing the ISE down to ~2200. Unlike the large set-point change where the error is the largest when the change first takes place and slowly decreases with each time-step as the process response approaches the new set-point; there is an average error (significantly smaller than that of the large set-point) that accumulates with each time-step and decreases when the slope of the set-point begins to change directions.

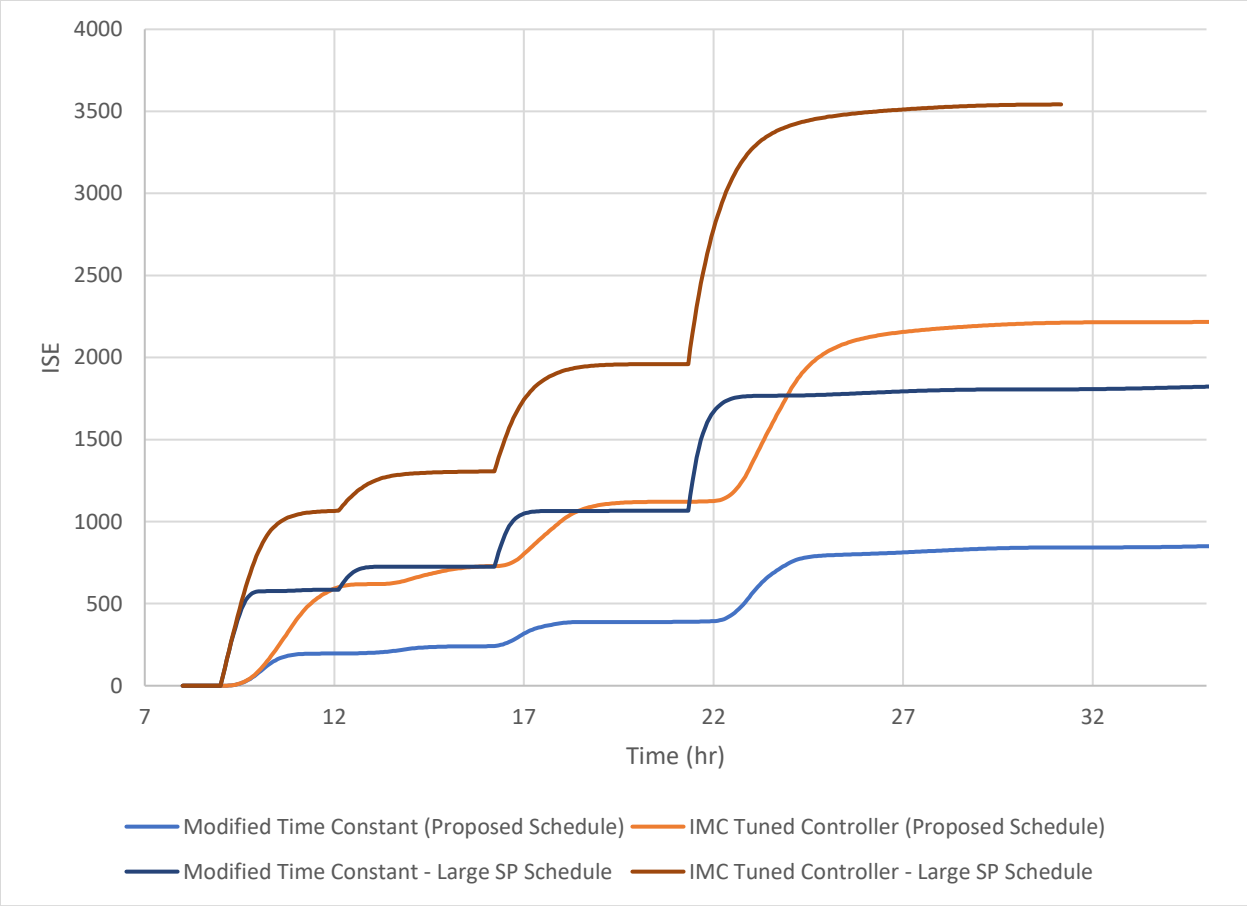

Figure 29 Integrated square error (%CC vs %CC SP) without disturbance

Updating the time constant for the controller to 100 significantly improves the performance of the controller in being able to control the process response closely to that of the set-point resulting in a lower error. Implementing the updated time constant on the large set-point and ramp set-point changes resulted in an overall ISE of ~1800 and ~850, respectively.

This shows an improvement of 48.6% for the large set-point change and 61.4% for the ramp set-point schedule over the originally tuned controllers. It is important to note that the original parameters were developed using IMC tuning guidelines. The IMC parameters were developed offline using a series of steady state gains and time constants resulting in parameters that were sub-optimal for the requirement of following the set-point schedule.

The influence of the disturbance in the flue-gas flowrate resulted in better response as the schedule was based on the disturbance. This is clearly seen in the following figure (Figure 30). The ISE of

the IMC controller dropped to ~1050 in comparison to ~2200 without the influence of the disturbance which translates to an improvement of ~52.3%. The performance of the tuned controller improved significantly as well; reducing from ~850 to ~390 resulting an improvement in achieving the set-point by ~54.1%.

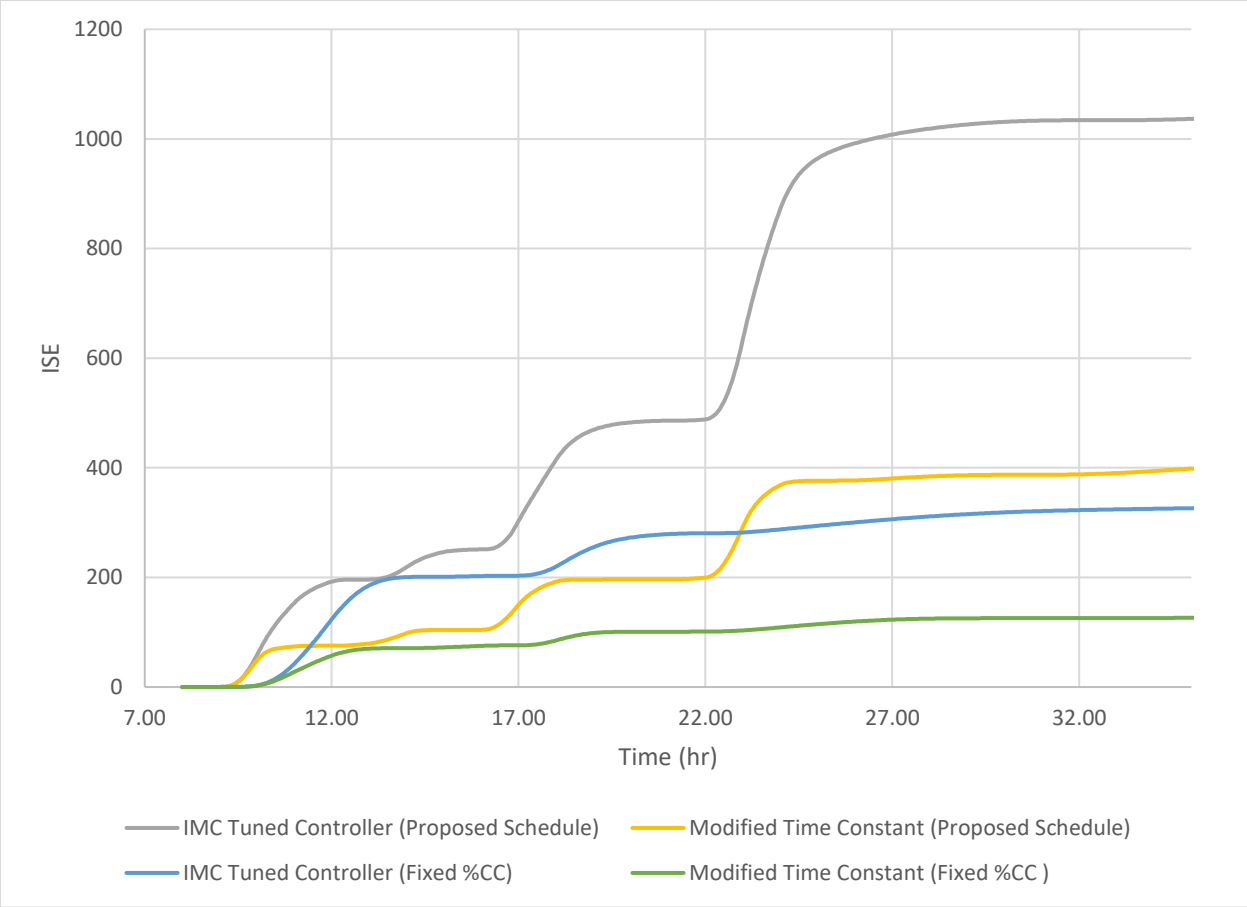

Figure 30 Integrated square error (%CC vs %CC SP) with disturbance

Comparing the performance of the controller in being able to maintain a steady state and reject the disturbance in the flue-gas flowrate; the modified controller appears to perform better. The IMC tuned controller resulted in an ISE of ~330 in comparison to ~125 of the modified controller which is ~62.1% lower.

Figure 30 also indicates the difficulty of servo-control related scenarios. Even though the schedule was designed around the disturbance and the disturbance improves the performance of the

controller, following the constantly changing set-points adds a layer of complexity for the controller.

Now switching over to comparing the performance of the controllers and set-point options to the schedule proposed in Figure 5. Since the ramp set-point schedule closely mimic's the proposal, the errors are identical to their respective errors of response in relation to set-points (Figure 31).

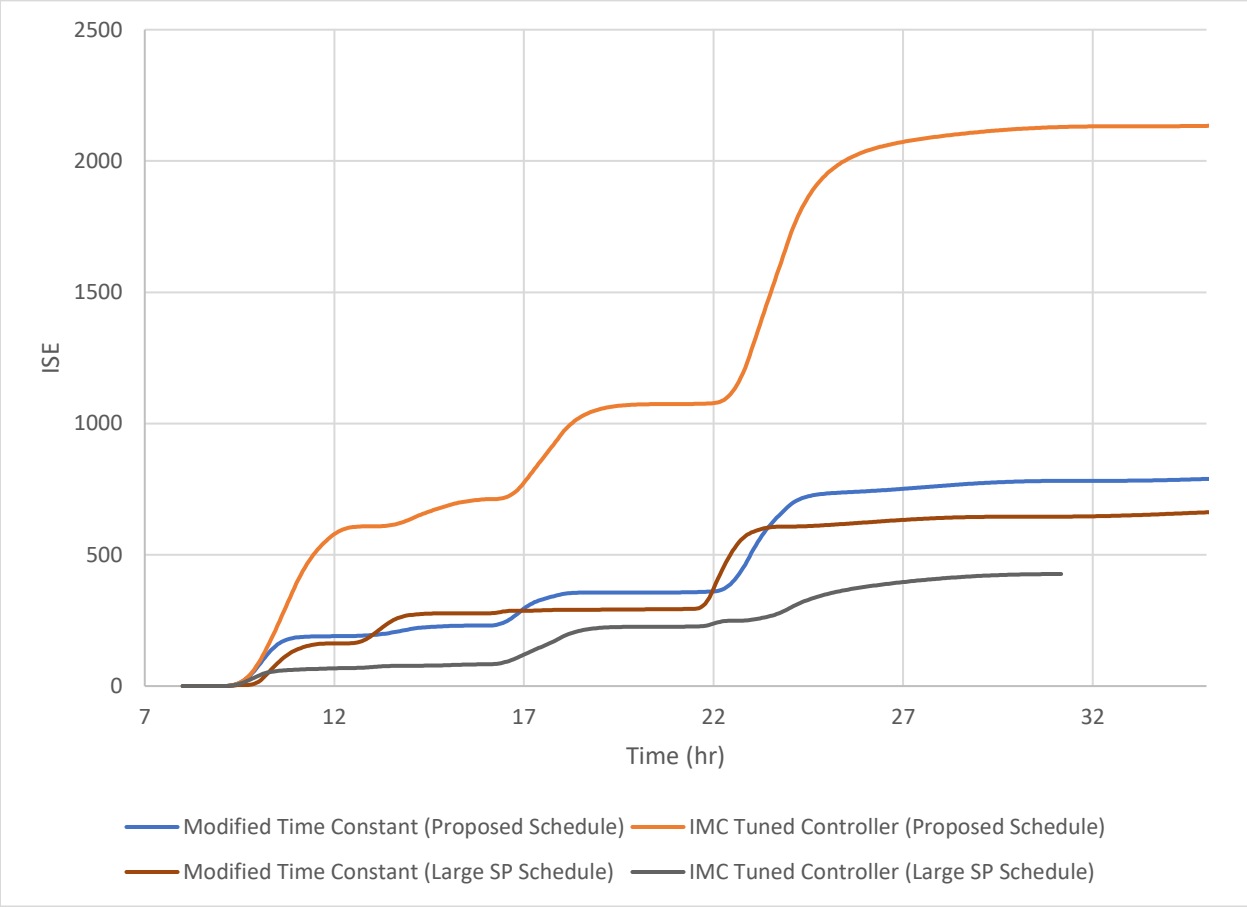

Figure 31 Integrated square error (%CC vs Alie Schedule) without disturbance

By contrast, the performance of the large (simple) set-point changes with both the IMC tuned parameter and the modified parameters resulted in significantly lower ISE's of ~430 and ~650 respectively. It is interesting to see that the modified controller parameter performed poorly to that of the original IMC controller. This emphasises the importance of appropriately tuning the controller for the application. In this scenario that compared the ISE of the responses without the influence of the disturbance, the best performance was by the simple set-point change with the

original IMC tuned parameter, followed by simple set-point change with the modified parameter, then the ramp schedule with the modified parameter at ~800 ISE and finally, the ramp schedule with the IMC parameter at last with an ISE of ~2132.

The final comparison is with the influence of disturbance on the ramp schedules (Figure 32). As expected, the ISE of both controllers are similar to the ISE of the response to their respective set-points. The IMC controller resulted with an ISE close to ~980 and the modified with ~350.

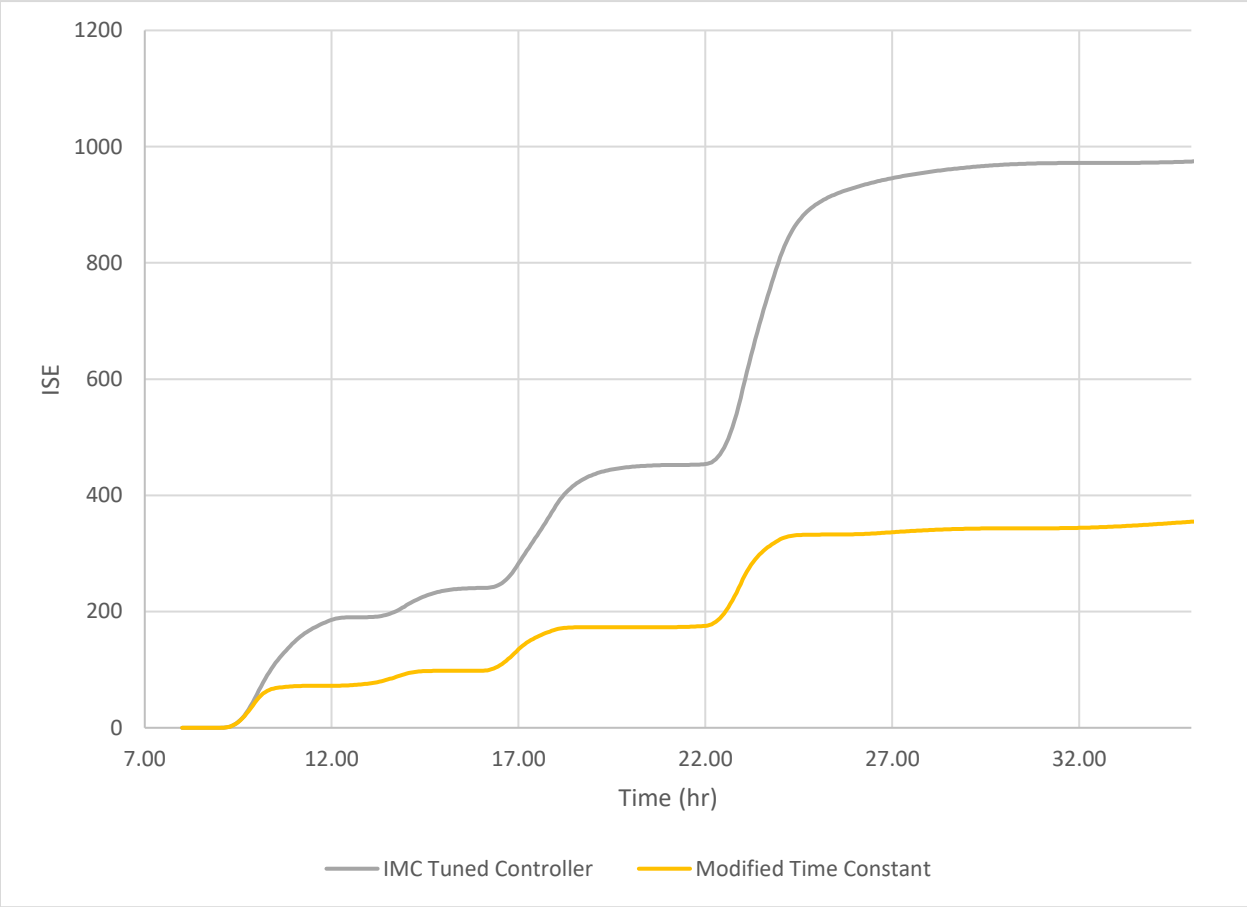

Figure 32 Integrated square error (%CC vs Proposed Schedule) with disturbance

4.14 Comparing Q reboilers

An alternate approach to the problem can be seen as minimizing the Q_{reb} over the course of the day since over 80% of the operating energy costs for the carbon capture system is the amount of energy spent in recovering MEA from the desorber.

The Q_{reb} or the energy supplied by the reboiler to the system between all the runs is divided into two sections. One with the influence of flue gas flowrate disturbance and the other without. The first data set shows the Q_{reb} without the influence of flue-gas flowrate with a fixed carbon capture set-point and a variable carbon capture set-point.

The proposed schedule (Figure 5) works along with the disturbance reducing the overall energy requirement by the carbon capture system. On the other hand, capturing a fixed amount of carbon throughout the day where the influence of flue-gas flowrate is working against the desired set-point leads to additional energy spent in capturing additional carbon. None of the runs presented in the figure below (Figure 33) are influenced by the effect of a disturbance in the flue-gas flowrate.

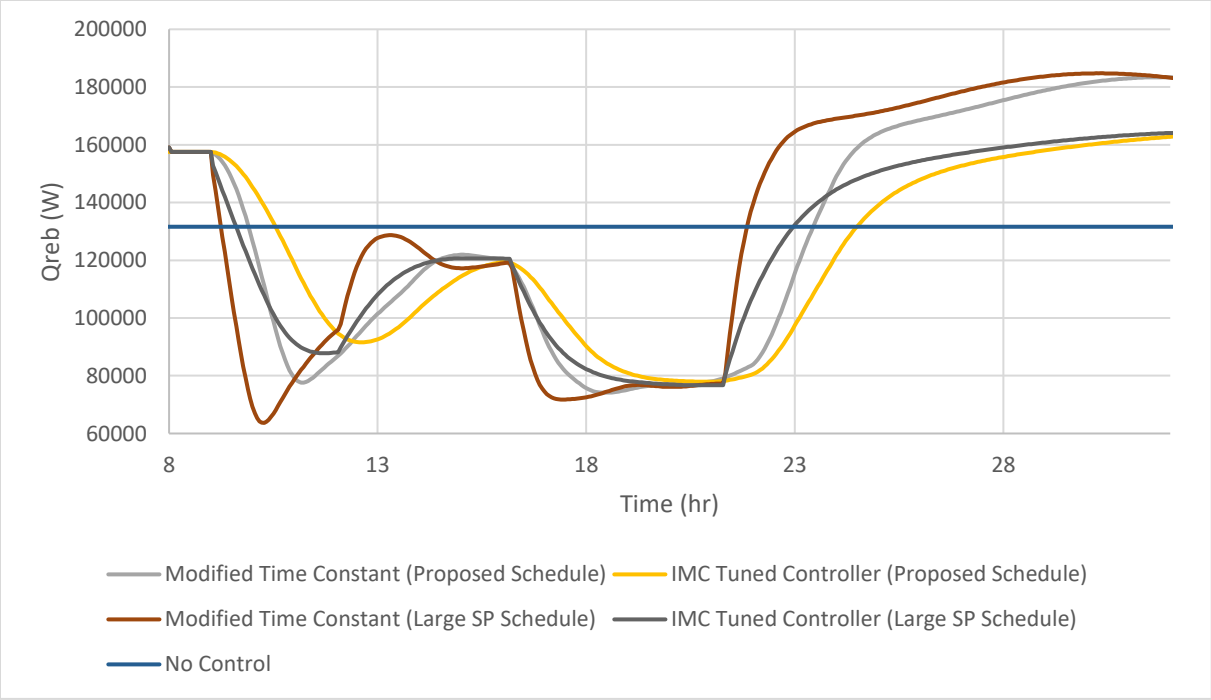

Figure 33 Qreb without disturbance

It is assumed that the all the variables are fixed initially for the run, then the set-points take effect on the 9th hour of the day. During these fluctuations, the set-point varies below the average capture rate during the day and is raised above the average capture rate (85%) during non-peak hours. Q_{reb} is manipulated by the controller to allow for the capture rates to follow in the direction of the set-point.

The averages are calculated from 1 hour before the set-point begins to change to 32 hours in order to include the changes in Q_{reb} before the next cycle takes place. The uncontrolled run consumes on average, 131 kW throughout the day in comparison to 127 kW and 121 kW for the ramp set-point changes with τ_I = 100 and 250 respectively. Changing the set-point erratically consumed an average of 131 kW and 124 kW for τ_I = 100 and 250 respectively. Without the influence of the disturbance in the flue-gas flowrate, following the schedule results a slightly lower consumption of energy for the carbon capture system.

When incorporating the disturbance into the runs, the patterns are similar for the set-point schedules with the two-time constants (Figure 34).

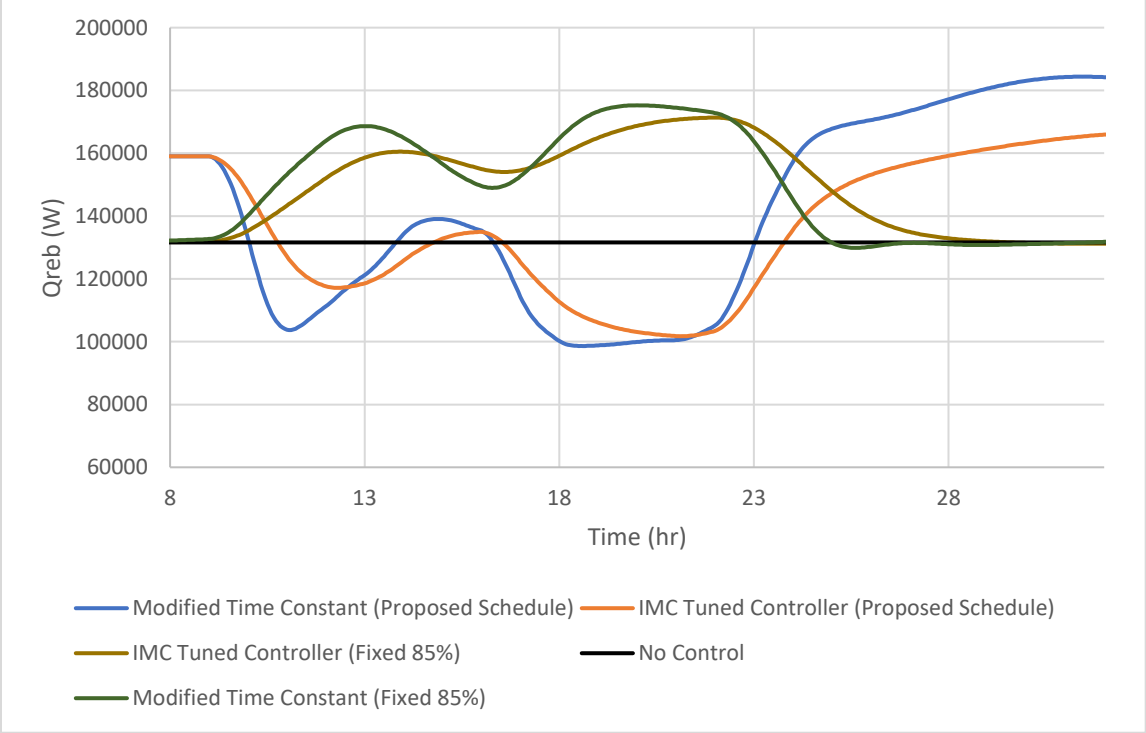

Figure 34 Q reboiler with disturbance

In comparison to the uncontrolled run, using the controller to capture a fixed %CC, the reboiler consumes much larger amounts of energy.

On average, the set-point schedule with τ_I = 100 and 250 under the influence of the disturbance consumed 139.8 kW and 134.9 kW of energy. This is relatively higher than the non-controlled run of 131.6 kW. Following the schedule is significantly lower than trying to capture a fixed amount of carbon using two controllers, that consumed 149.7 kW and 150.0 kW of energy.

There is a 10% and 11% increase in the Q_{reb} between the controllers following the set-point schedule with and without the disturbance of the inlet flue gas flowrate with the time constants for the controllers equal to 100 and 250 (seconds) respectively. This is attributed to the fluctuations in the disturbance. Since the nominal value of the inlet flue gas flowrate is the base value (based on the generation of power), the additional generation of power (Figure 32) will only result in an increase in the production of flue gas. For this schedule, the additional flue gas generation amounts to an increase by 10.5% in comparison to a steady-state power generation at the nominal value. The controllers take this additional increase in flue gas as an additional increase in CO_2 entering the absorber (that is required to be captured) resulting in the increase in Q_{reb}.

Comparing the performance of the controllers, the re-tuned controller (τ_I = 100) requires an additional ~5 - 6 kW of energy to follow the proposed schedule in comparison to the controller parameters proposed by Nittaya (2014). Not implementing the controller will result in significantly lower capture (due to added CO_2 in the system from the additional flue gas) requiring the operation to pay additional fines for not meeting the regulatory requirements.

The amount of energy while following the schedule is lower than capturing a fixed rate. However, it is important to note that following the schedule shifts capturing high amounts of CO_2 to off peak hours. This results in lowered costs due to the fluctuation in the cost of electricity throughout the day. This is because the price of energy varies throughout the day, on a typical day, the price of electricity (that is generated from the power plant) is higher during the day where capturing less CO_2 allows for additional power to be produced and distributed to the community. When the price drops later in the day and through the night, the CCS plant spends additional amounts of energy to

capture at a higher rate thereby resulting in a more economical operation of the carbon capture system throughout the day.

Of the controllers with the two sets of tuning parameters, for the proposed schedule (Figure 5) using an upper limit of 96.3%, the controller with τ_I equal to 100 performs significantly better than the controller with τ_I equal to 250 as shown in comparison for the ISE's (Integral Squared Errors). This shows the importance of implementing the appropriate tuning parameters based on the operating range of the system.

4.15 Model Predictive Schedule

The energy demand (and resultant flue gas flow rate) is expected to vary somewhat from day-to-day. The schedule use in this study was developed based on a given disturbance; therefore following the same schedule with a different flue gas disturbance (resulting from a different electricity demand) may not perform well and may lead to additional energy expenditures and/or the controller failing to maintain the CCS process at or close to the set point. Therefore, a simple correlation between the set-point and flue gas disturbance was developed to determine the schedule on-line as the flue gas changes. The correlation, shown in Figure 33 was developed by taking the %CC at each time step was ordered from smallest to largest value and plotted against its corresponding flue gas flow rate.

Figure 35 shows a close-to-linear relationship between the flue-gas and the %CC. Using Excel's linear trend line feature, a linear function with an R^2 value of 0.993 was estimated that provided a %CC value for an input value of flue-gas flowrate.

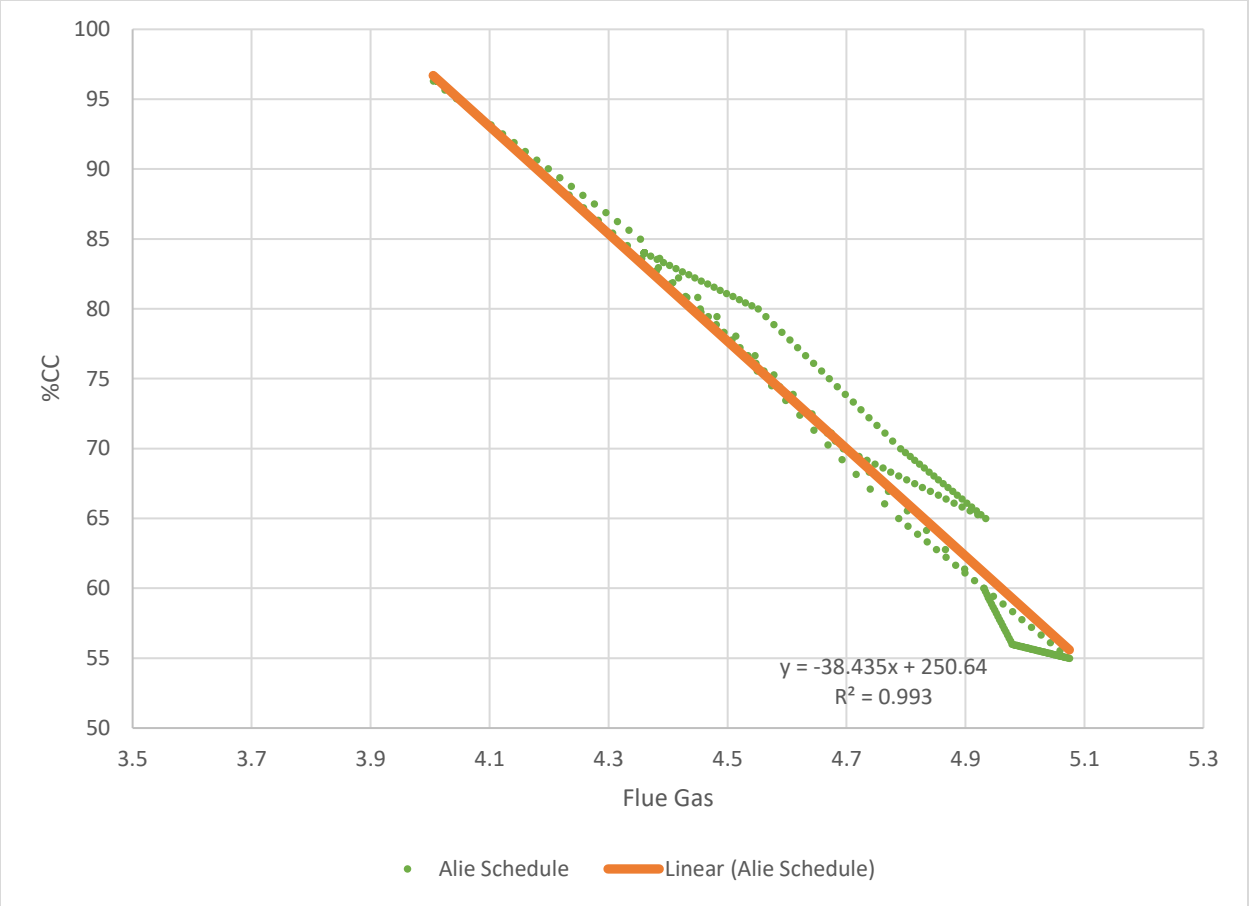

Figure 35 %CC vs Flue-gas

This trend was implemented in gProms by replacing the function for the set-point from a set-point to a linear function and removing the associated initialisation variable from the process section.

The estimated schedule and the original schedule are plotted against each other in Figure 36, the estimated schedule follows the same trajectory but is not able to meet the entire schedule at each point.

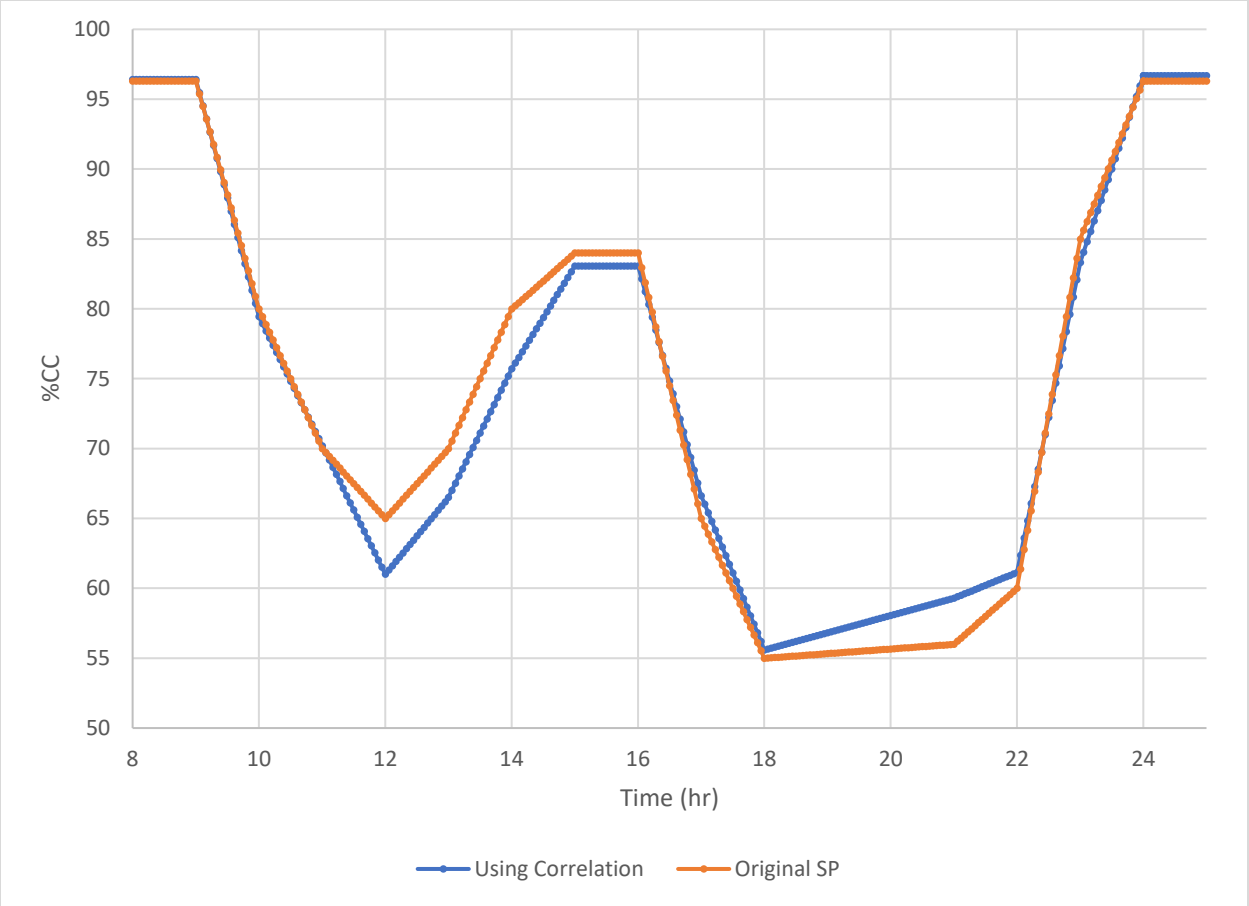

Figure 36 Correlated Schedule vs Original Schedule

The major difference appears between the 12th hour and the 14th hour, where the approximated schedule falls short of the desired set-point by ~4% CC. This along with the process dynamics, will result in performance different from expected as different changes in set-point will yield varying results as explained in the previous section.

On the other hand, using a simplified correlated schedule does have merits as well, analysing the demand of the fleet daily will require additional resources and are time consuming. Having a schedule that is able to adapt itself based on a given disturbance profile improves the controller's performance as the schedule will be in sync with the disturbance.

Although good, following this procedure is not perfect as in real world applications, predicting the demand may not be 100% accurate and will introduce errors between the model and the actual disturbance.

Finally, in order to implement this relation, a flow meter must be installed to monitor the flowrate of the flue-gas prior to the flue-gas entering the CCS absorber is measured. This will allow the model to adjust the set-point accordingly in real time.

Chapter 5: Conclusion

The objective of this work was to evaluate the control of the MEA process using a series of linear PI controllers attached to a power plant that is incorporated into a fleet of electric generators. This work also investigated the response of a controller in constantly changing set-point in the presence of a disturbance. The %CC set-point schedule used in this work was in relation to a specific disturbance experienced by the associated power plant.

In a typical scenario, the disturbance hinders the performance of the system staying in control. However, this work found that the influence of the disturbance on the ability of the process following the schedule is positive due the process dynamics.

This work demonstrated the importance of controller parameter tuning. A variation in the maximum limit of the capture rate resulted in vastly different performance for both the IMC and the re-tuned controllers.

Regarding the evaluation of the controller performance, the Integrated Square Error (ISE) for each run was assessed between the respective runs in comparison to the set-point and the proposed schedule. The evaluation showed an average of 57.6% decrease in ISE when updating the tuning parameter from the original IMC tuned controller (on large set-point change and ramp change with and without disturbance) and a decrease of 52.3% and 54.1% (from their respective ISE's that were measured without disturbance) with the incorporation of disturbance for the IMC tuned and the re-tuned controller parameter, respectively.

Reboiler duty for each configuration and run was evaluated as an approximation of the benefit of following the schedule in comparison to a fixed set-point or not implementing a control structure at all. The addition of an appropriately tuned controller reduced the energy consumed by the reboiler by ~7% in comparison to a fixed capture rate (with disturbance) and by ~4% in comparison to not having a controller at all.

If the demand is assumed to follow a similar pattern, slight fluctuations in day-to-day estimations of the flue-gas generation from the power plant can be incorporated into the system by allowing the process to estimate the set-point using a correlation between the flue-gas and the set-point used in the proposed schedule. This work displayed a implemented a linear correlation between the

disturbance and the corresponding %CC set-point to showcase the potential of an on-line schedule development.

In conclusion, the configuration chosen performs well; provided the tuning parameters are adjusted according to the proposed schedule for the %CC set-point.

Chapter 6: Recommendations for Future Work

As this work was conducted on a part of the fleet, incorporating the rigorous model and control to the fleet itself can provide a realistic performance of the fleet in the presence of various disturbances throughout the fleet of generators.

The simple model used to approximate the %CC set-point schedule can be modified to include the time of day or incorporate the fluctuation in demand of power to better approximate the appropriate set-point.

Evaluating alternate control schemes and configurations in a combined servo-control and disturbance related scenarios will help determine the most effective way of scheduling and controlling the post-combustion carbon capture process.

Possibly through the use of data analytics in the future, a close approximation of the upcoming demand can be estimated on a daily basis where a correlation between the disturbance and the set-point can assist in developing a daily set-point criterion. This simple schedule does not consider the minimum capture requirements as of now; it primarily adjusts according to the disturbance. The assumptions for the application of this trend line include that the fluctuations are in around the values for which the data is provided, and the flue-gas does not lower below the nominal value of 4.01 mol/s.

References

Abu-Zahra, M., Schneiders, L., Niederer, J., Feron, P., & Versteeg, G. (2007). CO2 capture from power plants: Part 1. A parametric study of the technical performance based on monoethanolamine. *International Journal of Greenhouse Gas Control, 1*(1), 37-46.

Alie, C. (2013). *A framework for assessing the CO2 mitigation options for the electricity generation sub-sector.* PhD Thesis, University of Waterloo.

Bristol, E. H. (1966). *On a new measure of interaction for multivariable process control.* IEEE Trans. Autom. Control, AC-11.

Chalmers, H., & Gibbins, J. (2007). Initial evaluation of the impact of post-combustion capture of carbon dioxide on supercritical pulverised coal power plant part load performance. *Fuel, 86*(14), 2109-2123.

Chapel, D., Marix, C., & Ernest, J. (1999). Recovery of CO2 from Flue Gases: Commercial Trends. *Candian Society of Chemical Engineers*.

Cooper, D. (2004). *Practical Process Control Using Control Station.* Storrs, CT: Control Station.

Douglas, P. (2018). *Personal Communication.*

Dugas, E. (2006). *Pilot plant study of carbon dioxide capture by aqueous monoethanolamine, M.S.E Thesis.* Austin: University of Texas at Austin.

Edward, J. (2008). *Design and rating shell and tube heat exchangers.* Teesside, UK: P&I Design Ltd.

EPA. (2016, April). *EPA*. Retrieved from Climate Change Indicators: Atmospheric Concentrations of Greenhouse Gases: https://www.epa.gov/climate-indicators/climate-change-indicators-atmospheric-concentrations-greenhouse-gases

Global CCS Institute. (2018). *Global Status Report.* Global CCS Institute.

Harun, N. (2012). Dynamic Simulation of MEA Absorption Process for CO2 Capture from Power Plants. *PhD Thesis*.

Herzog, H. (2010). Scaling up carbon dioxide capture and storage: From megatons to gigatons. *Energy Economics*. doi:10.1016/j.eneco.2010.11.004

Herzog, H. J. (2000). The Economics of CO2 Separation and Capture. *Journal of the Franklin Institute*, 20.

Hoegh-Guldberg, O. (1998). Climate change, coral bleaching and the future of the world's coral reefs. 50.

IEA. (2011). *World Energy Outlook.* Retrieved from https://www.iea.org/publications/freepublications/publication/WEO2011_WEB.pdf

IEEE Transactions on Power Systems. (1999). THe IEEE Reliability Test System - 1996. *14*(3), 1010-1020.

Jansen, D., Gazzani, M., Manzolini, G., Dijk, E. V., & Carbo, M. (2015). Pre-combustion CO2 capture. *International Journal of Greenhouse Gas Control, 40*, 167-187.

Lawal, A., Want, M., Stephenson, P., & Yeung, H. (2009). Dynamic modelling of CO2 absorption for post combustion capture in coal-fired power plants. *Fuel, 88*, 2455-2462.

Li, Z., Ding, Z., Wang, M., & Oko, E. (2018). Model-free adaptive control for MEA-based post-combustion carbon capture processes. *Fuel, 224*, 637-643.

Liao, P., Wu, X., Li, Y., Wang, M., Shen, J., Lawal, A., & Xu, C. (2018). Application of piece-wise linear system identification of solvent-based post-combustion carbon capture. *Fuel, 234*, 526-537.

Lin, Y.-J., Chang, C.-C., Wong, D. S.-H., Jang, S.-S., & Ou, J.-J. (2011). Control Strategies for Flexible Operation of Power Plant Integrated with CO2 Capture Plant. *AIChE, 58*(9), 2697-2704.

Lockwood, T. (2014). *Developments in Oxyfuel Combustion of Coal, CCC/240.* IEA Clean Coal Centre.

Luis, P. (2016). Use of monoethanolamine (MEA) for CO2 capture in a global scenario: Consequences and alternatives. *Desalination, 380*(15 February 2016), 93-99.

Mechleri, E., Lawal, A., Ramos, A., Davison, J., & Dowell, N. (2017). Process control strategies for flexible operation of post-combustion CO2 capture plants. *International Journal of Greenhouse Gas Control, 57*(February 2017), 14-25.

Natural Resources Canada. (2016, 02 17). Retrieved from Power Plant Modelling: https://www.nrcan.gc.ca/energy/coal/carbon-capture-storage/4311

Nittaya, T. (2014). Dynamic Modelling and Control of MEA Absorption Processes for CO2 Capture from Power Plants. *MASc Thesis*.

Oh, S.-Y., Binns, M., Cho, H., & Kim, J.-K. (2016). Energy minimization of MEA-based CO2 capture process. *Applied Energy, 169*, 353-362.

O'Neill, B. C. (2002). Dangerous Climate Impacts and the Kyoto Protocal. *Science Compass, 296*(5575), 1971-1972.

Oyenekan, B., & Rochelle, G. (2006). Energy Performance of Stripper Configurations for CO2 Capture by Aqueous Amines. *I&EC Research, 45*(8), 2457-2464.

Paris Climate Change Conference. (2015, November). Retrieved from United Nations Climate Change: https://unfccc.int/process-and-meetings/conferences/past-conferences/paris-climate-change-conference-november-2015/paris-climate-change-conference-november-2015

Peterson, T., Connolley, W., & Fleck, J. (2008, September 1). The myth of the 1970s global cooling scientific consensus. *AMS100*.

Rao, A. B. (2002). A Technical, Economic and Environmental Assessment of Amine-based CO2 Capture Technology for Power Plant Greenhouse Gas Control.

Rao, A., & Rubin, E. (2006). Identifying Cost-Effective CO2 Control Levels for Amine-Based CO2 Capture Systems. *Industrial Engineering, 45*, 2421-2429.

Salazar, J., Diwekar, U., Joback, K., Berger, A., & Bhown, A. (2013). Solvent Selection for Post-Combustion CO2 Capture. *Energy Procedia, 37*, 257-264.

Scott, V., Gilfillan, S., Markusson, N., Chalmers, H., & Haszeldine, R. (2012). Last chance for carbon capture and storage. *Nature Climate Change, 3*, 105-111. doi:https://doi.org/10.1038/nclimate1695

Singh, D. J. (2003). Simulation of CO2 Capture strategies for existing coal fired power plant - MEA scrubbing versus O2/CO2 recycle combustion. *Energy Conversion and Management, 44*, 3073-3091.

Song, C., Liu, Q., Deng, S., Zhao, J., Li, Y., Song, Y., & Li, H. (2018). Alternative pathways for efficient CO2 capture by hybrid processes - A review. *Renewable and Sustainable Energy Reviews, 82*(1), 215-231.

Stanger, R., Wall, T., Spörlb, R., Paneru, M., Grathwohl, S., Weidmann, M., . . . Santos, S. (2015). Oxyfuel combustion for CO2 capture in power plants. *Science Direct, 40*(September 2015), 55-125.

Wang, Y., Zhao, L., Otto, A., Robinius, M., & Stolten, D. (2017). A Review of Post-combustion CO2 Capture Technologies from Coal-fired Power Plants. *Energy Procedia, 114*(November 2016), 650-665.

Wu, X., Shen, J., Li, Y., Wang, M., & Lawal, A. (2018). Flexible operation of post-combustion solvent-based carbon capture for coal fired power plants using multi-model predictive control: A simulation study. *Fuel, 220*(February), 931-941.

Wu, X., Shen, J., Li, Y., Wang, M., Lawal, A., & Lee, K. (2018). Nonlinear dynamic analysis and control design of a solvent-based post-combustion CO2 capture process. *Computers and Chemical Engineering, 115*, 397-406.

Zhang, Q., Turton, R., & Bhattacharyya, D. (2016). Development of Model and Model-Predictive Control of an MEA-Based Postcombustion CO2 Capture Process. *I&EC Research, 55*, 1292-1308.

Appendix

Appendix A: Aspen Steady State Tests

Condensor Temperature Condenser Duty (Watts)	-11500	-12075	-12650	-13225	-13800	-10925	-10350	-9775	-9200
% Change from Nominal	-20%	-15%	-10%	-5%	0%	5%	10%	15%	20%
Inlet CO2 Conc (Side)/Inlet Flue Gas Flowrate (Down)	0.14								
3.21									
3.41									
3.61									
3.81	319.7	314.3	307.8	299.6	289.1	275.7	259.7	241.9	223.1
4.01	317.0	311.2	304.0	294.9	283.3	268.8	252.1	234.1	215.0
4.21	314.5	308.3	300.5	290.6	278.0	262.9	245.8	227.6	208.5
4.41	312.9	306.4	298.3	288.1	275.2	259.8	242.7	224.7	205.7
4.61	311.7	305.1	296.8	286.4	273.5	258.1	241.2	223.5	204.7
4.82	311.2	304.6	296.3	286.0	273.1	257.9	241.1	223.6	205.1

Reboiler Temperature Condenser Duty (Watts)	-11500	-12075	-12650	-13225	-13800	-10925	-10350	-9775	-9200
% Change from Nominal	-20%	-15%	-10%	-5%	0%	5%	10%	15%	20%
Inlet CO2 Conc (Side)/Inlet Flue Gas Flowrate (Down)	0.14								
3.21									
3.41									
3.61									
3.81	387.4	387.4	387.3	387.3	387.3	387.3	387.3	387.3	387.2
4.01	387.2	387.2	387.1	387.1	387.1	387.1	387.1	387.1	387.0
4.21	387.0	386.9	386.9	386.9	386.9	386.9	386.9	386.8	386.8
4.41	386.8	386.8	386.8	386.8	386.7	386.7	386.7	386.7	386.6
4.61	386.7	386.6	386.6	386.6	386.6	386.6	386.5	386.5	386.5
4.82	386.6	386.6	386.6	386.5	386.5	386.5	386.5	386.4	386.4

CO2 Purity Condenser Duty (Watts)	-11500	-12075	-12650	-13225	-13800	-10925	-10350	-9775	-9200
% Change from Nominal	-20%	-15%	-10%	-5%	0%	5%	10%	15%	20%
Inlet CO2 Conc (Side)/Inlet Flue Gas Flowrate (Down)	0.14								
3.21									
3.41									
3.61									
3.81	91.57%	93.12%	94.57%	95.86%	96.88%	97.55%	97.86%	97.96%	97.98%
4.01	92.58%	94.06%	95.42%	96.57%	97.42%	97.92%	98.12%	98.17%	98.18%
4.21	93.42%	94.84%	96.10%	97.13%	97.84%	98.20%	98.33%	98.36%	98.36%
4.41	93.84%	95.19%	96.38%	97.31%	97.93%	98.24%	98.34%	98.36%	98.36%
4.61	94.09%	95.39%	96.52%	97.40%	97.96%	98.23%	98.32%	98.33%	98.33%
4.82	94.18%	95.45%	96.55%	97.40%	97.95%	98.21%	98.29%	98.31%	98.31%

Condensor Temperature Condenser Duty (Watts)	-11500	-12075	-12650	-13225	-13800	-10925	-10350	-9775	-9200
% Change from Nominal	-20%	-15%	-10%	-5%	0%	5%	10%	15%	20%
Inlet CO2 Conc (Side)/Inlet Flue Gas Flowrate (Down)					0.14875				
3.21									
3.41									
3.61	319.8	314.5	307.9	299.8	289.3	276.0	260.0	242.2	223.4
3.81	316.6	310.7	303.4	294.1	282.3	267.8	250.9	232.8	213.7
4.01	314.3	308.0	300.1	290.1	277.5	262.2	245.0	227.0	207.6
4.21	312.6	306.0	297.8	287.5	274.5	259.0	241.9	223.9	204.9
4.41	311.4	304.7	296.4	286.0	272.9	257.6	240.6	222.9	204.1
4.61	311.0	304.3	296.0	285.7	272.6	257.4	240.6	223.1	204.6
4.82	310.8	304.2	295.9	285.6	272.7	257.6	241.0	223.6	205.1

Reboiler Temperature Condenser Duty (Watts)	-11500	-12075	-12650	-13225	-13800	-10925	-10350	-9775	-9200
% Change from Nominal	-20%	-15%	-10%	-5%	0%	5%	10%	15%	20%
Inlet CO2 Conc (Side)/Inlet Flue Gas Flowrate (Down)					0.14875				
3.21									
3.41									
3.61	387.4	387.4	387.4	387.3	387.3	387.3	387.3	387.3	387.2
3.81	387.1	387.1	387.1	387.1	387.1	387.1	387.0	387.0	387.0
4.01	386.9	386.9	386.9	386.9	386.9	386.9	386.8	386.8	386.8
4.21	386.8	386.8	386.7	386.7	386.7	386.7	386.7	386.6	386.6
4.41	386.6	386.6	386.6	386.6	386.6	386.5	386.5	386.5	386.5
4.61	386.6	386.5	386.5	386.5	386.5	386.5	386.4	386.4	386.4
4.82	386.5	386.5	386.5	386.5	386.5	386.4	386.4	386.4	386.4

CO2 Purity Condenser Duty (Watts)	-11500	-12075	-12650	-13225	-13800	-10925	-10350	-9775	-9200
% Change from Nominal	-20%	-15%	-10%	-5%	0%	5%	10%	15%	20%
Inlet CO2 Conc (Side)/Inlet Flue Gas Flowrate (Down)					0.14875				
3.21									
3.41									
3.61	91.52%	93.08%	94.54%	95.83%	96.85%	97.53%	97.85%	97.95%	97.97%
3.81	92.72%	94.20%	95.54%	96.67%	97.50%	97.96%	98.15%	98.20%	98.20%
4.01	93.51%	94.92%	96.18%	97.19%	97.88%	98.24%	98.36%	98.39%	98.39%
4.21	93.94%	95.29%	96.46%	97.39%	97.99%	98.28%	98.37%	98.39%	98.39%
4.41	94.19%	95.48%	96.59%	97.45%	98.00%	98.26%	98.35%	98.36%	98.36%
4.61	94.26%	95.52%	96.61%	97.45%	97.99%	98.24%	98.33%	98.34%	98.34%
4.82	94.28%	95.53%	96.61%	97.44%	97.97%	98.23%	98.31%	98.33%	98.33%

Condensor Temperature									
Condenser Duty (Watts)	-11500	-12075	-12650	-13225	-13800	-10925	-10350	-9775	-9200
% Change from Nominal	-20%	-15%	-10%	-5%	0%	5%	10%	15%	20%
Inlet CO2 Conc (Side)/Inlet Flue Gas Flowrate (Down)	0.1575								
3.21									
3.41									
3.61									
3.81	314.4	308.1	300.3	290.4	277.7	262.5	245.3	227.1	207.8
4.01	312.4	305.8	297.6	287.1	274.1	258.5	241.4	223.3	204.2
4.21	311.2	304.5	296.1	285.6	272.5	257.1	240.1	222.4	203.4
4.41	310.8	304.1	295.8	285.3	272.3	257.0	240.2	222.6	203.9
4.61	310.7	304.0	295.7	285.3	272.4	257.2	240.5	223.1	204.6
4.82	310.6	304.0	295.8	285.4	272.6	257.5	241.0	223.7	205.3

Reboiler Temperature									
Condenser Duty (Watts)	-11500	-12075	-12650	-13225	-13800	-10925	-10350	-9775	-9200
% Change from Nominal	-20%	-15%	-10%	-5%	0%	5%	10%	15%	20%
Inlet CO2 Conc (Side)/Inlet Flue Gas Flowrate (Down)	0.1575								
3.21									
3.41									
3.61									
3.81	386.9	386.9	386.9	386.9	386.9	386.9	386.8	386.8	386.8
4.01	386.8	386.7	386.7	386.7	386.7	386.7	386.6	386.6	386.6
4.21	386.6	386.6	386.6	386.6	386.5	386.5	386.5	386.5	386.4
4.41	386.5	386.5	386.5	386.5	386.5	386.4	386.4	386.4	386.4
4.61	386.5	386.5	386.5	386.5	386.4	386.4	386.4	386.4	386.3
4.82	386.5	386.5	386.4	386.4	386.4	386.4	386.4	386.3	386.3

CO2 Purity									
Condenser Duty (Watts)	-11500	-12075	-12650	-13225	-13800	-10925	-10350	-9775	-9200
% Change from Nominal	-20%	-15%	-10%	-5%	0%	5%	10%	15%	20%
Inlet CO2 Conc (Side)/Inlet Flue Gas Flowrate (Down)	0.1575								
3.21									
3.41									
3.61									
3.81	93.46%	94.88%	96.14%	97.16%	97.86%	98.22%	98.35%	98.37%	98.37%
4.01	94.00%	95.35%	96.52%	97.44%	98.03%	98.32%	98.41%	98.43%	98.43%
4.21	94.25%	95.54%	96.65%	97.51%	98.04%	98.30%	98.38%	98.39%	98.39%
4.41	94.32%	95.58%	96.67%	97.50%	98.03%	98.28%	98.36%	98.37%	98.37%
4.61	94.34%	95.59%	96.66%	97.49%	98.01%	98.26%	98.34%	98.36%	98.36%
4.82	94.34%	95.58%	96.65%	97.47%	98.00%	98.25%	98.33%	98.35%	98.35%

Condensor Temperature									
Condenser Duty (Watts)	-11500	-12075	-12650	-13225	-13800	-10925	-10350	-9775	-9200
% Change from Nominal	-20%	-15%	-10%	-5%	0%	5%	10%	15%	20%
Inlet CO2 Conc (Side)/Inlet Flue Gas Flowrate (Down)	0.16625								
3.21									
3.41	319.6	314.2	307.6	299.4	288.8	275.4	259.3	241.5	222.6
3.61	314.9	308.7	300.9	291.1	279.1	263.6	246.4	228.2	209.1
3.81	312.5	305.9	297.6	287.1	274.0	258.4	241.2	223.1	203.9
4.01	311.1	304.4	296.0	285.3	272.1	256.6	239.7	221.8	202.8
4.21	310.7	304.0	295.6	285.0	271.9	256.5	239.8	222.0	203.4
4.41	310.5	303.9	295.5	285.0	272.0	256.9	240.1	222.6	204.1
4.61	310.5	303.9	295.6	285.1	272.2	257.1	240.6	223.2	204.8
4.82	310.5	303.9	295.6	285.3	272.6	257.5	241.2	223.8	205.6

Reboiler Temperature									
Condenser Duty (Watts)	-11500	-12075	-12650	-13225	-13800	-10925	-10350	-9775	-9200
% Change from Nominal	-20%	-15%	-10%	-5%	0%	5%	10%	15%	20%
Inlet CO2 Conc (Side)/Inlet Flue Gas Flowrate (Down)	0.16625								
3.21									
3.41	387.4	387.3	387.3	387.3	387.3	387.3	387.3	387.3	387.2
3.61	387.0	387.0	387.0	386.9	386.9	386.9	386.9	386.9	386.8
3.81	386.8	386.7	386.7	386.7	386.7	386.7	386.6	386.6	386.6
4.01	386.6	386.6	386.6	386.5	386.5	386.5	386.5	386.4	386.4
4.21	386.5	386.5	386.5	386.5	386.5	386.4	386.4	386.4	386.4
4.41	386.5	386.5	386.5	386.4	386.4	386.4	386.4	386.3	386.3
4.61	386.5	386.5	386.4	386.4	386.4	386.4	386.3	386.3	386.3
4.82	386.4	386.4	386.4	386.4	386.4	386.4	386.3	386.3	386.3

CO2 Purity									
Condenser Duty (Watts)	-11500	-12075	-12650	-13225	-13800	-10925	-10350	-9775	-9200
% Change from Nominal	-20%	-15%	-10%	-5%	0%	5%	10%	15%	20%
Inlet CO2 Conc (Side)/Inlet Flue Gas Flowrate (Down)	0.16625								
3.21									
3.41	91.60%	93.15%	94.60%	95.88%	96.90%	97.55%	97.87%	97.96%	97.98%
3.61	93.30%	94.73%	96.01%	97.06%	97.76%	98.16%	98.30%	98.33%	98.33%
3.81	94.02%	95.37%	96.55%	97.48%	98.07%	98.35%	98.44%	98.46%	98.46%
4.01	94.31%	95.59%	96.70%	97.55%	98.09%	98.33%	98.41%	98.43%	98.43%
4.21	94.38%	95.64%	96.72%	97.55%	98.07%	98.31%	98.39%	98.41%	98.41%
4.41	94.40%	95.64%	96.71%	97.54%	98.05%	98.30%	98.38%	98.39%	98.39%
4.61	94.40%	95.63%	96.70%	97.52%	98.04%	98.28%	98.36%	98.38%	98.38%
4.82	94.39%	95.62%	96.68%	97.50%	98.02%	98.27%	98.35%	98.37%	98.37%

Condensor Temperature									
Condenser Duty (Watts)	-11500	-12075	-12650	-13225	-13800	-10925	-10350	-9775	-9200
% Change from Nominal	-20%	-15%	-10%	-5%	0%	5%	10%	15%	20%
Inlet CO2 Conc (Side)/Inlet Flue Gas Flowrate (Down)					0.175				
3.21	318.8	313.3	306.5	298.0	287.1	273.3	257.0	239.0	220.1
3.41	314.3	307.9	300.1	290.1	277.4	262.0	244.9	226.7	207.3
3.61	312.8	306.2	297.9	287.5	274.2	258.7	241.4	223.2	203.8
3.81	311.1	304.3	295.9	285.1	271.9	256.3	239.4	221.3	202.3
4.01	310.6	303.9	295.4	284.7	271.5	256.1	239.3	221.6	202.8
4.21	310.4	303.7	295.3	284.8	271.6	256.3	239.6	222.0	203.5
4.41	310.4	303.7	295.3	284.9	271.8	256.8	240.0	222.6	204.2
4.61	310.4	303.7	295.4	285.0	272.2	257.2	240.6	223.3	205.0
4.82	310.4	303.8	295.6	285.3	272.6	257.6	241.3	224.1	206.0

Reboiler Temperature									
Condenser Duty (Watts)	-11500	-12075	-12650	-13225	-13800	-10925	-10350	-9775	-9200
% Change from Nominal	-20%	-15%	-10%	-5%	0%	5%	10%	15%	20%
Inlet CO2 Conc (Side)/Inlet Flue Gas Flowrate (Down)					0.175				
3.21	387.3	387.3	387.3	387.3	387.2	387.2	387.2	387.2	387.2
3.41	386.9	386.9	386.9	386.9	386.9	386.8	386.8	386.8	386.8
3.61	386.8	386.8	386.8	386.7	386.7	386.7	386.7	386.7	386.6
3.81	386.6	386.6	386.6	386.5	386.5	386.5	386.5	386.4	386.4
4.01	386.5	386.5	386.5	386.5	386.4	386.4	386.4	386.4	386.4
4.21	386.5	386.5	386.5	386.4	386.4	386.4	386.4	386.3	386.3
4.41	386.5	386.4	386.4	386.4	386.4	386.4	386.3	386.3	386.3
4.61	386.4	386.4	386.4	386.4	386.4	386.3	386.3	386.3	386.3
4.82	386.4	386.4	386.4	386.4	386.3	386.3	386.3	386.3	386.2

CO2 Purity									
Condenser Duty (Watts)	-11500	-12075	-12650	-13225	-13800	-10925	-10350	-9775	-9200
% Change from Nominal	-20%	-15%	-10%	-5%	0%	5%	10%	15%	20%
Inlet CO2 Conc (Side)/Inlet Flue Gas Flowrate (Down)					0.175				
3.21	91.90%	93.44%	94.86%	96.10%	97.06%	97.67%	97.94%	98.02%	98.03%
3.41	93.50%	94.92%	96.17%	97.18%	97.88%	98.23%	98.35%	98.37%	98.37%
3.61	93.98%	95.35%	96.55%	97.49%	98.09%	98.38%	98.48%	98.49%	98.49%
3.81	94.34%	95.63%	96.74%	97.60%	98.13%	98.37%	98.45%	98.46%	98.46%
4.01	94.43%	95.69%	96.77%	97.60%	98.11%	98.35%	98.42%	98.44%	98.44%
4.21	94.45%	95.70%	96.76%	97.58%	98.09%	98.33%	98.41%	98.42%	98.42%
4.41	94.45%	95.69%	96.75%	97.56%	98.08%	98.32%	98.39%	98.41%	98.41%
4.61	94.44%	95.67%	96.73%	97.54%	98.06%	98.30%	98.38%	98.40%	98.40%
4.82	94.43%	95.65%	96.70%	97.52%	98.04%	98.29%	98.37%	98.39%	98.39%

Condensor Temperature									
Condenser Duty (Watts)	-11500	-12075	-12650	-13225	-13800	-10925	-10350	-9775	-9200
% Change from Nominal	-20%	-15%	-10%	-5%	0%	5%	10%	15%	20%
Inlet CO2 Conc (Side)/Inlet Flue Gas Flowrate (Down)	0.18375								
3.21	318.5	312.9	306.1	297.5	286.4	272.5	256.1	238.2	219.2
3.41	312.4	305.7	297.4	286.8	273.5	257.8	240.5	222.3	202.8
3.61	310.8	304.0	295.5	284.7	271.5	255.8	238.8	220.9	201.9
3.81	310.5	303.8	295.3	284.5	271.3	255.7	238.8	221.0	202.2
4.01	310.3	303.6	295.1	284.4	271.3	255.8	239.1	221.5	202.8
4.21	310.3	303.5	295.1	284.5	271.5	256.2	239.5	222.1	203.5
4.41	310.2	303.5	295.2	284.8	271.8	256.6	240.2	222.7	204.4
4.61	310.3	303.7	295.3	285.0	272.2	257.2	240.8	223.5	205.3
4.82	310.3	303.8	295.6	285.4	272.8	257.8	241.6	224.4	206.3

Reboiler Temperature									
Condenser Duty (Watts)	-11500	-12075	-12650	-13225	-13800	-10925	-10350	-9775	-9200
% Change from Nominal	-20%	-15%	-10%	-5%	0%	5%	10%	15%	20%
Inlet CO2 Conc (Side)/Inlet Flue Gas Flowrate (Down)	0.18375								
3.21	387.3	387.3	387.3	387.2	387.2	387.2	387.2	387.2	387.1
3.41	386.7	386.7	386.7	386.7	386.7	386.7	386.6	386.6	386.6
3.61	386.5	386.5	386.5	386.5	386.5	386.5	386.4	386.4	386.4
3.81	386.5	386.5	386.5	386.5	386.4	386.4	386.4	386.4	386.3
4.01	386.5	386.5	386.4	386.4	386.4	386.4	386.4	386.3	386.3
4.21	386.4	386.4	386.4	386.4	386.4	386.3	386.3	386.3	386.3
4.41	386.4	386.4	386.4	386.4	386.4	386.3	386.3	386.3	386.3
4.61	386.4	386.4	386.4	386.4	386.3	386.3	386.3	386.3	386.2
4.82	386.4	386.4	386.4	386.3	386.3	386.3	386.3	386.2	386.2

CO2 Purity									
Condenser Duty (Watts)	-11500	-12075	-12650	-13225	-13800	-10925	-10350	-9775	-9200
% Change from Nominal	-20%	-15%	-10%	-5%	0%	5%	10%	15%	20%
Inlet CO2 Conc (Side)/Inlet Flue Gas Flowrate (Down)	0.18375								
3.21	92.01%	93.54%	94.95%	96.18%	97.12%	97.70%	97.96%	98.04%	98.05%
3.41	94.11%	95.46%	96.64%	97.56%	98.14%	98.42%	98.50%	98.52%	98.52%
3.61	94.43%	95.70%	96.80%	97.64%	98.16%	98.39%	98.47%	98.48%	98.48%
3.81	94.47%	95.73%	96.82%	97.64%	98.15%	98.38%	98.45%	98.47%	98.47%
4.01	94.50%	95.74%	96.81%	97.63%	98.13%	98.36%	98.44%	98.45%	98.45%
4.21	94.50%	95.74%	96.80%	97.61%	98.11%	98.35%	98.43%	98.44%	98.44%
4.41	94.50%	95.73%	96.78%	97.59%	98.10%	98.33%	98.41%	98.43%	98.43%
4.61	94.49%	95.70%	96.76%	97.56%	98.08%	98.32%	98.40%	98.42%	98.42%
4.82	94.46%	95.68%	96.72%	97.53%	98.05%	98.30%	98.39%	98.41%	98.41%

Condensor Temperature Condenser Duty (Watts)	-11500	-12075	-12650	-13225	-13800	-10925	-10350	-9775	-9200
% Change from Nominal	-20%	-15%	-10%	-5%	0%	5%	10%	15%	20%
Inlet CO2 Conc (Side)/Inlet Flue Gas Flowrate (Down)	0.1925								
3.21	314.0	307.7	299.7	289.6	276.9	261.5	244.3	226.1	206.8
3.41	311.8	305.1	296.7	286.0	272.5	256.8	239.5	221.2	201.8
3.61	310.5	303.7	295.2	284.3	271.0	255.3	238.4	220.5	201.4
3.81	310.3	303.5	295.0	284.2	270.9	255.4	238.6	220.9	202.2
4.01	310.1	303.4	294.9	284.3	271.1	255.7	239.1	221.5	202.9
4.21	310.1	303.4	295.0	284.4	271.4	256.2	239.6	222.2	203.7
4.41	310.2	303.5	295.1	284.7	271.8	256.7	240.3	222.9	204.7
4.61	310.2	303.6	295.4	285.1	272.4	257.3	241.0	223.8	205.7
4.82	310.3	303.7	295.6	285.4	272.8	258.1	241.8	224.7	206.8

Reboiler Temperature Condenser Duty (Watts)	-11500	-12075	-12650	-13225	-13800	-10925	-10350	-9775	-9200
% Change from Nominal	-20%	-15%	-10%	-5%	0%	5%	10%	15%	20%
Inlet CO2 Conc (Side)/Inlet Flue Gas Flowrate (Down)	0.1925								
3.21	386.9	386.9	386.9	386.9	386.8	386.8	386.8	386.8	386.8
3.41	386.7	386.7	386.7	386.6	386.6	386.6	386.6	386.5	386.5
3.61	386.5	386.5	386.5	386.5	386.4	386.4	386.4	386.4	386.3
3.81	386.5	386.4	386.4	386.4	386.4	386.4	386.3	386.3	386.3
4.01	386.4	386.4	386.4	386.4	386.4	386.3	386.3	386.3	386.3
4.21	386.4	386.4	386.4	386.4	386.3	386.3	386.3	386.3	386.2
4.41	386.4	386.4	386.4	386.3	386.3	386.3	386.3	386.2	386.2
4.61	386.4	386.4	386.3	386.3	386.3	386.3	386.3	386.2	386.2
4.82	386.4	386.3	386.3	386.3	386.3	386.3	386.2	386.2	386.2

CO2 Purity Condenser Duty (Watts)	-11500	-12075	-12650	-13225	-13800	-10925	-10350	-9775	-9200
% Change from Nominal	-20%	-15%	-10%	-5%	0%	5%	10%	15%	20%
Inlet CO2 Conc (Side)/Inlet Flue Gas Flowrate (Down)	0.1925								
3.21	93.57%	94.98%	96.23%	97.23%	97.90%	98.24%	98.36%	98.39%	98.39%
3.41	94.25%	95.58%	96.74%	97.63%	98.19%	98.44%	98.53%	98.54%	98.54%
3.61	94.50%	95.77%	96.85%	97.68%	98.19%	98.42%	98.49%	98.50%	98.50%
3.81	94.55%	95.79%	96.86%	97.67%	98.17%	98.40%	98.47%	98.48%	98.48%
4.01	94.56%	95.79%	96.85%	97.66%	98.15%	98.38%	98.46%	98.47%	98.47%
4.21	94.55%	95.78%	96.83%	97.64%	98.13%	98.37%	98.44%	98.46%	98.46%
4.41	94.53%	95.76%	96.81%	97.61%	98.12%	98.35%	98.43%	98.45%	98.45%
4.61	94.51%	95.73%	96.78%	97.58%	98.09%	98.34%	98.42%	98.44%	98.44%
4.82	94.48%	95.70%	96.74%	97.55%	98.07%	98.32%	98.41%	98.43%	98.43%

Condensor Temperature									
Condenser Duty (Watts)	-11500	-12075	-12650	-13225	-13800	-10925	-10350	-9775	-9200
% Change from Nominal	-20%	-15%	-10%	-5%	0%	5%	10%	15%	20%
Inlet CO2 Conc (Side)/Inlet Flue Gas Flowrate (Down)	0.20125								
3.21	312.5	305.9	297.5	287.0	273.7	258.0	240.7	222.3	203.0
3.41	310.6	303.7	295.1	284.2	270.8	255.1	237.9	220.0	200.9
3.61	310.2	303.4	294.8	284.0	270.6	255.0	238.1	220.4	201.5
3.81	310.1	303.2	294.8	284.0	270.8	255.4	238.5	221.0	202.2
4.01	310.0	303.3	294.8	284.2	271.1	255.7	239.1	221.6	203.2
4.21	310.0	303.3	294.9	284.4	271.5	256.2	239.7	222.2	203.9
4.41	310.1	303.4	295.1	284.8	271.9	256.9	240.4	223.1	205.0
4.61	310.2	303.6	295.4	285.1	272.4	257.6	241.3	224.1	206.0
4.82	310.3	303.8	295.7	285.5	273.1	258.2	242.1	225.1	207.2

Reboiler Temperature									
Condenser Duty (Watts)	-11500	-12075	-12650	-13225	-13800	-10925	-10350	-9775	-9200
% Change from Nominal	-20%	-15%	-10%	-5%	0%	5%	10%	15%	20%
Inlet CO2 Conc (Side)/Inlet Flue Gas Flowrate (Down)	0.20125								
3.21	386.8	386.7	386.7	386.7	386.7	386.7	386.6	386.6	386.6
3.41	386.5	386.5	386.5	386.5	386.5	386.4	386.4	386.4	386.4
3.61	386.5	386.4	386.4	386.4	386.4	386.4	386.3	386.3	386.3
3.81	386.4	386.4	386.4	386.4	386.4	386.3	386.3	386.3	386.3
4.01	386.4	386.4	386.4	386.4	386.3	386.3	386.3	386.3	386.2
4.21	386.4	386.4	386.4	386.3	386.3	386.3	386.3	386.2	386.2
4.41	386.4	386.4	386.3	386.3	386.3	386.3	386.3	386.2	386.2
4.61	386.4	386.3	386.3	386.3	386.3	386.3	386.2	386.2	386.2
4.82	386.3	386.3	386.3	386.3	386.3	386.3	386.2	386.2	386.2

CO2 Purity									
Condenser Duty (Watts)	-11500	-12075	-12650	-13225	-13800	-10925	-10350	-9775	-9200
% Change from Nominal	-20%	-15%	-10%	-5%	0%	5%	10%	15%	20%
Inlet CO2 Conc (Side)/Inlet Flue Gas Flowrate (Down)	0.20125								
3.21	94.07%	95.44%	96.62%	97.55%	98.14%	98.42%	98.51%	98.52%	98.52%
3.41	94.52%	95.81%	96.89%	97.72%	98.22%	98.45%	98.52%	98.53%	98.53%
3.61	94.58%	95.83%	96.91%	97.71%	98.21%	98.43%	98.50%	98.51%	98.51%
3.81	94.60%	95.84%	96.89%	97.70%	98.19%	98.41%	98.49%	98.50%	98.50%
4.01	94.60%	95.83%	96.88%	97.68%	98.17%	98.40%	98.47%	98.49%	98.49%
4.21	94.59%	95.80%	96.86%	97.65%	98.15%	98.39%	98.46%	98.48%	98.48%
4.41	94.57%	95.78%	96.83%	97.63%	98.13%	98.37%	98.45%	98.47%	98.47%
4.61	94.54%	95.75%	96.79%	97.59%	98.11%	98.35%	98.44%	98.46%	98.46%
4.82	94.51%	95.71%	96.75%	97.56%	98.08%	98.34%	98.43%	98.45%	98.45%

Condensor Temperature Condenser Duty (Watts)	-11500	-12075	-12650	-13225	-13800	-10925	-10350	-9775	-9200
% Change from Nominal	-20%	-15%	-10%	-5%	0%	5%	10%	15%	20%
Inlet CO2 Conc (Side)/Inlet Flue Gas Flowrate (Down)	0.21								
3.21	310.3	303.4	294.8	283.9	270.4	254.6	237.6	219.6	200.6
3.41	310.2	303.3	294.7	283.8	270.3	254.7	237.7	219.8	200.8
3.61	310.0	303.2	294.6	283.8	270.4	254.8	238.0	220.3	201.4
3.81	309.9	303.1	294.6	283.8	270.7	255.2	238.5	220.9	202.2
4.01	309.9	303.1	294.8	284.1	271.0	255.7	239.2	221.6	203.3
4.21	310.0	303.3	294.9	284.3	271.4	256.3	239.8	222.5	204.1
4.41	310.0	303.4	295.1	284.8	271.9	257.1	240.6	223.4	205.3
4.61	310.1	303.6	295.4	285.2	272.6	257.7	241.5	224.4	206.4
4.82	310.3	303.8	295.8	285.7	273.2	258.6	242.5	225.5	207.7

Reboiler Temperature Condenser Duty (Watts)	-11500	-12075	-12650	-13225	-13800	-10925	-10350	-9775	-9200
% Change from Nominal	-20%	-15%	-10%	-5%	0%	5%	10%	15%	20%
Inlet CO2 Conc (Side)/Inlet Flue Gas Flowrate (Down)	0.21								
3.21	386.5	386.5	386.5	386.4	386.4	386.4	386.4	386.3	386.3
3.41	386.5	386.5	386.4	386.4	386.4	386.4	386.4	386.3	386.3
3.61	386.4	386.4	386.4	386.4	386.4	386.3	386.3	386.3	386.3
3.81	386.4	386.4	386.4	386.3	386.3	386.3	386.3	386.3	386.2
4.01	386.4	386.4	386.4	386.3	386.3	386.3	386.3	386.2	386.2
4.21	386.4	386.3	386.3	386.3	386.3	386.3	386.2	386.2	386.2
4.41	386.3	386.3	386.3	386.3	386.3	386.3	386.2	386.2	386.2
4.61	386.3	386.3	386.3	386.3	386.3	386.2	386.2	386.2	386.2
4.82	386.3	386.3	386.3	386.3	386.3	386.2	386.2	386.2	386.2

CO2 Purity Condenser Duty (Watts)	-11500	-12075	-12650	-13225	-13800	-10925	-10350	-9775	-9200
% Change from Nominal	-20%	-15%	-10%	-5%	0%	5%	10%	15%	20%
Inlet CO2 Conc (Side)/Inlet Flue Gas Flowrate (Down)	0.21								
3.21	94.59%	95.86%	96.94%	97.76%	98.25%	98.47%	98.54%	98.55%	98.55%
3.41	94.61%	95.87%	96.94%	97.75%	98.25%	98.46%	98.53%	98.54%	98.54%
3.61	94.64%	95.88%	96.94%	97.74%	98.23%	98.45%	98.52%	98.53%	98.53%
3.81	94.65%	95.88%	96.93%	97.72%	98.21%	98.43%	98.50%	98.52%	98.52%
4.01	94.63%	95.86%	96.90%	97.70%	98.19%	98.42%	98.49%	98.50%	98.51%
4.21	94.61%	95.83%	96.88%	97.68%	98.17%	98.40%	98.48%	98.50%	98.49%
4.41	94.59%	95.80%	96.85%	97.64%	98.15%	98.39%	98.47%	98.49%	98.49%
4.61	94.56%	95.77%	96.81%	97.61%	98.12%	98.37%	98.46%	98.48%	98.48%
4.82	94.52%	95.73%	96.76%	97.57%	98.10%	98.35%	98.45%	98.47%	98.47%

Condensor Temperature									
Reboiler Duty (Watts)	124000	131750	139500	147250	155000	162750	170500	178250	186000
% Change from Nominal	-20%	-15%	-10%	-5%	0%	5%	10%	15%	20%
Inlet CO2 Conc (Side)/Inlet Flue Gas Flowrate (Down)					0.14				
3.21									
3.41									
3.61									
3.81			205.65	255.01	289.11	308.51	317.69	329.45	344.59
4.01				249.32	283.27	303.95	315.79	321.86	339.17
4.21			198.72	244.77	278.05	299.37	312.86	317.56	332.98
4.41			199.61	243.09	275.18	296.07	310.13	317.11	327.12
4.61			201.51	242.93	273.52	293.65	307.44	316.45	321.74
4.82			203.67	243.49	273.05	292.67	306.16	315.77	319.03

Reboiler Temperature									
Reboiler Duty (Watts)	124000	131750	139500	147250	155000	162750	170500	178250	186000
% Change from Nominal	-20%	-15%	-10%	-5%	0%	5%	10%	15%	20%
Inlet CO2 Conc (Side)/Inlet Flue Gas Flowrate (Down)					0.14				
3.21									
3.41									
3.61									
3.81			385.74	386.60	387.32	387.91	388.40	388.75	388.91
4.01				386.34	387.11	387.74	388.25	388.68	388.88
4.21			385.14	386.09	386.90	387.57	388.12	388.59	388.85
4.41			384.91	385.89	386.74	387.44	388.02	388.50	388.84
4.61			384.71	385.72	386.60	387.33	387.94	388.43	388.84
4.82			384.60	385.63	386.52	387.28	387.90	388.40	388.83

CO2 Purity									
Reboiler Duty (Watts)	124000	131750	139500	147250	155000	162750	170500	178250	186000
% Change from Nominal	-20%	-15%	-10%	-5%	0%	5%	10%	15%	20%
Inlet CO2 Conc (Side)/Inlet Flue Gas Flowrate (Down)					0.14				
3.21									
3.41									
3.61									
3.81			97.46%	97.67%	96.88%	94.62%	92.53%	88.04%	77.91%
4.01				97.93%	97.42%	95.59%	93.21%	91.41%	82.36%
4.21			97.97%	98.15%	97.84%	96.40%	94.11%	92.95%	86.47%
4.41			97.98%	98.16%	97.93%	96.77%	94.72%	93.07%	89.46%
4.61			97.96%	98.14%	97.96%	96.99%	95.24%	93.23%	91.62%
4.82			97.95%	98.12%	97.95%	97.05%	95.45%	93.40%	92.53%

Condensor Temperature									
Reboiler Duty (Watts)	124000	131750	139500	147250	155000	162750	170500	178250	186000
% Change from Nominal	-20%	-15%	-10%	-5%	0%	5%	10%	15%	20%
Inlet CO2 Conc (Side)/Inlet Flue Gas Flowrate (Down)	0.14875								
3.21									
3.41									
3.61			205.93	255.23	289.32	308.69	317.75	329.73	344.75
3.81			201.12	248.54	282.30	303.18	315.36	320.78	338.19
4.01			198.32	244.24	277.46	298.88	312.50	317.45	332.26
4.21			199.04	242.51	274.47	295.46	309.47	317.07	326.07
4.41			201.43	242.31	272.91	293.05	306.86	316.20	320.56
4.61			203.22	242.97	272.63	292.29	305.79	315.57	318.37
4.82			204.71	243.67	272.73	291.99	305.26	315.18	317.30

Reboiler Temperature									
Reboiler Duty (Watts)	124000	131750	139500	147250	155000	162750	170500	178250	186000
% Change from Nominal	-20%	-15%	-10%	-5%	0%	5%	10%	15%	20%
Inlet CO2 Conc (Side)/Inlet Flue Gas Flowrate (Down)	0.14875								
3.21									
3.41									
3.61			385.76	386.61	387.33	387.91	388.40	388.75	388.91
3.81			385.39	386.30	387.07	387.71	388.23	388.67	388.88
4.01			385.12	386.06	386.87	387.55	388.10	388.57	
4.21			384.87	385.85	386.70	387.42	387.99	388.48	388.84
4.41			384.66	385.67	386.55	387.30	387.91	388.41	388.83
4.61			384.56	385.59	386.49	387.25	387.88	388.38	388.82
4.82			384.51	385.55	386.46	387.23	387.86	388.37	388.82

CO2 Purity									
Reboiler Duty (Watts)	124000	131750	139500	147250	155000	162750	170500	178250	186000
% Change from Nominal	-20%	-15%	-10%	-5%	0%	5%	10%	15%	20%
Inlet CO2 Conc (Side)/Inlet Flue Gas Flowrate (Down)	0.14875								
3.21									
3.41									
3.61			97.44%	97.66%	96.85%	94.58%	92.50%	87.89%	77.76%
3.81			97.75%	97.96%	97.50%	95.73%	93.35%	91.81%	83.08%
4.01			98.00%	98.19%	97.88%	96.48%	94.21%	93.00%	86.90%
4.21			98.02%	98.20%	97.99%	96.87%	94.89%	93.10%	89.95%
4.41			98.00%	98.17%	98.00%	97.07%	95.37%	93.32%	92.06%
4.61			97.99%	98.15%	97.99%	97.11%	95.54%	93.48%	92.76%
4.82			97.98%	98.14%	97.97%	97.13%	95.61%	93.57%	93.07%

Condensor Temperature									
Reboiler Duty (Watts)	124000	131750	139500	147250	155000	162750	170500	178250	186000
% Change from Nominal	-20%	-15%	-10%	-5%	0%	5%	10%	15%	20%
Inlet CO2 Conc (Side)/Inlet Flue Gas Flowrate (Down)					0.1575				
3.21									
3.41									
3.61									
3.81			198.34	244.22	277.73	299.10	312.72	317.53	332.58
4.01			198.34	241.98	274.10	295.19	309.26	317.06	325.69
4.21			200.54	241.89	272.53	292.73	306.58	316.08	320.05
4.41			202.64	242.96	272.31	292.00	305.54	315.43	317.96
4.61			204.17	243.14	272.42	291.71	305.02	315.04	317.00
4.82			205.48	243.92	272.57	291.60	304.69	314.75	316.41

Reboiler Temperature									
Reboiler Duty (Watts)	124000	131750	139500	147250	155000	162750	170500	178250	186000
% Change from Nominal	-20%	-15%	-10%	-5%	0%	5%	10%	15%	20%
Inlet CO2 Conc (Side)/Inlet Flue Gas Flowrate (Down)					0.1575				
3.21									
3.41									
3.61									
3.81			385.13	386.07	386.88	387.56	388.10	388.57	388.85
4.01			384.85	385.83	386.69	387.40	387.98	388.46	388.83
4.21			384.63	385.64	386.54	387.28	387.90	388.39	388.82
4.41			384.54	385.58	386.47	387.24	387.86	388.37	388.81
4.61			384.49	385.53	386.44	387.21	387.84	388.35	388.81
4.82			384.45	385.49	386.41	387.19	387.83	388.35	388.80

CO2 Purity									
Reboiler Duty (Watts)	124000	131750	139500	147250	155000	162750	170500	178250	186000
% Change from Nominal	-20%	-15%	-10%	-5%	0%	5%	10%	15%	20%
Inlet CO2 Conc (Side)/Inlet Flue Gas Flowrate (Down)					0.1575				
3.21									
3.41									
3.61									
3.81			97.98%	98.17%	97.86%	96.44%	94.15%	92.97%	86.71%
4.01			98.07%	98.24%	98.03%	96.92%	94.96%	93.13%	90.13%
4.21			98.04%	98.21%	98.04%	97.12%	95.44%	93.38%	92.25%
4.41			98.03%	98.19%	98.03%	97.17%	95.60%	93.54%	92.90%
4.61			98.01%	98.17%	98.01%	97.18%	95.68%	93.63%	93.18%
4.82			98.00%	98.16%	98.00%	97.18%	95.72%	93.70%	93.34%

Condensor Temperature Reboiler Duty (Watts)	124000	131750	139500	147250	155000	162750	170500	178250	186000
% Change from Nominal	-20%	-15%	-10%	-5%	0%	5%	10%	15%	20%
Inlet CO2 Conc (Side)/Inlet Flue Gas Flowrate (Down)	0.16625								
3.21									
3.41			205.31	254.70	288.80	308.36	317.65	329.16	344.38
3.61			198.84	245.15	279.13	299.98	313.32	317.87	333.91
3.81			197.54	241.53	273.99	295.29	309.49	317.13	326.11
4.01			200.18	241.35	272.16	292.52	306.42	316.03	319.80
4.21			202.06	242.03	271.86	291.77	305.38	315.34	317.73
4.41			203.46	242.78	272.00	291.46	304.82	314.92	316.77
4.61			204.87	243.45	272.19	291.35	304.49	314.62	316.23
4.82				244.22	272.59	291.35	304.28	314.40	315.92

Reboiler Temperature Reboiler Duty (Watts)	124000	131750	139500	147250	155000	162750	170500	178250	186000
% Change from Nominal	-20%	-15%	-10%	-5%	0%	5%	10%	15%	20%
Inlet CO2 Conc (Side)/Inlet Flue Gas Flowrate (Down)	0.16625								
3.21									
3.41			385.73	386.59	387.31	387.90	388.39	388.74	388.91
3.61			385.18	386.12	386.93	387.59	388.13	388.60	388.85
3.81			384.86	385.84	386.69	387.40	387.98	388.46	388.82
4.01			384.62	385.63	386.52	387.27	387.89	388.38	388.81
4.21			384.52	385.55	386.45	387.22	387.85	388.36	388.80
4.41			384.46	385.51	386.42	387.19	387.83	388.34	388.80
4.61			384.43	385.48	386.39	387.17	387.82	388.33	388.79
4.82				385.45	386.38	387.16	387.81	388.33	388.79

CO2 Purity Reboiler Duty (Watts)	124000	131750	139500	147250	155000	162750	170500	178250	186000
% Change from Nominal	-20%	-15%	-10%	-5%	0%	5%	10%	15%	20%
Inlet CO2 Conc (Side)/Inlet Flue Gas Flowrate (Down)	0.16625								
3.21									
3.41			97.46%	97.67%	96.90%	94.65%	92.54%	88.18%	78.09%
3.61			97.92%	98.11%	97.76%	96.29%	93.97%	92.83%	85.91%
3.81			98.11%	98.28%	98.07%	96.94%	94.94%	93.14%	89.97%
4.01			98.08%	98.25%	98.09%	97.17%	95.50%	93.42%	92.35%
4.21			98.06%	98.23%	98.07%	97.22%	95.66%	93.59%	93.00%
4.41			98.05%	98.21%	98.05%	97.23%	95.74%	93.69%	93.27%
4.61			98.04%	98.20%	98.04%	97.22%	95.78%	93.75%	93.41%
4.82				98.18%	98.02%	97.21%	95.81%	93.80%	93.49%

Condensor Temperature									
Reboiler Duty (Watts)	124000	131750	139500	147250	155000	162750	170500	178250	186000
% Change from Nominal	-20%	-15%	-10%	-5%	0%	5%	10%	15%	20%
Inlet CO2 Conc (Side)/Inlet Flue Gas Flowrate (Down)	0.175								
3.21			204.02	252.98	287.06	307.02	317.19	326.92	342.89
3.41			198.03	243.85	277.36	298.82	312.46	317.48	332.12
3.61			196.69	241.45	274.24	295.88	310.08	317.23	327.38
3.81			199.19	240.90	271.87	292.49	306.52	316.09	320.04
4.01			201.13	241.60	271.57	291.56	305.24	315.30	317.61
4.21			202.60	242.14	271.59	291.29	304.70	314.87	316.68
4.41			204.31	242.86	271.84	291.13	304.33	314.53	316.11
4.61				243.76	272.23	291.12	304.11	314.29	315.83
4.82				244.53	272.61	291.18	303.96	314.08	315.67

Reboiler Temperature									
Reboiler Duty (Watts)	124000	131750	139500	147250	155000	162750	170500	178250	186000
% Change from Nominal	-20%	-15%	-10%	-5%	0%	5%	10%	15%	20%
Inlet CO2 Conc (Side)/Inlet Flue Gas Flowrate (Down)	0.175								
3.21			385.64	386.52	387.25	387.85	388.35	388.73	388.90
3.41			385.11	386.05	386.86	387.54	388.09	388.56	388.84
3.61			384.91	385.88	386.72	387.42	388.00	388.48	388.82
3.81			384.63	385.64	386.52	387.27	387.88	388.38	388.80
4.01			384.51	385.55	386.45	387.21	387.84	388.35	388.79
4.21			384.45	385.50	386.41	387.18	387.82	388.33	388.79
4.41			384.42	385.46	386.38	387.17	387.81	388.32	388.78
4.61				385.44	386.36	387.15	387.80	388.32	388.78
4.82				385.42	386.35	387.14	387.79	388.31	388.78

CO2 Purity									
Reboiler Duty (Watts)	124000	131750	139500	147250	155000	162750	170500	178250	186000
% Change from Nominal	-20%	-15%	-10%	-5%	0%	5%	10%	15%	20%
Inlet CO2 Conc (Side)/Inlet Flue Gas Flowrate (Down)	0.175								
3.21			97.53%	97.74%	97.06%	94.95%	92.71%	89.27%	79.40%
3.41			97.98%	98.17%	97.88%	96.48%	94.21%	92.98%	86.97%
3.61			98.14%	98.31%	98.09%	96.91%	94.84%	93.13%	89.43%
3.81			98.12%	98.29%	98.13%	97.20%	95.51%	93.42%	92.30%
4.01			98.10%	98.26%	98.11%	97.26%	95.71%	93.62%	93.05%
4.21			98.09%	98.25%	98.09%	97.27%	95.78%	93.72%	93.32%
4.41			98.08%	98.23%	98.08%	97.27%	95.83%	93.80%	93.47%
4.61				98.22%	98.06%	97.26%	95.86%	93.85%	93.54%
4.82				98.21%	98.04%	97.24%	95.87%	93.90%	93.57%

Condensor Temperature									
Reboiler Duty (Watts)	124000	131750	139500	147250	155000	162750	170500	178250	186000
% Change from Nominal	-20%	-15%	-10%	-5%	0%	5%	10%	15%	20%
Inlet CO2 Conc (Side)/Inlet Flue Gas Flowrate (Down)	0.18375								
3.21			203.58	252.30	286.42	306.54	317.02	326.00	342.31
3.41			196.05	240.67	273.49	295.06	309.35	317.15	325.91
3.61			199.14	240.56	271.47	291.93	305.87	315.75	318.88
3.81			200.29	241.11	271.26	291.45	305.23	315.31	317.67
4.01			201.94	241.61	271.32	291.07	304.61	314.81	316.61
4.21			203.26	242.48	271.52	290.92	304.22	314.47	316.12
4.41				243.07	271.81	290.90	303.95	314.21	315.77
4.61				243.98	272.24	291.41	303.80	313.99	315.62
4.82				244.88	272.76	291.09	303.72	313.83	315.58

Reboiler Temperature									
Reboiler Duty (Watts)	124000	131750	139500	147250	155000	162750	170500	178250	186000
% Change from Nominal	-20%	-15%	-10%	-5%	0%	5%	10%	15%	20%
Inlet CO2 Conc (Side)/Inlet Flue Gas Flowrate (Down)	0.18375								
3.21			385.61	386.49	387.23	387.83	388.33	388.72	388.89
3.41			384.84	385.82	386.67	387.39	387.97	388.45	388.81
3.61			384.56	385.59	386.48	387.24	387.86	388.36	388.79
3.81			384.51	385.54	386.44	387.21	387.84	388.34	388.79
4.01			384.44	385.49	386.40	387.17	387.81	388.32	388.78
4.21			384.40	385.46	386.38	387.15	387.80	388.32	388.78
4.41				385.42	386.35	387.14	387.79	388.31	388.77
4.61				385.40	386.34	387.15	387.78	388.30	388.77
4.82				385.39	386.32	387.11	387.77	388.30	388.77

CO2 Purity									
Reboiler Duty (Watts)	124000	131750	139500	147250	155000	162750	170500	178250	186000
% Change from Nominal	-20%	-15%	-10%	-5%	0%	5%	10%	15%	20%
Inlet CO2 Conc (Side)/Inlet Flue Gas Flowrate (Down)	0.18375								
3.21			97.55%	97.77%	97.12%	95.05%	92.77%	89.68%	79.88%
3.41			98.18%	98.34%	98.14%	97.02%	95.01%	93.17%	90.10%
3.61			98.15%	98.31%	98.16%	97.27%	95.64%	93.53%	92.69%
3.81			98.14%	98.30%	98.15%	97.30%	95.73%	93.64%	93.05%
4.01			98.13%	98.28%	98.13%	97.31%	95.82%	93.76%	93.35%
4.21			98.11%	98.27%	98.11%	97.31%	95.87%	93.84%	93.49%
4.41				98.25%	98.10%	97.30%	95.91%	93.90%	93.57%
4.61				98.24%	98.08%	97.26%	95.92%	93.94%	93.60%
4.82				98.23%	98.05%	97.27%	95.92%	93.98%	93.61%

Condensor Temperature Reboiler Duty (Watts)	124000	131750	139500	147250	155000	162750	170500	178250	186000
% Change from Nominal	-20%	-15%	-10%	-5%	0%	5%	10%	15%	20%
Inlet CO2 Conc (Side)/Inlet Flue Gas Flowrate (Down)	0.1925								
3.21			197.48	243.39	276.89	298.35	312.13	317.43	331.42
3.41			195.85	239.89	272.53	294.00	308.33	316.92	323.85
3.61			199.12	240.36	271.00	291.41	305.34	315.41	317.91
3.81			201.00	241.02	270.90	290.95	304.56	314.82	316.65
4.01			202.33	241.81	271.11	290.75	304.14	314.43	316.05
4.21				242.54	271.44	290.60	303.85	314.14	315.74
4.41				243.35	271.77	290.72	303.66	313.91	315.60
4.61				244.32	272.35	290.86	303.57	313.75	315.57
4.82				245.24	272.83	291.04	303.53	313.63	315.60

Reboiler Temperature Reboiler Duty (Watts)	124000	131750	139500	147250	155000	162750	170500	178250	186000
% Change from Nominal	-20%	-15%	-10%	-5%	0%	5%	10%	15%	20%
Inlet CO2 Conc (Side)/Inlet Flue Gas Flowrate (Down)	0.1925								
3.21			385.07	386.02	386.84	387.52	388.07	388.55	388.84
3.41			384.76	385.75	386.61	387.34	387.93	388.42	388.80
3.61			384.51	385.54	386.44	387.21	387.83	388.34	388.78
3.81			384.44	385.48	386.39	387.17	387.81	388.32	388.78
4.01			384.39	385.45	386.36	387.15	387.79	388.31	388.77
4.21				385.42	386.34	387.13	387.78	388.30	388.77
4.41				385.39	386.32	387.12	387.77	388.29	388.76
4.61				385.38	386.31	387.11	387.76	388.29	388.76
4.82				385.36	386.30	387.10	387.76	388.29	388.76

CO2 Purity Reboiler Duty (Watts)	124000	131750	139500	147250	155000	162750	170500	178250	186000
% Change from Nominal	-20%	-15%	-10%	-5%	0%	5%	10%	15%	20%
Inlet CO2 Conc (Side)/Inlet Flue Gas Flowrate (Down)	0.1925								
3.21			98.00%	98.18%	97.90%	96.54%	94.30%	93.00%	87.35%
3.41			98.21%	98.37%	98.19%	97.14%	95.23%	93.25%	90.96%
3.61			98.17%	98.33%	98.19%	97.33%	95.74%	95.74%	93.00%
3.81			98.16%	98.31%	98.17%	97.35%	95.85%	93.78%	93.36%
4.01			98.15%	98.30%	98.15%	97.35%	95.91%	93.87%	93.52%
4.21				98.29%	98.13%	97.35%	95.95%	93.93%	93.60%
4.41				98.27%	98.12%	97.33%	95.97%	93.99%	93.63%
4.61				98.26%	98.09%	97.31%	97.31%	94.02%	93.63%
4.82				98.25%	98.07%	97.29%	95.97%	94.04%	93.61%

Condensor Temperature Reboiler Duty (Watts)	124000	131750	139500	147250	155000	162750	170500	178250	186000
% Change from Nominal	-20%	-15%	-10%	-5%	0%	5%	10%	15%	20%
Inlet CO2 Conc (Side)/Inlet Flue Gas Flowrate (Down)	0.20125								
3.21			195.68	240.67	273.72	295.36	309.66	317.23	326.54
3.41			197.99	239.78	270.79	291.44	305.51	315.55	318.27
3.61			200.05	240.38	270.63	290.83	304.08	314.90	316.78
3.81			201.57	240.99	270.85	290.58	304.08	314.43	316.07
4.01				241.89	271.06	290.49	303.75	314.11	315.74
4.21				242.73	271.45	290.51	303.53	313.86	315.59
4.41				243.50	271.89	290.60	303.42	313.67	315.56
4.61				244.69	272.39	290.79	303.38	313.56	315.60
4.82				245.80	273.07	291.03	303.39	313.46	315.69

Reboiler Temperature Reboiler Duty (Watts)	124000	131750	139500	147250	155000	162750	170500	178250	186000
% Change from Nominal	-20%	-15%	-10%	-5%	0%	5%	10%	15%	20%
Inlet CO2 Conc (Side)/Inlet Flue Gas Flowrate (Down)	0.20125								
3.21			384.87	385.84	386.69	387.40	387.97	388.45	388.81
3.41			384.52	385.56	386.45	387.21	387.84	388.34	388.78
3.61			384.45	385.48	386.40	387.17	387.78	388.32	388.77
3.81			384.39	385.44	386.36	387.14	387.79	388.30	388.76
4.01				385.41	386.34	387.12	387.77	388.29	388.76
4.21				385.38	386.32	387.11	387.76	388.29	388.76
4.41				385.36	386.30	387.10	387.76	388.28	388.75
4.61				385.35	386.29	387.08	387.75	388.28	388.75
4.82				385.34	386.28	387.08	387.75	388.28	388.75

CO2 Purity Reboiler Duty (Watts)	124000	131750	139500	147250	155000	162750	170500	178250	186000
% Change from Nominal	-20%	-15%	-10%	-5%	0%	5%	10%	15%	20%
Inlet CO2 Conc (Side)/Inlet Flue Gas Flowrate (Down)	0.20125								
3.21			98.18%	98.35%	98.14%	96.99%	94.95%	93.15%	89.83%
3.41			98.21%	98.37%	98.22%	97.36%	95.74%	93.62%	92.91%
3.61			98.20%	98.35%	98.21%	97.39%	95.97%	93.78%	93.35%
3.81			98.18%	98.33%	98.19%	97.39%	95.94%	93.89%	93.54%
4.01				98.32%	98.17%	97.39%	95.99%	93.97%	93.62%
4.21				98.31%	98.15%	97.38%	96.01%	94.02%	93.65%
4.41				98.29%	98.13%	97.36%	96.02%	94.06%	93.65%
4.61				98.28%	98.11%	97.34%	96.02%	94.08%	93.63%
4.82				98.27%	98.08%	97.31%	96.01%	94.10%	93.60%

Condensor Temperature Reboiler Duty (Watts)	124000	131750	139500	147250	155000	162750	170500	178250	186000
% Change from Nominal	-20%	-15%	-10%	-5%	0%	5%	10%	15%	20%
Inlet CO2 Conc (Side)/Inlet Flue Gas Flowrate (Down)	0.21								
3.21			198.13	239.19	270.41	291.03	305.02	315.25	317.54
3.41			198.89	239.75	270.32	290.82	304.72	315.01	317.02
3.61			200.48	240.21	270.39	290.45	304.08	314.47	316.15
3.81				241.24	270.66	290.30	303.69	314.10	315.75
4.01				242.09	270.99	290.31	303.45	313.82	315.59
4.21				242.92	271.40	290.37	303.30	313.62	315.56
4.41				244.02	271.93	290.56	303.24	313.46	315.60
4.61				245.05	272.60	290.77	303.23	313.36	315.70
4.82				246.14	273.22	291.07	303.28	313.30	315.82

Reboiler Temperature Reboiler Duty (Watts)	124000	131750	139500	147250	155000	162750	170500	178250	186000
% Change from Nominal	-20%	-15%	-10%	-5%	0%	5%	10%	15%	20%
Inlet CO2 Conc (Side)/Inlet Flue Gas Flowrate (Down)	0.21								
3.21			384.49	385.70	386.42	387.19	387.81	388.32	388.77
3.41			384.46	385.49	386.40	387.17	387.80	388.31	388.77
3.61			384.40	385.43	386.36	387.14	387.78	388.30	388.76
3.81				385.41	386.33	387.12	387.77	388.29	388.75
4.01				385.38	386.31	387.10	387.76	388.28	388.75
4.21				385.36	386.29	387.09	387.75	388.28	388.75
4.41				385.34	386.27	387.08	387.74	388.27	388.74
4.61				385.33	386.27	387.07	387.74	388.27	388.74
4.82				385.31	386.26	387.06	387.73	388.27	388.74

CO2 Purity Reboiler Duty (Watts)	124000	131750	139500	147250	155000	162750	170500	178250	186000
% Change from Nominal	-20%	-15%	-10%	-5%	0%	5%	10%	15%	20%
Inlet CO2 Conc (Side)/Inlet Flue Gas Flowrate (Down)	0.21								
3.21			98.24%	98.42%	98.25%	97.41%	95.84%	93.72%	93.15%
3.41			98.23%	98.38%	98.25%	97.42%	95.88%	93.78%	93.30%
3.61			98.22%	98.36%	98.23%	97.43%	95.97%	93.90%	93.54%
3.81				98.35%	98.21%	97.43%	96.02%	93.99%	93.64%
4.01				98.34%	98.19%	97.42%	96.05%	94.05%	93.67%
4.21				98.33%	98.17%	97.40%	96.06%	94.09%	93.67%
4.41				98.32%	98.15%	97.38%	96.06%	94.12%	93.65%
4.61				98.30%	98.12%	97.35%	96.05%	94.14%	93.62%
4.82				98.29%	98.10%	97.32%	96.04%	94.15%	93.58%

Appendix B: Model Equations

A summary of the model equations used is provided below

B.1 Packed Columns

The packed columns used in the simulation were developed by (Harun, 2012) using a rate based calculation for the absorber column and a equilibrium model for the desorption column.

B.1.1 Mass Balance

$$\frac{dC_{g,i}}{dt} = -u_g \frac{\partial C_{g,i}}{\partial z} - C_{g,i} \frac{\partial u_g}{\partial z} - a_{gl} N_i \tag{1}$$

$$\frac{\partial C_{l,i}}{dt} = u_l \frac{\partial C_{l,i}}{\partial z} + a_{gl} N_i \tag{2}$$

B.1.2 Energy Balance

$$\frac{\partial T_g}{\partial t} = -u_g \frac{\partial T_g}{\partial z} - T_g \frac{\partial u_g}{\partial z} + \frac{q_g a_{gl}}{\sum C_{l,i} C_{p,i}} \tag{3}$$

$$\frac{\partial T_l}{\partial t} = -u_l \frac{\partial T_l}{\partial z} - \frac{q_l a_{gl}}{\sum C_{l,i} C_{p,i}} \tag{4}$$

B.1.3 Rate Equations

$$N_{g,i} = k_{g,i}\left(p_{g,i} - p_i^l\right) \tag{5}$$

$$N_{l,i} = k_{l,i}(C_{l,i}^l - C_{l,i}) \tag{6}$$

$$N_i = N_{g,i} = N_{l,i} \tag{7}$$

$$N_i = E k_{g,i}\left(p_{g,i} - p_i^l\right) = E k_{l,i}(C_{l,i}^l - C_{l,i}) \tag{8}$$

B.1.4 Mass Transfer coefficients

$$k_g = 5.23 \left(\frac{\rho_g u_g}{a_p \mu_g}\right)^{0.7} \left(\frac{\mu_g}{\rho_g D_g}\right)^{\frac{1}{3}} \left(\frac{D_g}{R_g T_g a_p d_p^2}\right) \tag{9}$$

$$k_l = 0.0051\,(\frac{\mu_l g}{\rho_l})^{\frac{1}{3}}\left(\frac{\rho_l u_l}{a_w \mu_l}\right)^{\frac{2}{3}}\left(\frac{\mu_l}{\rho_l D_l}\right)^{-\frac{1}{2}}(a_p d_p)^{0.4} \quad (10)$$

Wetted Surface Area

$$\frac{a_w}{a_p} = 1 - \exp\left\{-1.45\left(\frac{L}{\mu_l a_p}\right)^{0.1}\left(\frac{a_p L^2}{g\rho_l^2}\right)^{-0.05}\left(\frac{L^2}{\rho_l a_p \sigma_l}\right)^{0.2}\left(\frac{\sigma_{ct}}{\sigma_l}\right)^{0.75}\right\} \quad (11)$$

Enhancement Factor

$$E_2 = \frac{\sqrt{M\frac{E_i - E_2}{E_i - 1}}}{tanh\sqrt{M\frac{E_i - E_2}{E_i - 1}}} \quad (12)$$

B.2 Reboiler

$$\frac{dM_{i,reb}}{dt} = F_{in}x_{i,in} - F_v y_{i,out} - F_l x_{i,out} \quad (13)$$

$$\frac{dE_{reb}}{dt} = F_{in,reb}H_{in,reb} - F_{V,reb}H_{V,reb} - F_{L,reb}H_{L,reb} - Q_{reb} \quad (14)$$

$$M_{i,reb} = \frac{\pi}{4} d_c^2 L_B \rho_m x_i \quad (15)$$

$$E_{reb} = \frac{\pi}{4} d_c^2 L_B H_l \rho_m \quad (16)$$

B.3 Condenser

$$\frac{dE_{cond}}{dt} = F_{in,cond}H_{in,cond} - F_{V,cond}H_{V,cond} - F_{L,cond}H_{L,cond} - Q_{cond} \quad (17)$$

$$T_{cond} = 5351.5(y_{CO_2 out,Cond})^2 + 9777.7(y_{CO_2 out,Cond}) - 4143.3 \quad (18)$$

B.4 Heat Exchanger

$$\frac{\partial T_{tube}}{\partial t} = \frac{-u_{tube}}{L}\frac{\partial T_{tube}}{\partial z} + UT_{LM}\frac{\pi D_{tube}}{\rho_{tube}A_{tube}C_{p,tube}} \quad (19)$$

$$\frac{\partial T_{shell}}{\partial t} = \frac{-u_{shell}}{L}\frac{\partial T_{shell}}{\partial z} + UT_{LM}\frac{n_{tube}\pi D_{tube}}{\rho_{shell}A_{shell}C_{p,shell}} \quad (20)$$

B.5 Buffer Tank

$$F_{mkpH_2O} = F_{v,out,Cond,H_2O} + F_{v,out,Abs,H_2O} - F_{v,in,Abs,H_2O} \quad (21)$$

$$F_{mkpMEA} = F_{v,out,Cond,MEA} + F_{v,out,Abs,MEA} - F_{v,in,Abs,MEA} \quad (22)$$

$$A_T\frac{dh_T}{dt} = \frac{F_{in,tot}}{\rho_{in}} - \frac{F_{out,tot}}{\rho_{out}} \quad (23)$$

$$F_{out,tot} = \frac{C_v\alpha}{mw_L}\sqrt{\rho_{out}\Delta P} \quad (24)$$

$$\frac{dE_{tank}}{dt} = F_{in,tank}H_{in,tank} + F_{mkpH_2O}H_{mkpH_2O} + F_{mkpMEA}H_{mkpMEA} - F_{out,tank}H_{out,tank} - Q_{tank} \quad (25)$$

B.6 Valves

$$\tau_v\frac{dV_{SP}^{act}}{dt} = V_{SP} - V_{SP}^{act} \quad (26)$$

$$\alpha = \frac{V_{SP}^{act} + f_{Leak}}{1 + f_{Leak}} \quad (27)$$

B.7 CO_2 Capture Equation

$$\%CC(t) = 1 - \frac{y_{CO_2,out,Abs}(t)F_{v,out,abs}(t)}{y_{CO_2,in,Abs}(t)F_{v,in,abs}(t)} \quad (28)$$